TECHNISCHE UNIVERSITÄT MÜNCHEN

Fakultät für Chemie

Lehrstuhl für Biotechnologie

Aspects of immunoglobulin biosynthesis

Eva Seedig

Vollständiger Abdruck der von der Fakultät für Chemie der Technischen Universität München zur Erlangung des akademischen Grades eines

Doktors der Naturwissenschaften (Dr. rer. nat.)

genehmigten Dissertation.

Vorsitzender: Univ.- Prof. Dr. B. Reif

Prüfer der Dissertation:

1. Univ.- Prof. Dr. J. Buchner

2. Univ.- Prof. Dr. V. A. Sieber

Die Dissertation wurde am 30.04.2012 bei der Technischen Universität München eingereicht und durch die Fakultät für Chemie am 25.06.2012 angenommen.

Summary

In higher vertebrates, the immune system represents an essential barrier against various pathogens. Antibodies, the humoral branch of the immune system, fold and assemble in the endoplasmic reticulum (ER) assisted by several folding helpers such as chaperones and thiol oxidoreductases. Besides experimental research, antibodies are broadly used in medicine representing an important therapeutic and diagnostic tool. Consequently, the importance of antibodies has been continuously growing over the past years.

Currently, therapeutic antibodies are preferentially produced in mammalian cell cultures which is connected with high production costs. Therefore, the production of antibodies in microorganisms would be more useful. Microorganisms can be cultivated up to high densities with cheap media and the process time of expression is shorter compared to mammalian cell cultures. Yeast combines the advantages of microorganisms with the eukaryotic ability of adding the correct post-translational modifications.

In this work, an expression system for antibody fragments in *S. cerevisiae* was established. MAK33, a mouse IgG against creatine kinase from human heart muscle, was used as a model antibody. Both, the light chain and the Fd-fragment, were expressed from either CEN or 2µ plasmids and were found to fold and associate within the ER. This system provides now an opportunity for further investigations focusing on the improvement of antibody expression in yeast.

One of the possible avenues for improvement might be a co-expression of different proteins known to be important for antibody folding. One of these proteins is pERp1, a small ER resident protein dedicated to antibody folding in mammalian cells. pERp1 harbors six cysteines which are connected via disulfide bonds in a specific pattern. In this work, pERp1 and its six mutants lacking defined cysteines were characterized *in vitro* by biophysical methods. pERp1 was found to be a monomeric protein which has predominantly an α-helical secondary structure. In addition, an interesting destabilizing effect of one of the three disulfide bonds was identified. Finally, pERp1 was found to bind to BiP in the presence of nucleotides. However, pERp1 does not seem to have any effect on the ATPase activity of BiP.

Taken together, this work sheds light on immunoglobulin biosynthesis regarding possible improvements for the expression of recombinant antibodies in yeast.

Zusammenfassung

In höheren Wirbeltieren stellt das Immunsystem eine unverzichtbare Verteidigungslinie gegen unterschiedlichste Pathogene dar. Antikörper, der humorale Teil des Immunsystems, werden im endoplasmatischen Retikulum (ER) gefaltet und assembliert, unterstützt durch eine Reihe von Faltungshelfern wie Chaperone und Thiol-Oxidoreduktasen. Neben der experimentellen Forschung werden Antikörper auch viel in der Medizin zu Therapie und Diagnostik verwendet. In den vergangenen Jahren ist die Bedeutung von Antikörpern kontinuierlich gewachsen.

Aktuell werden therapeutische Antikörper vorzugsweise in Säugerzellkulturen produziert, was aber mit hohen Kosten verbunden ist. Daher wäre eine Antikörper-Produktion in Mikroorganismen vorteilhafter. Mikroorganismen können in hohen Dichten auf günstigem Medium kultiviert werden und Expressionszeit ist im Vergleich mit Säugerzellkulturen kürzer. Hefe kombiniert die Vorteile von Mikroorganismen mit der eukaryotischen Fähigkeit zu post-translationalen Modifikationen.

In dieser Arbeit wurde ein Expressionssystem für Antikörperfragmente in *S. cerevisiae* etabliert. Als Modellantikörper wurde MAK33 verwendet, ein IgG gegen Kreatinkinase aus menschlichem Herzmuskel. Sowohl die leichte Kette also auch das Fd-Fragment wurden entweder aus CEN oder 2µ Plasmiden exprimiert und wurden innerhalb des ER gefaltet und assoziiert. Dieses System erlaubt nun weitere Untersuchungen mit dem Ziel die Antikörperexpression in Hefe zu verbessern.

Eine der möglichen Stoßrichtungen für Verbesserungen könnte die Co-Expression anderer faltungsunterstützender Proteine sein. Eines dieser Proteine ist pERp1, ein kleines ER-Protein das in Säugerzellen zur Antikörperfaltung beiträgt. Es enthält sechs Cysteine, die über Disulfidbrücken zu einem bestimmten Muster verbunden sind. In dieser Arbeit wurden pERp1 und seine sechs Mutanten in denen bestimmte Cysteine fehlten *in vitro* mittels biophysikalischer Methoden charakterisiert. Es wurde festgestellt, dass pERp1 ein monomeres Protein mit einer vorwiegend α-helikalen Sekundärstruktur ist. Zusätzlich wurde ein interessanter destabilisierender Effekt von einer der drei Disulfidbrücken identifiziert. Außerdem wurde gezeigt, dass pERp1 in Gegenwart von Nukleotiden BiP bindet, es scheint jedoch keine Auswirkung auf die ATPase-Aktivität von BiP zu haben.

Zusammengefasst beleuchtet die Arbeit die Biosynthese von Immunoglobulinen in Bezug auf mögliche Verbesserungen der Expression rekombinanter Antikörper in Hefe.

Index

1 Introduction

1.1 Protein folding

During their translation at a ribosome, proteins are synthesized in an unfolded linear form (random-coil). However, in order to fulfill their functions they have to adopt their functional three-dimensional structure (native conformation). The term "protein folding" describes the transition between the unfolded and the native state of proteins and was established in the middle of the last century (Anfinsen et al., 1961). Anfinsen et al. could show in experiments with denatured and reduced ribonuclease A for the first time that the folding of proteins is a reversible process which is thermodynamically driven and that the native conformation represents the thermodynamic minimum with the lowest energy. Additionally, it was suggested that the information about correct folding is coded in the primary structure, the amino acid sequence (Anfinsen et al., 1961). However, it remained open how a protein finds its native conformation. A small theoretical protein with 150 amino acids could adopt 10^{300} possible configurations (Levinthal, 1969). This astronomical number is the basis of the Levinthal paradox which argues that proteins fold in a defined way, in which they reach their native structure via a series of stable folding intermediates, not via random testing of various conformations (Levinthal, 1968). Consequently, three folding models were proposed (Figure 1) which uncoupled the formation of the secondary and tertiary protein structure and thereby simplified the search for the native structure (Fersht, 1999). The *framework model* suggests that well-defined elements of the secondary structure are formed first independently from the tertiary structure (Kim and Baldwin, 1982) . The native elements of secondary structure then form the tertiary structure, e.g., by a diffusion-collision mechanism (Karplus and Weaver, 1994). The *nucleation model* proposes that interactions of some neighboring residues lead to a nucleus of the native secondary structure from which it then grows and the tertiary structure is formed as a consequence of the secondary structure (Wetlaufer, 1973). The *hydrophobic-collapse model* suggests that the protein collapses rapidly around its hydrophobic residues and that the tertiary structure directs the secondary structure by native-like interactions (Ptitsyn, 1995). The collapsed state of the protein is also termed a "molten globule" state, which is characterized by a very weak native-like secondary structure and fluctuating tertiary interactions. On the contrary, the *jigsaw model* proposes that each molecule of a given protein folds by a different path to its native state (Harrison and Durbin, 1985).

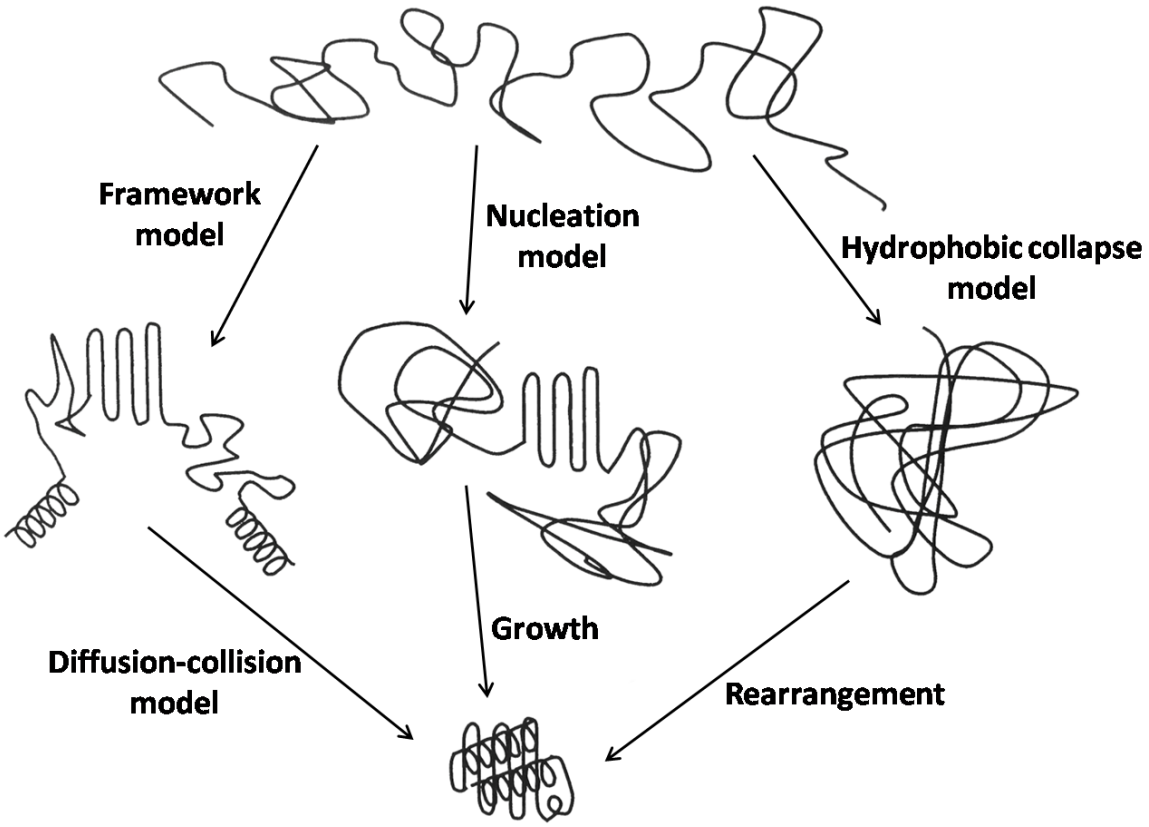

Figure 1: Mechanisms of protein folding, adapted from Fersht (1999). In the framework model, elements of the secondary structure are proposed to form first and then diffuse until they collide and form the tertiary structure. In the nucleation model, the native-like secondary structure serves as a nucleus from which the native structure can propagate. In the hydrophobic collapse model, the protein collapses around its hydrophobic residues and the native structure is formed by a rearrangement of the protein.

Later on, the "new view" of the protein folding kinetics has emerged putting the models proposing only one defined way into question (Dill and Chan, 1997). It has been suggested that protein folding proceeds down the folding funnel (Figure 2) with many possible routes which are more or less energetically favorable. The top of the funnel correlates to the energetic maximum and the protein exists in many random unfolded states. On its way down the folding funnel, the protein might have to overcome energetic barriers and non-native folding intermediates might get caught within kinetic traps (Dill and Chan, 1997). During the progress down the funnel, the amount of native-like structures increases until the protein reaches its native conformation which correlates to the energetic minimum (Dill and Chan, 1997). In the native state, both enthalpy and free energy are decreased because of the stabilizing intramolecular interactions such as hydrogen bonds, salt bridges and van der Waals´ inte-

ractions (Creighton, 1990). Additionally, formation of the native structures reduces configuration entropy (Onuchic et al., 1995). Therefore, the process of protein folding might also be described as a competition between entropy, which tries to keep the protein unfolded, and minimization of enthalpy, which drags the protein down the funnel to fold (Fersht, 1999). The width of the folding funnel represents the configuration entropy and the depth corresponds to the free energy (Onuchic et al., 1995).

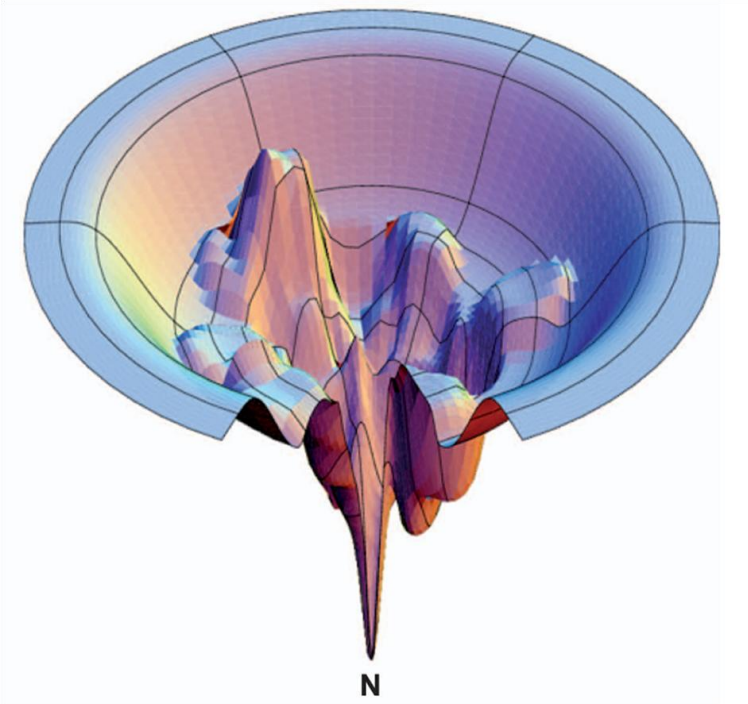

Figure 2: Folding funnel according to Dill and Chan (1997). The top of the funnel represents energetic maximum and the protein might be present in many random unfolded states. Protein folding proceeds down the folding funnel towards the native state (N) which corresponds to the energetic minimum. The width of the funnel represents entropy, whereas the depth represents free energy.

1.1.1 Protein misfolding

Only correctly folded proteins are able to fulfill their functions and therefore it is necessary to keep the amount of folding mistakes as low as possible. For this purpose, cells developed powerful mechanisms one of which is represented by folding helpers (chaperones). Until now, many chaperones have been identified. Some of them are constitutively present in a cell but the expression of most of them is up-regulated during stress conditions. A variety of stresses such as elevated temperatures, presence of toxic chemicals etc. can disturb protein homeostasis and lead to protein misfolding and aggregation (Richter et al., 2010). Misfolded

or damaged proteins are extremely harmful for the host organism and therefore they have to be degraded. Cells developed sophisticated pathways how to cope with aberrant proteins. Besides chaperones which help nascent proteins to fold and to correct mistakes that occurred during folding or prevent unfolded proteins from aggregation, signaling pathways such as the unfolded protein response (UPR) and the endoplasmic reticulum associated degradation (ERAD) pathway developed. These pathways are activated during severe stresses upon which unfolded proteins accumulate within the endoplasmic reticulum (see section 1.3).

1.1.2 Molecular Chaperones

There are five major classes of molecular chaperones which are broadly conserved: the Hsp100 family, Hsp90 family, Hsp70 family, Hsp60 family and the family of small heat shock proteins (sHsps). Apart from these ubiquitous chaperones also other heat-inducible chaperones are known, like e.g. Hsp33 the activity of which is redox regulated (Jakob et al., 1999), however they are not included in a separate class (Richter et al., 2010).

All molecular chaperones react promiscuously with a wide range of unfolded proteins. Aberrant proteins are recognized by molecular chaperones via hydrophobic residues, which would be normally buried in a hydrophobic core of the correctly folded proteins. Chaperones bind to this exposed hydrophobic sequences and prevent the protein from misfolding or aggregation. During protein folding, the affinity state of the chaperone for its substrate changes, which is controlled by ATP-hydrolysis in most of the chaperone families except of small Hsps. sHsps are also referred to as “holdases”, which are mostly expressed only upon stress conditions and are very efficient in binding of aberrant proteins, functioning as a first line of defense. Comparing to that, “foldases” like Hsp70 and Hsp90, exist in a constitutively expressed and also in a stress induced forms, e.g. Hsc70 and Hsp70 (Richter et al., 2010).

Hsp70 chaperones consist of an N-terminal ATPase domain and a C-terminal substrate binding domain. They can be found in nucleus, cytosol, mitochondria, chloroplast and ER, where they bind to exposed hydrophobic residues and keep proteins in a folding-compatible conformation (Bukau et al., 2006). The Hsp70 chaperone in the lumen of the endoplasmic reticulum (ER) is called BiP and it plays a significant role in antibody folding (see section 1.4.2).

1.2 Protein folding in Endoplasmic Reticulum

The ER is an important organelle present in all nucleated eukaryotic cells which not only enables the folding of certain proteins, their modification and assembly, but it also contains distinct quality control mechanisms responsible for degradation or recycling of misfolded proteins. Around one third of all cellular proteins are folded in ER (Hoseki et al., 2010). The ER provides conditions similar to the extracellular environment in terms of oxidizing capabilities and ion conditions (Feige and Hendershot, 2011) which allows post-translational modifications such as formation of disulfides. The folding capacity of the ER can be extremely high for example in antibody-producing plasma cells. Folding of a single IgM pentamer requires folding of 70 Ig domains, their assembly into light and heavy chains connected to J chain, attachment of 26 N-glycans, and introduction of ~100 disulfide bonds. It was shown that lipopolysaccharide-stimulated B cells can secrete 3000 IgM molecules $cell^{-1}sec^{-1}$ (King and Corley, 1989).

New synthesized proteins interact in the cytoplasm with ribosome-associated chaperones (Hsc70 and Hsp40 in eukaryotes, trigger factor in prokaryotes) which hand them over to the cytoplasmic folding machinery (Wegrzyn and Deuerling, 2005). Proteins which are targeted into endoplasmic reticulum are translocated through the ER membrane and folded within ER upon the help of the ER chaperoning machinery. The translocation pore consists of the conserved heterotrimeric membrane protein Sec61, identified by Deshaies and Schekman (1987). In *Saccharomyces cerevisiae* additional binding partners, namely the membrane complex Sec62/Sec63 (consisting of Sec62, Sec63, Sec71 and Sec72) exist (Deshaies et al., 1991; Green et al., 1992). Besides import of the nascent proteins into the ER, Sec61 was also shown to be involved in the export of misfolded proteins out of the ER (Pilon et al., 1997).

Translocation of proteins through the ER membrane starts with insertion of a loop into the translocation channel (Shaw et al., 1988). Translocation occurs mostly co-translational which prevents synthesis of large protein regions that would be unable to cross the ER membrane (High, 1995). Usually, the N-terminal end of co-translational translocated proteins contains a signal peptide (Martoglio and Dobberstein, 1998). The signal peptide is recognized by the signal recognition particle (SRP), which binds to a ribosome synthesizing a nascent polypeptide chain (Walter and Johnson, 1994). SRP delivers the ribosome to the ER membrane, where it interacts with the SRP receptor and then with the translocation pore. The growing nascent peptide moves directly from the ribosomal tunnel into the translocation channel

(Rapoport, 2007). For the peptide chain elongation by the ribosome, GTP hydrolysis is necessary, but the movement of the nascent protein through the translocation channel is independent of nucleotide hydrolysis (Connolly and Gilmore, 1986).

Post-translational translocation starts with the binding of the nascent protein to the translocational channel and the translocation occurs by a ratcheting mechanism (Matlack et al., 1999). As soon as the nascent peptide enters the ER lumen, BiP binds to it and prevents its movement back to the cytosol. At the beginning, BiP is in its ATP-bound state and its substrate binding pocket is open. However, upon interaction with the J domain of Sec63, ATP is rapidly hydrolyzed and the pocket closes around the translocating peptide (Misselwitz et al., 1999). After the protein moved partially into the ER, another BiP molecule can bind to it. This is repeated until the nascent protein completely crosses the ER membrane. Finally, BiP is released from the nascent peptide upon exchange of ADP for ATP which opens the substrate binding pocket (Rapoport, 2007).

Once the polypeptide chain is translocated into the ER, its folding is assisted by the ER chaperoning machinery. After the protein is folded correctly, it can be released from the ER and transported via the Golgi apparatus to the cell surface or another final destination. In case of an unsuccessful folding process, the protein might react again with ER folding assistant proteins and try to reach the native conformation. If the folding process fails completely, the protein is retrotranslocated through the ER membrane back to the cytosol and is degraded there in proteasome (Braakman and Bulleid, 2011). The ER quality control, ensuring that only correctly folded proteins leave the ER, is discussed separately in section 1.3.

Yeast ER and the ER of mammalian cells contain different chaperones and other folding helpers such as thiol oxidoreductases (Table 1). In this work, all experiments were performed in yeast, therefore in the following part only the ER of yeast will be discussed. For better illustration, molecular chaperones and folding enzymes of the yeast ER were divided into four groups (Table 1). In the first group, there are heat shock proteins such as Hsp70 (BiP) and its Hsp40 co-chaperones. The second group involves the nucleotide exchange factors for BiP. The third group is represented by lectin chaperones and the fourth group contains thiol oxidoreductases of the protein disulfide isomerase (PDI) family.

ER chaperones and folding enzymes	
Yeast	Mammals
Heat Shock Proteins	
Hsp90	
	Grp94
Hsp70	
Kar2	BiP
Hsp40 (J-domain containing proteins, co-chaperones of BiP)	
Sec63, Jem1, Scj1	ERdj1/Mtj1, ERdj2, ERdj3 ERdj4/Mdj1, ERdj6, ERdj7
Nucleotide Exchange Factors for BiP	
Lhs1, Sil1	BAP, Grp170
Lectin-like chaperons	
Folding of glycoproteins	
Cne1	calnexin, calreticulin
Degradation of terminally misfolded glycoproteins	
Mns1p, Mnl1p (Htm1p)	EDEM
Thiol oxidoreductases	
Pdi1, Eug1, Mpd1, Mpd2, Eps1	ERp57, ERp72, P5, PDI, pERp1*, ERdj5 (reductase)

Table 1: Chaperones and folding enzymes in the ER of *Saccharomyces cerevisiae* and in the ER of mammalian cells, adapted from Feige et al. (2010a) and Nishikawa et al. (2005). EDEM – endoplasmic reticulum degradation-enhancing α-mannosidase like proteins. * – pERp1 was proposed to be either a unique type of oxidoreductase or a chaperone dedicated to antibody folding (Shimizu et al., 2009; van Anken et al., 2009).

1.2.1 BiP/Kar2

BiP (Kar2 in yeast) is a ~78 kDa big Ca^{2+}-binding protein that associates with newly synthesized, unfolded or unassembled proteins in the lumen of ER. BiP is the major ER luminal chaperone and beside this function, BiP was also shown to be involved in the control of ER luminal Ca^{2+} homeostasis (Lievremont et al., 1997). BiP was identified as a glucose-regulated protein which binds antibody heavy chains (Haas and Wabl, 1983), however, it was shown

that BiP binds immunoglobulin light chains as well (Knittler and Haas, 1992). BiP preferentially binds to aliphatic residues which normally would be buried in correctly folded proteins (Flynn et al., 1991).

In *S. cerevisiae*, Kar2 was shown to participate in the translocation of secretory proteins through the ER membrane (Nguyen et al., 1991). Furthermore, upon ER stress, Kar2 can activate the unfolded protein response by its dissociation from Ire1 (Okamura et al., 2000).

Similar to other Hsp70 proteins, BiP consists of an N-terminal ATPase domain and a C-terminal substrate binding domain with a flexible lid, which confines the substrate. Binding and release of the substrate protein is coupled to ATP hydrolysis and conformational changes in both domains (Awad et al., 2008). ATP hydrolysis is stimulated by Hsp40/DnaJ-like proteins and generated ADP is then released by two nucleotide exchange factors (NEFs), which enables ATP binding again (Figure 3A). Recently, single molecule experiments with BiP and C_H1 antibody domain as its authentic substrate showed movements of BiP domains upon substrate binding (Marcinowski et al., 2011). It was shown that according to the conformational transition of the lid domain, BiP can discriminate between peptide and protein substrates (Figure 3B). Furthermore, it was shown that the BiP chaperone cycle is modulated by ERdj3 at several steps (Marcinowski et al., 2011). ERdj3 is the main BiP co-chaperone in antibody folding in mammalian cells (Shen and Hendershot, 2005). However, a homologue of ERdj3 in yeast has not been identified so far.

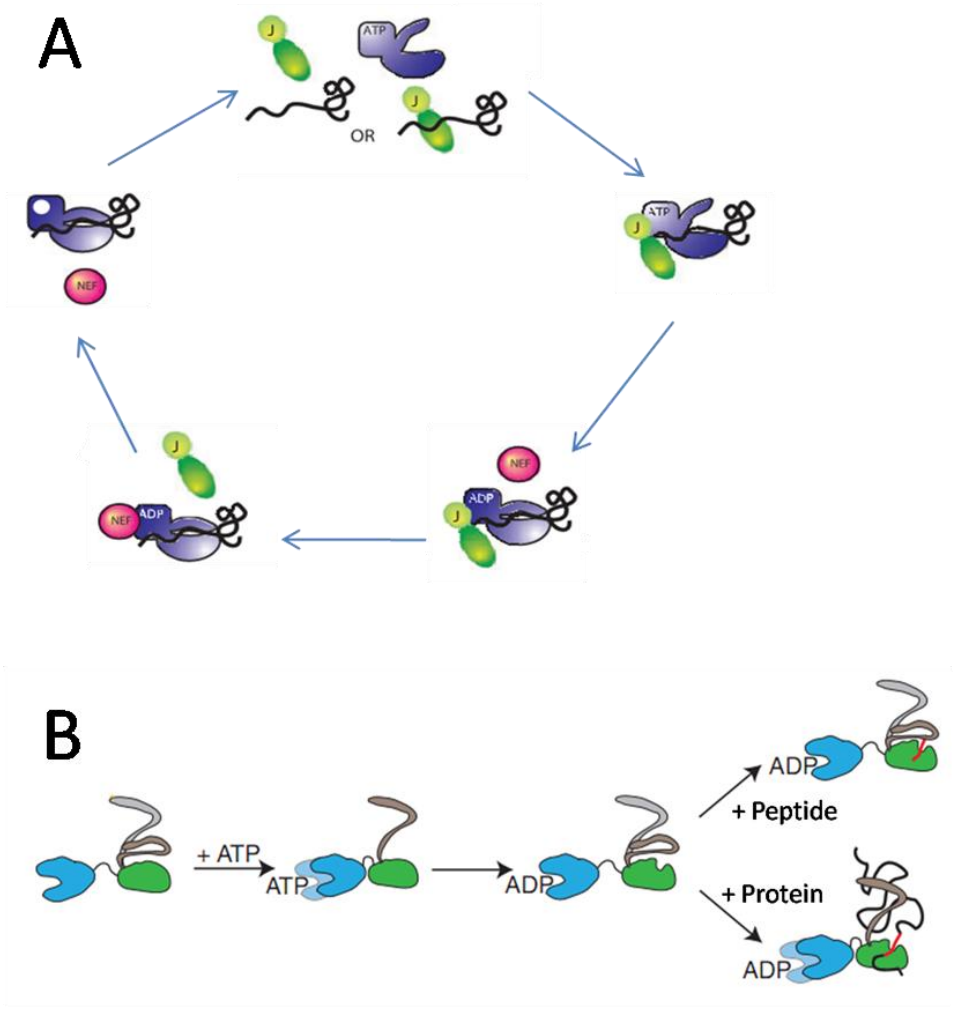

Figure 3: Chaperone cycle of BiP.
A) ATPase cycle of BiP, adapted from Christis et al. (2008). BiP binds the substrate which may be presented by a J-protein. J-protein stimulates hydrolysis of BiP-bounded ATP to ADP, which is then released from BiP by nucleotide exchange factor, making BiP accessible for the next chaperoning cycle.
B) The interdomain distance (ATPase domain in blue, substrate binding domain in green) of BiP changes upon nucleotide binding, adapted from Marcinowski et al. (2011). The peptide (in red) is bound in a conformation similar to ADP-only state, whereas binding of the protein (in black) results in a widely opened conformation and closer domain coupling. In addition, the lid (in grey) also interacts directly with the bound protein. The predominant conformation is depicted in darker colors.

In ER lumen of *S. cerevisiae*, so far two NEFs for BiP have been found, Lhs1p and Sil1p (Hale et al., 2010). Lhs1p is member of an ER Hsp70 subfamily (Craven et al., 1997) which is ubiquitously present among eukaryotes. A mammalian homologue of Lhs1 is Grp170, a glucose-regulated stress protein that binds immunoglobulin (Chen et al., 1996; Lin et al., 1993). Lhs1p was shown to be required for protein refolding after heat shock (Saris and Makarow,

1998) and deletion of LHS1 (*ΔLhs1*) activates the unfolding protein response, but it is not lethal. *ΔSil1* cells are viable as well, however, the double deletion (*ΔLhs1, ΔSil1*) disrupts the translocation of proteins into the ER and is lethal (Tyson and Stirling, 2000). Recent data suggests that Lhs1p and Sil1p bind to Kar2 in a very different manner and that the mechanisms of the Kar2 interaction with Lhs1p and Sil1p are distinct (Hale et al., 2010).

1.2.2 Hsp40/J domain proteins

Hsp40 proteins are co-chaperones of Hsp70. They stimulate its ATPase activity and some of them also deliver substrates to Hsp70. Hsp40 and Hsp70 interact via the Hsp40 J domain (Figure 3A). A single Hsp70 protein can interact with several Hsp40s to promote diverse cellular processes (Vembar et al., 2010).

Within the endoplasmic reticulum of *S. cerevisiae*, so far three Hsp40s (Sec63p, Scj1p and Jem1p) have been found to interact with Kar2.

Sec63 is an integral ER membrane protein containing three domains imbedded in the membrane and a J domain loop presented in the ER lumen. The highly charged C-terminal segment is positioned in the cytosol (Feldheim et al., 1992). Sec63p together with Kar2 are necessary for the co- and posttranslational translocation of nascent proteins into the yeast ER (Brodsky et al., 1995).

Jem1p is peripherally associated with the luminal side of the ER membrane (Nishikawa and Endo, 1997), whereas Scj1p is a soluble ER-luminal protein (Schlenstedt et al., 1995). Jem1p and Scj1p play a role in the ERAD, because they maintain the solubility of proteins designated for retrotranslocation from ER and degradation (Nishikawa et al., 2001). *ΔJem1* cells grow normally, but the double deletion *ΔJem1* and *ΔScj1* shows defective growth at elevated temperatures (Nishikawa and Endo, 1997). Deletion of *Scj1* activates the UPR and *ΔScj1* cells are hypersensitive to the reducing agents, tunicamycin and hypoglycosylation. The double deletion *ΔScj1, ΔJem1* increases the sensitivity to hypoglycosylation and activation of the UPR (Silberstein et al., 1998).

Recently, it was shown that a mutation in the Kar2 surface that interacts with a Hsp40 J domain impaired the interaction between Sec63p and Kar2 but not between Kar2 and Jem1p. Consequently, yeast expressing mutated Kar2 showed a defect in the protein translocation, but

the ERAD remained unaffected. This data suggests that the role of BiP/Kar2 in protein translocation is defined by the specificity of its J domain co-chaperones (Vembar et al., 2010).

Jem1p and Sec63p also play a role during the mating of budding yeast. Mutants, which are Sec63p or Jem1p defective, are unable to undergo karyogamy (Nishikawa and Endo, 1997; Nishikawa et al., 2008).

1.2.3 Lectin chaperones

In mammalian cells, two lectin chaperones are known, transmembrane calnexin and soluble calreticulin, which facilitate glycoprotein folding (Christis et al., 2008). Calnexin and calreticulin recognize the $GlcMan_9GlcNAc_2$ moieties which were produced before by trimming with glucosidase I and II (see section 1.3.2). After the glycoprotein adapted its native conformation, the third glucose is removed, the correctly folded glycoprotein dissociates from calnexin/calreticulin and is secreted from the ER (Hoseki et al., 2010). Calnexin and calreticulin also form a complex with ERp57 (Russell et al., 2004), a member of the protein disulfide isomerase family dedicated to the folding of glycosylated disulfide bonded substrates (Oliver et al., 1997).

The homologue of calnexin in *S. cerevisiae* is Cne1p, a membrane protein, that in contrast to calnexin does not exhibit calcium binding activity and lacks the cytoplasmic tail (Parlati et al., 1995). Cne1p was shown to function as a molecular chaperone (Xu et al., 2004b) and to be involved in the ER quality control (Xu et al., 2004a). In addition to that, Cne1p was found to interact with Mpd1, a member of the yeast PDI family (see section 1.2.4). Cne1p increases the reductive activity of Mpd1p, whereas Mpd1p inhibits the chaperone activity of Cne1p. It was suggested, that Mpd1p might act as a homologue of ERp57 (Kimura et al., 2005).

1.2.4 Thiol oxidoreductases

Thiol oxidoreductases are proteins from the protein disulfide isomerase family. Protein disulfide isomerases (PDI) possess a signal sequence, an ER retention signal, and one or more thioredoxin domains with the active site motif CXXC. The two cysteines can cycle between the reduced and oxidized state, in which they form an intramolecular disulfide bond. In *S. cerevisiae*, five members of the PDI family have been identified so far: Eps1p, Eug1p, Mpd1p, Mpd2p, Pdi1p (Norgaard et al., 2001). The most prominent member of the PDI family is the Pdi1p that contains two thioredoxin domains. Two thioredoxin domains are also

present in Eug1p that shares about 40% sequence homology with Pdi1p. In contrast to all other members of the PDI family, the active site of Eug1p consists of a CXXS motif. Therefore, Eug1p cannot form an intramolecular disulfide bond. In contrast to Pdi1p and Eug1p, Mpd1p, Mpd2p and Eps1p contain only one thioredoxin domain (Norgaard et al., 2001).

From all PDI family members, only Pdi1p is essential. Overexpression of any of the remaining members (Eps1p, Eug1p, Mpd1p, Mpd2p) suppresses the lethality of Pdi1p deletion, however, Mpd1p is the only protein capable of performing all the essential functions of Pdi1p (Norgaard et al., 2001).

PDI is the key enzyme involved in the formation of the correct disulfide bond pattern in proteins. It catalyzes oxidation, reduction, and isomerization of disulfide bonds. In addition to that, PDI harbors also chaperone activity, because it is able to promote folding of proteins without disulfide bonds as well (Wang and Tsou, 1993).

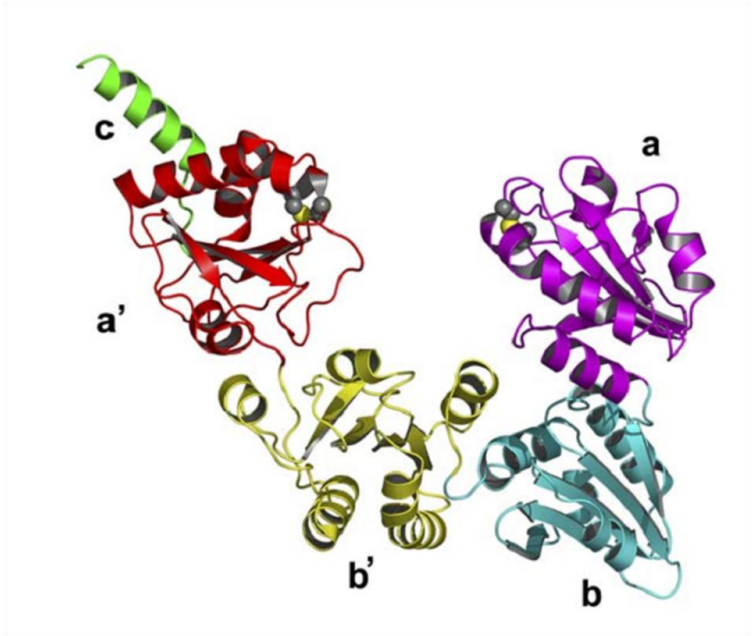

Figure 4: Structure of yeast protein disulfide isomerase Pdi1p according to Tian et al (2006). The a domain is shown in magenta, the a´ domain in red, the b domain in blue, the b´ domain in yellow and the C-terminal extension is shown in green. Cysteines of both thioredoxin active sites are represented by grey, sulfur atoms by yellow spheres respectively.

Pdi1p consists of four thioredoxin domains followed by a C-terminal extension with the HDEL motif. The four thioredoxin domains are arranged in the form of a “twisted U” and are labeled as a, b, b´, a´ in order of appearance from N- to C-terminus. Flexible domains a and a´

contain both a CGHC active site and are catalytically active, whereas b and b´ domains are responsible for the binding of the substrate, see figure 4 (Tian et al., 2006).

During the oxidative protein folding, the CXXC active site of PDI becomes reduced in order to form a disulfide bond in a client protein. To be able to form further disulfide bonds, PDI has to be oxidized again, which is carried out in a reaction with a FAD-bound sulfhydryl oxidase Ero1p (Frand and Kaiser, 1999). Ero1 is an essential, evolutionary conserved protein that directly oxidizes reduced PDI and regenerates itself by oxidation with molecular oxygen or other electron acceptors. An asymmetry in the rate of oxidation of the two active sites was shown which suggested that the a domain of PDI acts as an isomerase and the a´ domain as an oxidase (Kulp et al., 2006). However, Ero1p was recently shown to preferentially interact with the a´ domain of Pdi1p, which should therefore consequently function as an oxidase (Vitu et al., 2010). Presumably, further studies will be necessary to elucidate the main activities of the two catalytical domains.

PDI also plays a role in the ERAD (section 1.3.2). It was shown that Pdi1p associates with Mnl1p (Clerc et al., 2009) in which it is responsible for the formation of a disulfide bond within the mannosidase homology domain that is necessary for its activity (Sakoh-Nakatogawa et al., 2009).

1.3 Quality control in ER

During the folding in the ER, proteins interact with various folding helpers such as chaperones and oxidoreductases. Only proteins that achieved their native conformation and are stable without chaperones can leave the ER. Otherwise, chaperones retain them within the ER and help them to fold. Additionally, chaperones also monitor the protein conformation, which is commonly referred to as the ER quality control. The ER quality control ensures that only correctly folded and assembled proteins are secreted form the ER. Misfolded proteins are either subjected to further folding cycles or they are discarded in a process called endoplasmic reticulum associated degradation (ERAD).

1.3.1 Unfolded Protein Response (UPR)

Upon various stresses such as hypoxia, nutrient starvation, strong reducing conditions etc., but also during normal cellular development, protein folding pathways might be interrupted. This leads to an overload of the ER folding capacity and accumulation of misfolded protein in

the ER. Cells developed mechanisms how to cope with this suboptimal conditions: the ER expands, the synthesis of chaperones is upregulated, general protein synthesis is downregulated and the ERAD pathway (see section 1.3.2) becomes activated. Together, these response mechanisms are known as the "unfolded protein response" (UPR). UPR is an intracellular signaling pathway leading from the ER to the cytosol/nucleus that restores the ER protein-folding homeostasis and enables adaptation to new conditions. However, if the ER stress persists, UPR induces the cell cycle arrest and the release of Ca^{2+} into the cytosol which leads to apoptosis (Christis et al., 2008).

Ire1, identified in *S. cerevisiae* by Cox et al. (1993), is a transmembrane protein conserved among eukaryotes that functions as a stress sensor in the ER and activates the UPR. The luminal N-terminal domain of yeast Ire1 consists of five subregions as depicted in figure 5A (Kimata et al., 2004). It is proposed, that subregions I and V are loosely folded, whereas subregions II and IV form a tightly folded domain termed as a "core stress-sensing region" (CSSR) which harbors an intrinsic ability to form higher oligomers. Subregion III is a loosely folded loop that sticks out from the CSSR (Credle et al., 2005). Crystal structure of the conserved core region of the luminal domain is shown in figure 5B.

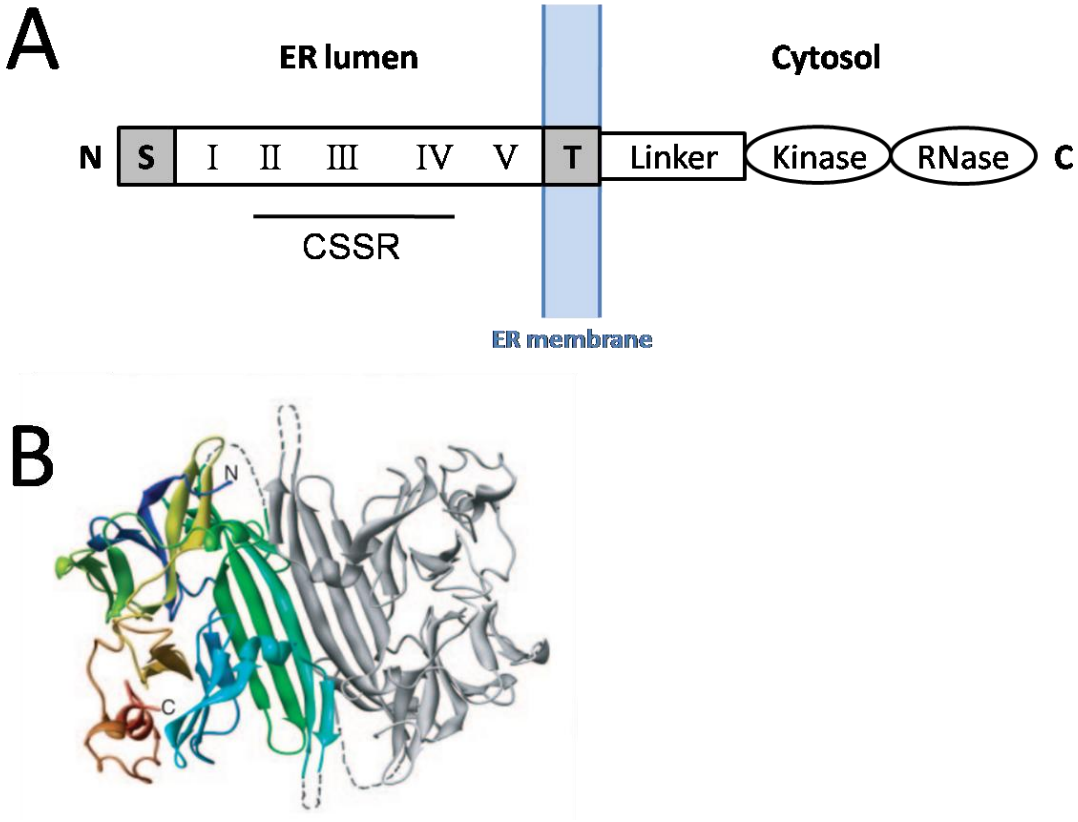

Figure 5: Structure of Ire1.
A) Schematic structure of Ire1, adapted from Kohno (2010). S-signal sequence, T-transmembrane region, Kinase – kinase domain, RNase – ribonuclease domain, N – N-terminus, C – C-terminus, CSSR – core stress sensing region, I-V luminal domain subregions.
B) Ribbon diagram of the conserved core region of the luminal domain (cLD) according to Credle et al. (2005). The two independent core domains in the asymmetric unit associate in a twofold symmetric head-to-head arrangement, colored with a rainbow gradient from N-terminus (blue) to C-terminus (red).

The UPR is regulated by BiP/Kar2 that is associated with the subregion V of the inactive monomeric Ire1 under non-stress conditions. Upon ER stress, Kar2 rapidly dissociates from Ire1 allowing its oligomerization (Figure 6). The luminal domain of Ire1 contains two interfaces. The interface I forms a dimer with a deep groove that was proposed to bind unfolded peptides and the interface II enables further oligomerization (Credle et al., 2005).

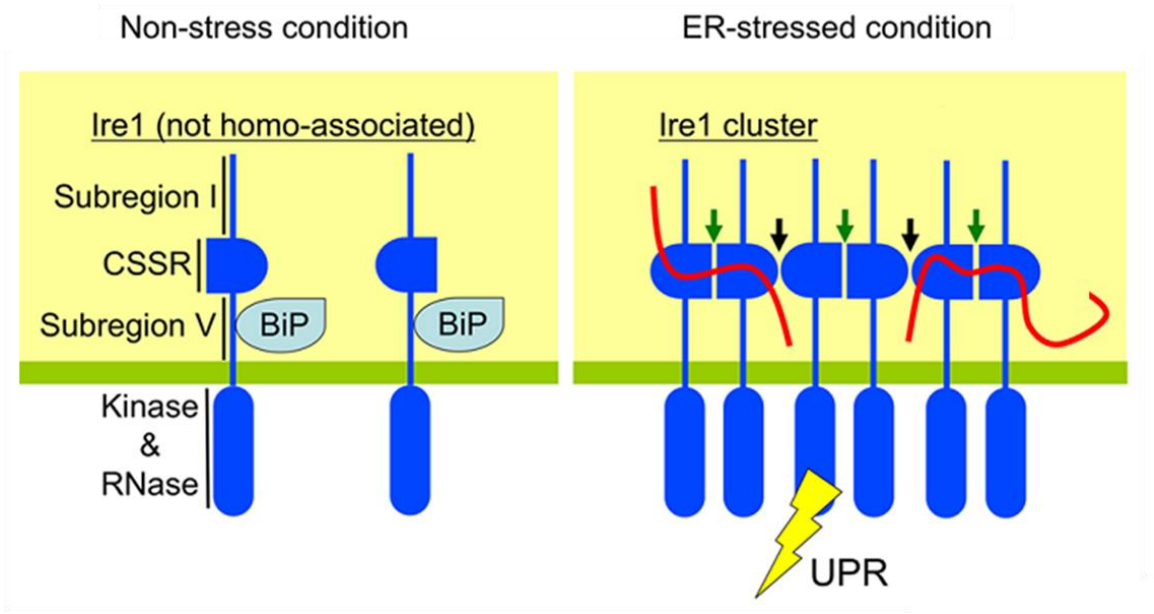

Figure 6: Model of Ire1 function, adapted from Promlek et al. (2011). BiP associates with the subregion V of the Ire1 luminal domain under non-stressed conditions. Upon stress, BiP dissociates from Ire1 which causes Ire1 clustering. Unfolded proteins (red lines) then can directly interact with the cluster of Ire1 which leads to its full activation and induction of the unfolded protein response (UPR).
Green arrows – interface I, black arrows – interface II.

Upon ER stress, Ire1 oligomerizes and undergoes trans-autophosphorylation which activates its kinase and ribonuclease domains (Shamu and Walter, 1996; Welihinda and Kaufman, 1996). This leads to the nonconventional cytosolic splicing of *HAC1* mRNA which is then translated into transcription factor HAC1 that upregulates genes responsible for the synthesis of ER chaperones and ERAD components (Cox and Walter, 1996; Sidrauski and Walter, 1997). Additionally, the Ire1-*HAC1* pathway also activates enzymes important for ER membrane biogenesis. In yeast, Ire1 is induced by the depletion of inositol which is an important component of phosphatidylinositol that is present in high amounts in the yeast ER membrane (Cox et al., 1997). Recently, it was shown that although inositol depletion leads to UPR, it is not the main factor that activates Ire1 (Promlek et al., 2011). It was proposed that unfolded proteins activate Ire1 in a different manner than membrane aberrancies. This was suggested by experiments with an Ire1 mutant where the subregion III of the luminal domain, which forms a peptide-binding groove, was deleted (ΔIII Ire1). It was shown that unfolded proteins induced with DTT, that prevents the formation of disulfide bonds, or tunicamycin, which blocks glycosylation, activate ΔIII Ire1 much less than WT Ire1 and that activation

proceeds rapidly (Promlek et al., 2011). However, if the membrane structure was affected (e.g. by inositol depletion) ΔIII Ire1 and WT Ire1 were activated almost equally and the activation was rather slow. Therefore it was proposed, that ER stress leading to UPR is not always connected to the accumulation of unfolded proteins in the ER and that membrane-related stress is sensed by Ire1 in a different way (Promlek et al., 2011).

Previously, a titration model of Ire1 activation was suggested, where the increasing amount of unfolded proteins competes Kar2 away from Ire1 (Bertolotti et al., 2000; Okamura et al., 2000). However, after the possible peptide-binding groove within the Ire1 dimers was identified and the CSSR was proposed to interact directly with unfolded proteins (Credle et al., 2005), a two-step sensor mechanism was proposed. In the first step, BiP dissociates from Ire1 which leads to the formation of Ire1 clusters and then unfolded proteins directly interact with Ire1 clusters leading to their full activation (Kimata et al., 2007). Indeed, an evidence that Ire1 senses stress by direct binding of unfolded proteins was provided recently, showing that peptide binding leads to oligomerization of the CSSR *in vitro* (Gardner and Walter, 2011). Therefore, it was suggested that, whereas BiP association fine-tunes Ire1 signaling, unfolded proteins are the actual activating ligands.

1.3.2 ER-associated degradation (ERAD)

Most newly synthesized proteins are modified by N-linked glycans in the ER. After the nascent protein entered the ER lumen, glucose$_3$-mannose$_9$-*N*-acetylglucosamine$_2$ ($Glc_3Man_9GlcNAc_2$) oligosaccharides are covalently attached by oligosaccharyltransferase to asparagines in Asn-X-Ser/Thr motifs. The two outermost glucose residues are then immediately removed by the glucosidases Gls1 and Gls2 producing $GlcMan_9GlcNAc_2$ oligosaccharides. Further trimming by Gls2 leads to $Man_9GlcNAc_2$ oligosaccharides that prevent the disposal of the protein (Christis et al., 2008; Hoseki et al., 2010).

Proteins that do not reach their final folded state are discarded in a process referred to as ER-associated degradation (ERAD). In this process, aberrant proteins are retrotranslocated back to the cytosol where they are degraded in a proteasome (Werner et al., 1996). Selection of the ERAD substrates is mediated by BiP and lectin chaperones (Nishikawa et al., 2005). In aberrant proteins, BiP binds hydrophobic regions, which are normally buried in proteins with native structure (Flynn et al., 1991). Terminally misfolded proteins are released from BiP and targeted for ERAD. In contrast, aberrant glycoproteins are bound by lectin chaperones (sec-

tion 1.2.3) and in case of unsuccessful folding they are sorted for ERAD. For ERAD of some proteins also several cytosolic chaperones are required (Huyer et al., 2004; Zhang et al., 2001). One of these chaperones is the Hsp70 Ssa1p, which maintains the solubility of aberrant cytosolic domains of several integral ERAD substrates which enables their transport to proteasome (Nishikawa et al., 2005).

In *S. cerevisiae*, three different ERAD pathways can be distinguished according to which protein is degraded. In the ERAD-L pathway, proteins with misfolded luminal domains are degraded; in the ERAD-M pathway, proteins with misfolded membrane domains and in the ERAD-C pathway, proteins with misfolded cytoplasmic domains are degraded (Carvalho et al., 2006; Vashist and Ng, 2004).

The ERAD-L pathway in *S. cerevisiae* is shown in figure 7. $Man_9GlcNAc_2$ *N*-glycans (M9) of misfolded gylcoproteins are cleaved by ER mannosidase Mns1p. Mns1p removes the outermost mannose moiety from the B branch generating a $Man_8GlcNAc_2$ *N*-glycan (M8) that functions as a signal for degradation (Jakob et al., 1998). Afterwards, another mannose residue of M8 is removed by Mns1p in combination with Mnl1p, an Mns1p homologue previously known as Htm1p (Jakob et al., 2001; Nakatsukasa et al., 2001). The resulting $Man_7GlcNAc_2$ N-glycan (M7) has a terminal non-reducing α-1,6-mannose and tags the glycoprotein for ERAD (Clerc et al., 2009).

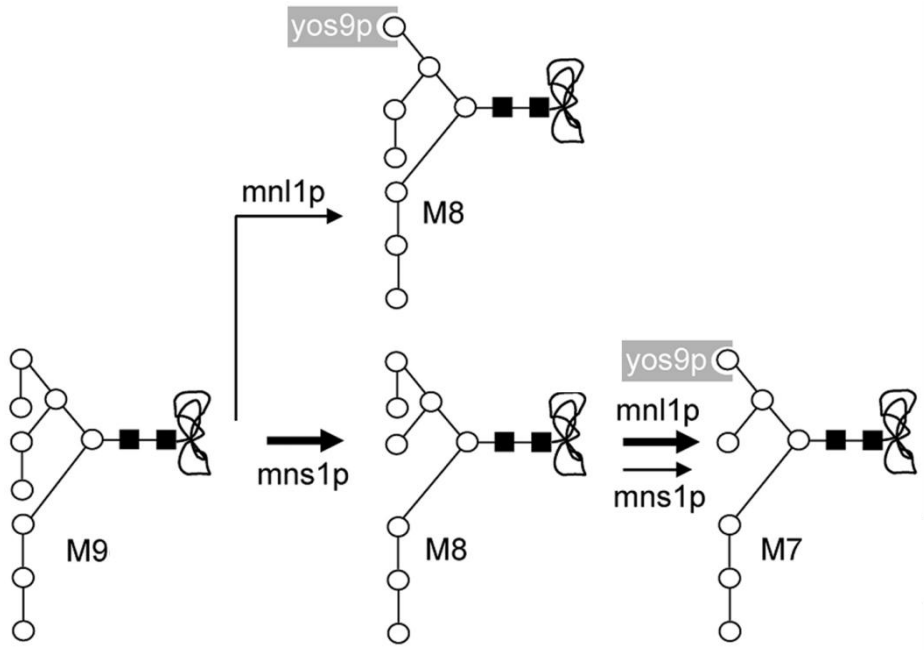

Figure 7: The ERAD-L pathway in *S. cerevisiae*, adapted from Chantret et al. (2011).
M9 – $Man_9GlcNAc_2$, M8 – $Man_8GlcNAc_2$, M7 – $Man_7GlcNAc_2$, mns1p – ER mannosidase I, mnl1p – ER mannosidase-like protein, Yos9p – lectin Yos9p, which targets the misfolded glycoprotein to an ubiquitin ligase complex. White circles – mannose moiety, black squares – GlcNAc.
Glc – glucose, Man – mannose, Ac – acetylglucosamine.

Pdi1p was also shown to play a role in the recognition of ERAD substrates and in the processing of their glycans. Pdi1p associates with Mnl1p and the Mnl1p-Pdi1p complex was suggested to be a functional unit that initiates the degradation of unfolded proteins (Gauss et al., 2011). It was proposed that aberrant proteins bind to the Mnl1p-Pdi1p complex and to free Pdi1p with the same affinity and that, besides oxidoreductase and chaperone activity, the Mnl1p-Pdi1p complex also exhibits exomannosidase activity.

Aberrant glycoproteins processed by Mns1p and Mnl1p have to be transferred to the ubiquitin ligase complex for ubiquitinylation. In yeast, there are two E3 ligases dedicated to ubiquitinylation of different substrates: Hrd1 ligase, which is involved in both the ERAD-M and the ERAD-L pathways, and Doa10 ligase involved in the ERAD-C pathway (Carvalho et al., 2006). Hrd1p forms a complex with the luminal protein Hrd3p that interacts with a lectin-like protein Yos9p (Buschhorn et al., 2004). Yos9p possesses a mannose-6-phosphate receptor homology (MRH) domain that recognizes the terminal α-1,6-mannose moiety. Other components of the Hrd1p/Hrd3p complex are Ubc7p/Cue1p (E2 complex), Der1p, Ubx2p and Usa1p (Carvalho et al., 2006). It was proposed that Kar2 transfers the misfolded proteins to the

Hrd1p/Hrd3p complex. Hrd3p binds hydrophobic patches of the misfolded protein and Yos9p examines it for the presence of an α-1,6-mannose residue. Substrates that were recognized by both Hrd3p and Yos9p are then ubiquitinylated by Hrd1p (Hirsch et al., 2009).

Ubiquitinylated proteins which were selected for ERAD have to be translocated through the ER membrane. Retrotranslocation of most ERAD substrates requires the chaperone-like AAA-ATPase Cdc48. Cdc48 forms a complex with its cofactors Udf1 and Npl4 and translocates misfolded protein across the membrane upon ATP hydrolysis (Ye et al., 2001). Ubx2p and Usa1p connect Der1p and cytosolic Cdc48 (Hoseki et al., 2010). It was proposed that misfolded proteins are retrotranslocated through the Sec61 translocon, the same pore which is used for the import of proteins into ER. In mammalian cells, other candidates for translocation channel are also proteins of the Derlin family (homologue of yeast Der1) (Hirsch et al., 2009; Hoseki et al., 2010).

Besides polyubiquitinylation, misfolded glycoproteins are also deglycosylated by the peptide *N*-glycanase Png1p and afterwards degraded in the proteasome. It also has been suggested that some misfolded glycoproteins might be degraded in an Mnl1p-dependent, Mns1p-independent manner, see figure 7 (Chantret et al., 2011).

The ERAD pathway can be generally considered as a system of sequential checkpoints that recognize aberrant protein domains (Vashist and Ng, 2004). The first checkpoint monitors the cytosolic domains of the membrane proteins and in case of a lesion the protein is degraded without considering the state of other domains. If the protein passes the first checkpoint, it is examined at the second checkpoint which monitors luminal domains and is common to both membrane and soluble proteins. In certain cases, when misfolded proteins manage to escape detection by the ER quality control, they can be sorted out in the Golgi apparatus and are directly transported for degradation into the vacuole (yeast lysosome). Therefore, the Golgi apparatus functions as a distal checkpoint and the pathway is also known as a "Golgi quality control" (Arvan et al., 2002). This pathway can be also used to bypass ERAD under severe ER stress, when ERAD becomes saturated, as an alternative pathway for direct degradation of misfolded proteins. Proteins that escape both the ER and the Golgi control mechanisms and reach the plasma membrane are endocytosed and degraded by vacuolar/lysosomal proteases (Vashist and Ng, 2004).

1.4 Antibodies

Immunoglobulins are proteins of the immune system which represents an essential defense barrier against various pathogens in higher vertebrates. Upon antigen stimulation, immunoglobulins are secreted as soluble molecules in high amounts by plasma cells. According to their structure and function, antibodies can be divided into five classes: IgA, IgD, IgE, IgG and IgM, which differ from each other by the constant region of the heavy chain. In contrast to the five types of heavy chains (α, δ, ε, γ and μ respective for each immunoglobulin class) only two types of light chains can be expressed (κ and λ) which can assemble with every type of heavy chain. Within a given cell, only one allele for a light chain and one allele for a heavy chain are expressed which ensures a single specificity of the produced antibody (Janeway et al., 2008).

The basic structure unit of all immunoglobulins is a four chain structure composed of two identical light chains (LC) and two identical heavy chains (HC).

IgA [$(2HC, 2LC)_n$, n=1,2,3] is the main antibody class present in secretions like saliva, tears and mucus. It represents the first line of defense against diverse viral and bacterial antigens.

IgD (2HC, 2LC) is found in low concentrations in serum, however its role has remained uncertain for a long time. Recently, the function and regulation of IgD was reviewed (Chen and Cerutti, 2011). IgD was suggested to enhance the mucosal immunogenity and to orchestrate the surveillance system at the interface between immunity and inflammation (Chen and Cerutti, 2011; Chen et al., 2009).

IgE (2HC, 2LC) plays a role in the defense against parasitic diseases, but it is also responsible for allergic reactions.

IgG (2HC, 2LC) is divided in four subclasses (IgG1-IgG4) and represents the most prominent antibody class in serum. IgG belongs to the most studied antibody type and it was also used in this work.

IgM $(2LC, 2HC)_5$ is the first antibody made in an immune response after contact with an antigen. Due to its pentameric structure it is very efficient in leading to the lysis of microorganisms as a consequence of binding and activating of the complement.

1.4.1 Structure of IgG

IgG is a "Y"-shaped molecule the structure of which is depicted in figure 8. Every IgG molecule consists of two identical light chains (LC) and two identical heavy chains (HC) which are connected by disulfide bonds. Heavy chains possess three constant domains (C_H1, C_H2 and C_H3) whilst light chains contain only one constant domain (C_L). The sequence of the constant domains is conserved within antibody classes and is responsible for its effector functions (e.g. activation of the complement or recruitment of immune cells). Additionally, the second constant domain (C_H2) contains a conserved asparagine (Asn297) which is covalently N-glycosylated (Deisenhofer, 1981).

At the N-terminus of each chain, there is a variable domain (V_L for a light chain, V_H for a heavy chain) harboring three hypervariable (CDR) regions responsible for the specific binding capacity of the antibody molecule. Together, both variable domains form the antigen binding site. The orientation of the "Y"-arms is flexible due to an unstructured hinge region between C_H1 and C_H2. In the hinge region, IgG can be proteolytically cleaved by papain into three functional fragments (Figure 8). One Fc-fragment (fragment crystallizable) and two Fab-fragments (fragment antigen binding), each consisting of the complete light chain and a Fd-fragment (V_H and C_H1 domains). The Fc-fragment is responsible for effector functions such as antibody-dependent cellular toxicity and complement-dependent cytotoxicity (Jeong et al., 2011).

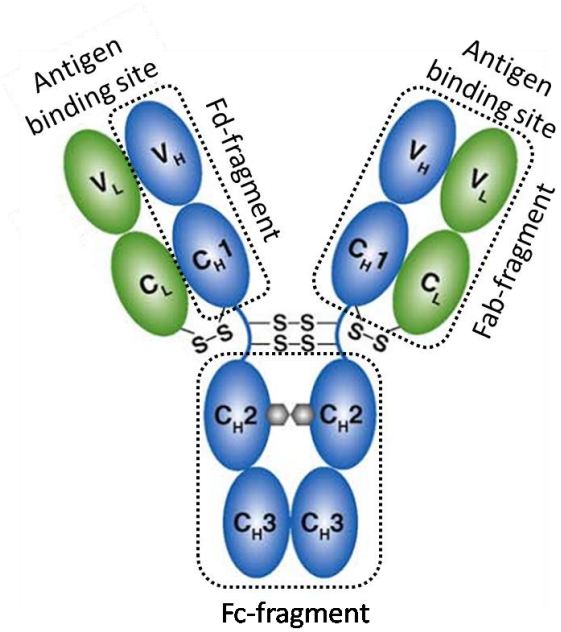

Figure 8: Schematic structure of an IgG molecule, adapted from Feige et al. (2010a). Light chains are depicted in green, heavy chains in blue and sugar moieties are represented by grey hexagons.

All antibody domains are composed of approximately 100 aminoacids and they are characterized by a typical folding motif known as an "immunoglobulin fold". This topology consists of a greek-key β-barrel with two β-sheets forming a sandwich-like structure (Figure 9). Constant domains consist of seven strands (a, b, c, d, e, f, g) and variable domains of nine strands (a, b, c, c´, c´´, d, e, f, g). In most antibody domains, there is a disulfide bridge connecting the strands b and f (Bork et al., 1994). The Ig-fold is one of the most widespread topologies in nature, which gave rise to the immunoglobulin superfamily (Feige et al., 2010a). However, Ig-like domains have been found also in numerous non-immunoglobulin molecules with different functions such as cell surface receptors, growth hormone receptor and diverse enzymes (Bork et al., 1994).

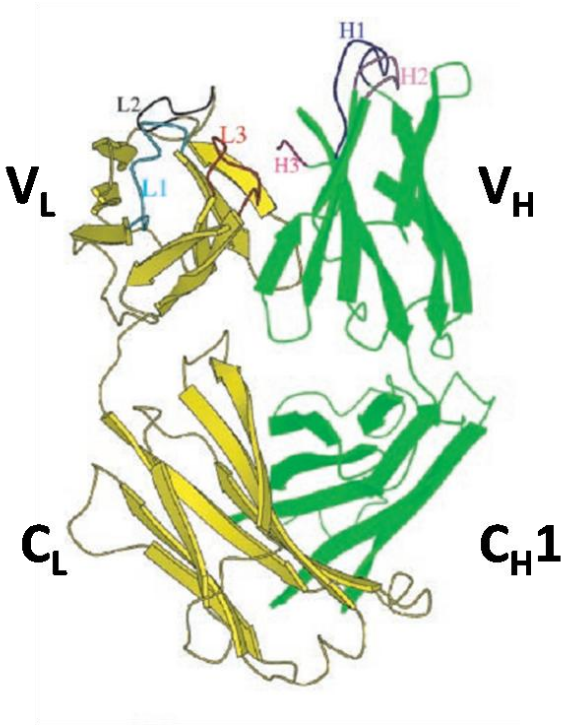

Figure 9: Structure of MAK33 Fab-fragment, adapted from Augustine et al. (2001). Light chain is depicted in yellow, heavy chain in green. Hypervariable regions within both variable domains are highlighted. V_L – variable domain of the light chain, C_L – constant domain of the light chain, V_H – variable domain of the heavy chain, C_H1 – first constant domain of the heavy chain.

1.4.2 Folding of IgG

How antibody molecules fold and assemble was recently reviewed by Feige et al. (2010a). Antibodies fold and assemble in the lumen of the ER. During B cell development, light and heavy chains are synthesized asynchronously (Burrows et al., 1979). Both chains are translocated already during translation into ER where they immediately start to fold even before the translation is finished (Bergman and Kuehl, 1979). In contrast to light chains, which can be secreted alone (Dul et al., 1996; Leitzgen et al., 1997), heavy chains are retained in the ER until they are correctly assembled with the light chain (Mains and Sibley, 1983) or eventually degraded by ERAD.

Most IgG molecules assemble first as heavy chain dimers to which light chains are then attached via a covalent disulfide bond between the C_H1 and C_L domains (Baumal et al., 1971) as shown in (Figure 10). The C_H1 domain is intrinsically disordered (Feige et al., 2009a) and is stable bound to BiP in the absence of a light chain (Hendershot et al., 1987). It was shown that BiP interacts with unassembled Ig intermediates but not with completely assembled anti-

body molecules (Bole et al., 1986). Association of the folded light chain together with the heavy chain induces folding of the C_H1 domain. Afterwards, the assembled IgG molecule is stabilized by a disulfide bond (Figure 10) and can be released from the ER.

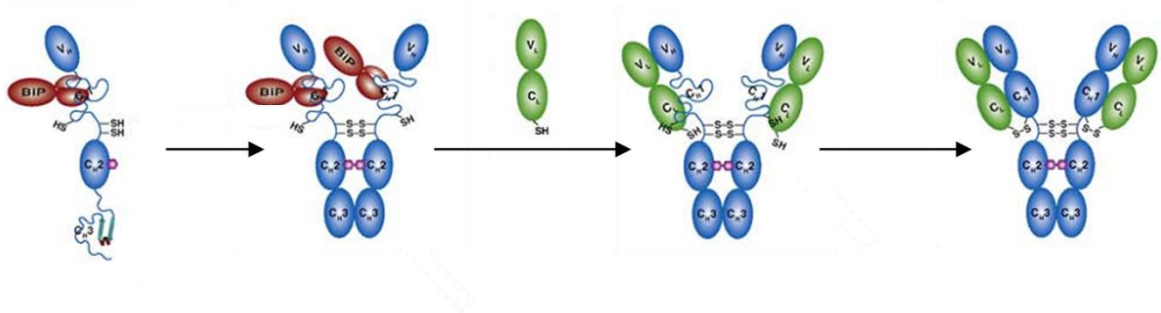

Figure 10: Folding and assembly of an IgG molecule, adapted from Feige et al. (2010a). Folding of the C_H3 domain induces dimerization of the heavy chains that are stabilized by disulfide bonds in the hinge region. The unfolded C_H1 domain remains bound to BiP until the correctly folded light chain is attached and its constant domain induces folding of the C_H1 domain. After the C_H1 domain was folded correctly, HCs and LCs are stabilized via disulfide bonds and the assembled IgG molecule can be secreted.

1.4.3 Production of antibodies

Almost 40 years ago, the monoclonal antibody technology was developed by fusion of myeloma cells with antibody-producing cells (Kohler and Milstein, 1975) which enabled the isolation and production of specific antibodies against a broad range of antigens. With this technology, it became possible to develop methods using antibodies in diagnostics, human therapeutics and of course experimental research. Especially the importance of therapeutic antibodies, enabling potential treatment of inflammatory and infectious diseases as well as cancer has been continuously growing over the years. In 2003, at least ten recombinant antibodies were approved by the US Food and Drug Administration (Joosten et al., 2003), in 2010 there were already 25 monoclonal antibodies in clinical use and more than 250 undergoing clinical trials (Yamada, 2011). Connected with this trend, also sales of antibodies for diagnostic/therapeutic purposes are continuously growing. The sales have risen from about $26 billion in 2006 to over $30 billion in 2008 and the expectation is that in 2012 the sales will reach $56 billion (Jeong et al., 2011).

It should also be mentioned that not only full length-antibodies but also antibody fragments find applications as therapeutics (Nelson and Reichert, 2009). Antibody fragments such

as the Fab-fragment and single-chain variable fragments (scFv fragments) have several advantages compared to full-sized antibodies. Advantages of antibody fragments with respect to clinical applications especially in the treatment of inflammatory diseases and cancer are lower retention times in non-target tissues, more rapid kidney clearance and possible fusion to drugs (Gasser and Mattanovich, 2007). In addition to that, because of their small size they can penetrate better and deeper into tissues and they are also able to pass the blood-brain barrier (Hackel et al., 2006) making them interesting also for the treatment of brain-related diseases. Antibody fragments can also bind to some epitopes which are inaccessible to full-length antibodies due to steric hindrance (Nelson and Reichert, 2009). On the other hand, in contrast to full-size antibodies, antibody fragments lack the Fc-fragment and therefore are not able to activate cellular and humoral effector functions (Gasser and Mattanovich, 2007). Recently, the possible therapeutic use of single domain antibodies derived from heavy chain antibodies from llamas and sharks was discussed as well (Wesolowski et al., 2009).

Besides medicine, antibodies also represent an interesting tool for industry. In the past, there have already been some experimental attempts to make use of antibodies in waste water decontamination (Graham et al., 1995), to add antibodies fused with an enzyme to toothpaste for protection against caries (Frenken et al., 1998) or as an additive in a shampoo as a prevention of hair dandruff (Dolk et al., 2005). However, for industrial applications it is necessary to produce antibodies in large amounts. This is one of the main obstacles together with production costs and low stability of antibodies under harsh conditions (Joosten et al., 2003).

Up to date, many ways of antibody production were described. Currently, antibodies are produced in prokaryotic cells e.g. *E.coli, L. zeae, B. subtilis* as well as in eukaryotic organisms like yeast, insect and mammalian cells, plants and transgenic animals (Schirrmann et al., 2008). Monoclonal therapeutic antibodies are currently produced in mammalian cell cultures, which is connected to very high production costs (300-3000 US$/g (Farid, 2007)). Therefore, microorganisms are more suitable for production of antibodies in high amounts. Antibody production in microorganisms harbors many advantages such as rapid growth on simple inexpensive media, which enables cheap production of large protein amounts. Additionally, microorganisms are easy to handle in terms of genetic modifications and the process time of expression is shorter in comparison to mammalian cell cultures.

1.4.3.1 Antibody production in Escherichia coli

Generally, there are two possible ways how to produce antibody fragments in *E.coli*. The first one is the expression of the desired antibody as inclusion bodies followed by *in vitro* refolding and the second one is the secretion of antibody fragments into the medium or/and periplasmic space. However, despite being an applicable host for antibody expression, *E. coli* is not ideally suited for large-scale production of antibodies. The main reason is the loss of expressed antibody due to e.g. cell lysis in case of secretion of soluble antibodies or during purification steps in the case of antibody expression into inclusion bodies (Better and Horwitz, 1989). Another disadvantage of *E.coli* is that it is not able to perform eukaryotic posttranslational modifications such as glycosylation.

1.4.3.2 Antibody production in yeast

As a microorganism, yeast provides the same advantage as *E.coli*, namely the large scale production of antibodies on cheap media. Yeast can be cultivated to cell densities up to 100 g/l dry biomass (Gasser and Mattanovich, 2007) and it is able of carrying out post-translational modifications. Another aspect which make yeast very interesting from an industrial point of view is that many yeast strains and their products are considered as GRAS ("Generally Regarded As Safe"). In addition to that, yeast secrete only low numbers of endogenous proteins into the medium (Schirrmann et al., 2008) which might facilitate the purification of secreted antibodies.

Currently, the methylotrophic yeast *Pichia pastoris* in combination with the alcohol oxidase (AOX1) promotor is the preferred yeast strain used for antibody production (Jeong et al., 2011). *P. pastoris* is mostly used for the production of antibody fragments (Damasceno et al., 2007; Gasser et al., 2006), allowing to achieve yields up to 300 mg/l of a Fc-fragment by cultivation with extended pre-induction glycerol feeding (Khatri et al., 2011) or ~450 mg/l of a Fab-fragment by fermentation (Ning et al., 2005). Furthermore, a glycoengineered *P. pastoris* strain was also successfully used for the production of a functional, fully assembled IgG1 with a yield of 1 g/l (Potgieter et al., 2009). In addition to that, in *P. pastoris* it is also possible to produce antibodies with human N-glycosylation (Li et al., 2006). A general disadvantage of *P. pastoris* is that products obtained from this yeast do not have the GRAS status (Joosten et al., 2003).

Hansenula polymorpha, another methylotrophic yeast strain, was used for the expression of MAK33, a mouse antibody against human creatine kinase (Abdel-Salam et al., 2001). However, the light chain and the Fd-fragment actually did not assemble into a functional heterodimeric form.

Compared with *P. pastoris*, antibody levels achieved in *S. cerevisiae* are quite low, as summarized e.g. by Gasser and Mattanovich (2007). There are few known cases, where it was possible to obtain antibody fragments from *S. cerevisiae*. In an early study, minor amounts of functional mouse-human chimeric Fab-fragment were obtained from a culture medium (Horwitz et al., 1988). In other studies, expression of an scFv fragment could be achieved by lowering the temperature to 20 °C and co-expression of BiP and PDI (Hackel et al., 2006; Shusta et al., 1998). However, *S. cerevisiae* generally does not seem to be an advantageous host for the expression of scFv-fragments, because of their improper folding and their accumulation in the ER and vacuole. One possible reason for the intracellular accumulation of scFv-fragments might be the exposure of the hydrophobic surfaces of V_H and V_L (Joosten et al., 2003). This theory was supported by the work of Frenken et al. (2000), who studied the expression of a llama V_{HH} antibody fragment. The heavy-chain only antibodies from camelids are devoid of hydrophobic surfaces (Hamers-Casterman et al., 1993) and Frenken et al. (2000) were able to express a llama V_{HH} antibody fragment into a medium of 100 ml *S. cerevisiae* culture to the concentrations 2.5-9.3 mg/ml which would correspond to 100-250 mg/l in a shake flask experiment.

In general, one of the main problems of antibody expression in yeast is the accumulation of (partly) unfolded protein in the ER leading to an overload of secretory pathways and causing intracellular stress. Another problem might be improper folding and assembly of LC-HC dimers (Gasser and Mattanovich, 2007).

1.4.4 Folding helpers dedicated to antibody folding

There are at least twelve mammalian chaperones and other folding helpers such as nucleotide exchange factors, oxidoreductases and peptidyl-prolyl isomerase known so far to be involved in the biosynthesis of antibodies (Feige et al., 2010a). One of these folding helpers is the recently discovered protein pERp1. pERp1 is a small (23 kDa) ER luminal protein involved in immunoglobulin folding. Until now, only three publications about pERp1 have emerged (Flach et al., 2010; Shimizu et al., 2009; van Anken et al., 2009).

pERp1, also known as Mzb1 (Flach et al., 2010), is heavily up-regulated during B cell differentiation and its expression is the highest in lymphocyte-rich tissues such as spleen (van Anken et al., 2009) or thymus (Shimizu et al., 2009). pERp1 shows homology to the human gene MGC29506, that is transcriptionally downregulated during gastric cancer and to a PACAP protein involved in apoptosis.

pERp1 contains six cysteines which are connected by intracellular disulfide bonds (Figure 11B). Four of these cysteines form CXXC and $C(X)_6C$ motifs (Figure 11A). The CXXC motif is a typical active site of thiol oxidoreductases such as PDI, however it was shown that pERp1 posses only very modest oxidoreductase activity (van Anken et al., 2009).

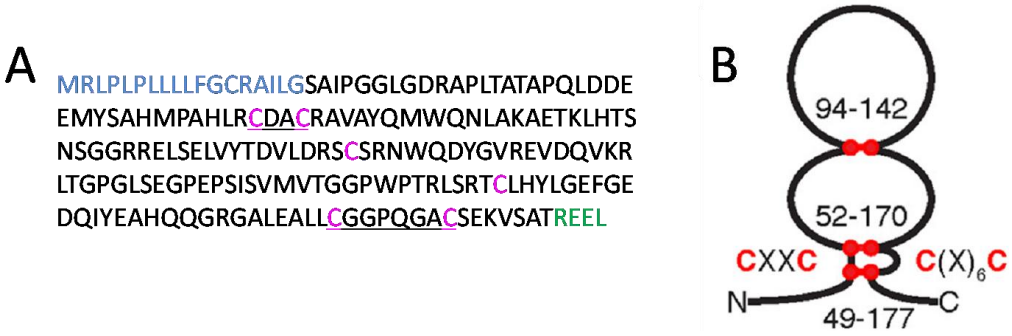

Figure 11: Sequence and structure of pERp1.
A) pERp1 sequence according to Shimizu et al. (2009) and van Anken et al. (2009). The signal sequence is marked in blue, the ER retention signal in green and cysteines in magenta. The CXXC and C(X)6C motifs are underlined.
B) Schematic structure of the native pERp1 as published by van Anken et al. (2009). Cysteines and disulfide bonds are shown in red.

pERp1 was found in a complex with BiP and was identified as a conditional target of the unfolded protein response (Shimizu et al., 2009). pERp1 was shown to promote the oxidation and stability of Ig HC *in vivo* and to stimulate the assembly and secretion of IgM. In conclusion, pERp1 was suggested to be either an unique type of oxidoreductase or to represent a new class of chaperone, which is dedicated to enhancing the oxidative folding of Ig precursors (Shimizu et al., 2009; van Anken et al., 2009).

In another recent publication, pERp1 was found to be abundantly expressed in B1 and marginal zone (MZ) B cells (Flach et al., 2010). B1 and MZ B cells are termed “innate-like” B cells and they differ from conventional (folicullar) B cells in several ways such as cell proliferation and altered calcium signaling (Chumley et al., 2002), fast secretion of antibodies as

a response to lipopolysaschariде (LPS) stimulation and abundant expression of integrins. Integrins are cell-surface receptors that facilitate anchoring of MZ B cells to the marginal zone of the spleen (Lu and Cyster, 2002). The cell adhesion is regulated by three different integrin conformation states, from the low–affinity bent conformation to the more affine extended-closed conformation and finally to the extended-open conformation with the highest ligand affinity (Luo et al., 2007). It was proposed, that one of the genes important for these special characteristic of the innate-like B cells is *Mzb1*. Mzb1, also known as pERp1, modulates the calcium store in the ER, decreases Ca^{2+} mobilization and thus regulates Ca^{2+} signaling (Flach et al., 2010). In addition to that, pERp1 promotes integrin-mediated adhesion and antibody secretion in LPS-stimulated cells (Flach et al., 2010). pERp1 was found to associate with chaperones BiP and Grp94 as well as with thiol oxidoreductases ERp57 and PDIA6 (CaBP1). It was suggested that pERp1 associates with Grp94, BiP and ERp57 in a calcium-dependent manner and that the interaction of ERp57 and pERp1 results in an exchange of calnexin and calreticulin (Flach et al., 2010).

Finally, it should be mentioned that the function of pERp1 was found to be independent of the CXXC motif (Shimizu et al., 2009; van Anken et al., 2009). However, until now nothing has been known about pERp1´s oligomeric state and secondary structure as well as about the influence of its six cysteines on the structure and stability which are topics addressed in this work.

1.5 Aim of this work

Yeast would be a very suitable host for antibody production. However, antibody expression in yeast, especially in *S. cerevisiae*, is so far connected with several hindrances, e.g. intracellular retention of expressed antibodies or their improper folding and assembly into functional molecules (Gasser and Mattanovich, 2007).

In this work, we wanted to establish an expression system for antibody fragments in *S. cerevisiae* which could be used as a model for future detailed studies of bottlenecks along the expression and secretory pathway. We decided to use MAK33, a mouse IgG against creatine kinase from human heart muscle, as a model antibody because MAK33 has been well studied over the past years and a lot is known about its structure and stability. See, e.g., Feige et al. (2009a), Feige et al. (2007), Feige et al. (2009b), Feige et al. (2010b), Simpson et al. (2009), Vinci et al. (2004).

One of the possible problems causing the accumulation of the expressed antibody fragments within the yeast cells might be the lack of some chaperones known to assist antibody folding in mammalian cells. One of these chaperones is the recently identified ER-resident protein pERp1 found in B cells (Flach et al., 2010; Shimizu et al., 2009; van Anken et al., 2009). pERp1 was shown to promote antibody folding, assembly and secretion *in vivo*. However, so far nothing has been known about its structure and stability. In this work, we wanted to analyze pERp1 *in vitro*, focusing especially on its oligomeric state, its secondary structure as well as on the effects of its six cysteines with respect to structure and stability.

2 Results

2.1 Expression of antibodies in yeast

2.1.1 Cloning and expression of MAK33 antibody fragments

2.1.1.1 Cloning of MAK33 antibody fragments

In order to study the expression of antibody fragments in yeast, several constructs of MAK33 light chain and Fd-fragment were cloned. Yeast codon-optimized sequences of MAK33 light chain (LC) and Fd-fragment were excised from a pMA-T vector and cloned into different pRS vectors. Every construct was designed in the same way with an N-terminal affinity tag and an invertase signal sequence which targets the endoplasmatic reticulum (Figure 12). Amino acid sequences of the respective antibody fragments are shown in figure 13.

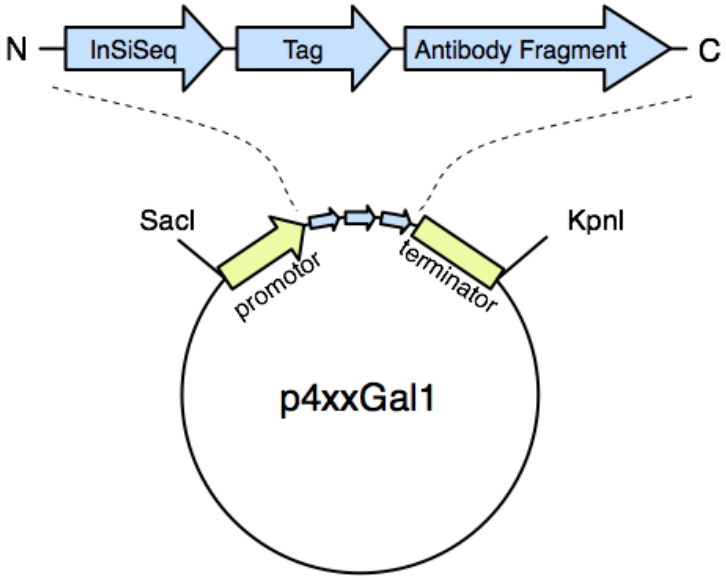

Figure 12: Schematic figure of MAK-33 expression constructs for yeast.
InSiSeq – invertase signal sequence.

Flag-Fd-fragment

MLLQAFLFLLAGFAAKISAS↓M**DYKDDDDK**EVQGVESGGGLVKPGGSLKLSCAASGFTF
SDYYMYWVRQTPEKRLEWVATISDGGSYTYYPDSVKGRFTISRDNAKNNLYLQMSSLKS
EDTAMYYCARDKAYYGNYGDAMDYWGQGTSVTVSSAKTTPPSVYPLAPGSAAQTNSMVT
LGCLVKGYFPEPVTVTWNSGSLSSGVHTFPAVLQSDLYTLSSSVTVPSSTWPSETVTCN
VAHPASSTKVDKKIVPRDCG

HA-light chain

MLLQAFLFLLAGFAAKISAS↓M**YPYDVPDYA**DIVLTQSPATLSVTPGDSVSLSCRASQS
ISNNLHWYQQKSHESPRLLIKYASQSISGIPSRFSGSGSGTDFTLSINSVETEDFGMYF
CQQSNSWPLTFGAGTKLELKRADAAPTVSIFPPSSEQLTSGGASVVCFLNNFYPKDINV
KWKIDGSERQNGVLNSWTDQDSKDSTYSMSSTLTLTKDEYERHNSYTCEATHKTSTSPI
VKSFNRNEC

Figure 13: Amino acid sequence of the respective MAK33 antibody fragments. Affinity tags are highlighted in bold, the invertase signal sequence is underlined. The cleavage site of the invertase signal sequence is marked with a magenta arrow.

Saccharomyces cerevisiae cells (strain BY4741) were transformed with several different plasmids (Table 2). In total, six yeast cultures producing MAK33 fragments under a galactose promotor were created: two cultures expressing the HA-light chain only (in a single-copy CEN and a multi-copy 2µ vector), two cultures expressing the Flag-Fd-fragment only (in a single-copy CEN and a multi-copy 2µ vector) and two cultures expressing the Fab-Fragment. For this, cells were co-transformed with HA-LC and Flag-Fd-fragment both in CEN vectors or both in 2µ vectors respectively.

Construct	Antibody fragment	Plasmid (origin)	Selection marker	Restriction enzymes	Affinity tag
Light chain (single copy)	MAK33 light chain	p416Gal1 (CEN)	Ampicillin, URA	XbaI/XhoI	N-HA
Fd-fragment (single copy)	MAK33 Fd-fragment	p413Gal1 (CEN)	Ampicillin, HIS	XbaI/XhoI	N-Flag
Fab-fragment (single copy)	MAK33 light chain, MAK33 Fd-fragment	p416Gal1 (CEN), p413Gal1 (CEN)	Ampicillin, URA, HIS	XbaI/XhoI	N-HA, N-Flag
Light chain (multi copy)	MAK33 light chain	p426Gal1 (2µ)	Ampicillin, URA	BamHI/HindIII	N-HA
Fd-fragment (multi copy)	MAK33 Fd-fragment	p423Gal1 (2µ)	Ampicillin, HIS	BamHI/XhoI	N-Flag
Fab-fragment (multi copy)	MAK33 light chain, MAK33 Fd-fragment	p426Gal1 (2µ), p423Gal1 (2µ)	Ampicillin, URA, HIS	BamHI/HindIII, BamHI/XhoI	N-HA, N-Flag

Table 2: *S. cerevisiae* cultures expressing different antibody fragments.

2.1.1.2 Growth of antibody expressing yeast cultures

After the transformation, the growth of each *S. cerevisiae* culture in a liquid minimal medium was examined. For this, 1 ml of a fresh over-night culture was inoculated into 100 ml of the corresponding medium and was cultivated at 30 °C upon orbital shaking. All cell cultures grew well until the stationary phase was reached. However, cells which were transformed with expression vectors were growing slower and they also reached lower OD_{600} values in the stationary phase compared to the wild type (Figure 14). This was the case not only for cells which were transformed with vectors containing antibody fragments but also for cells transformed with empty plasmids. This means that the worse growth of the transformed cultures compared to the wild type is not caused by antibody expression itself but it is rather an effect caused by the vectors in general.

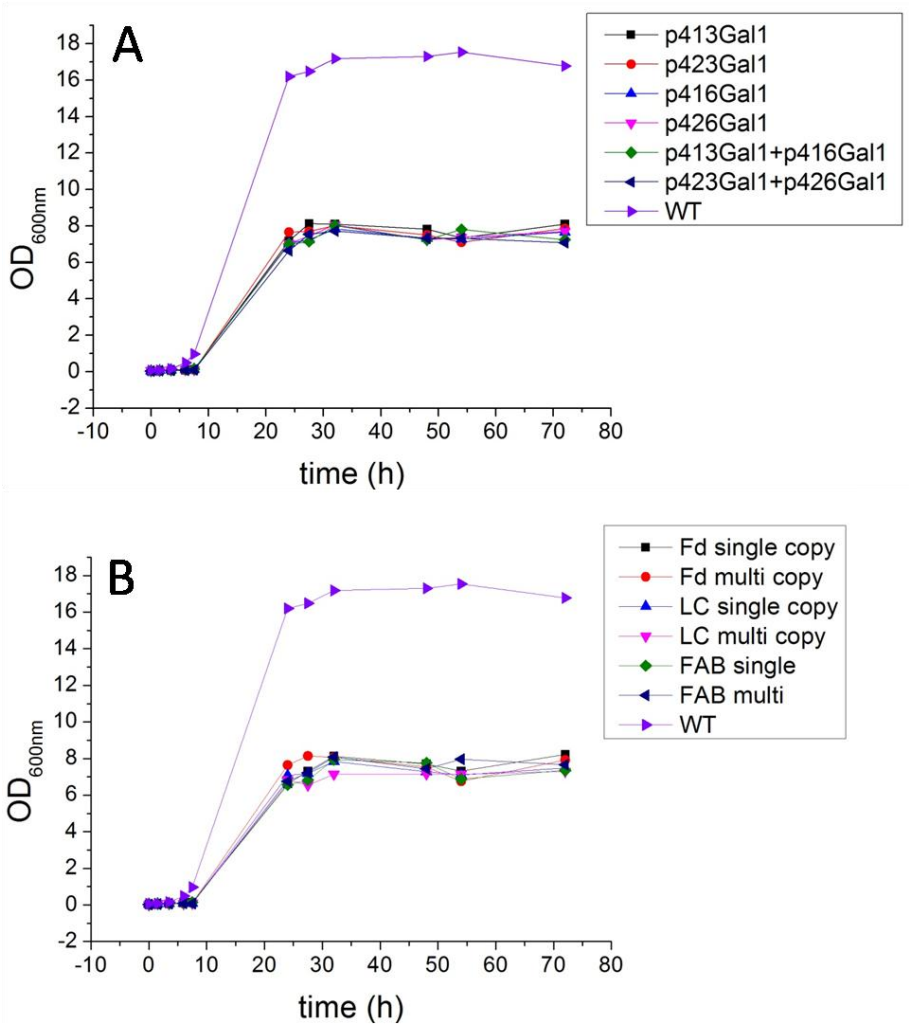

Figure 14: Growth kinetics of antibody-expressing yeast cultures in glucose medium.
A) Cells transformed with empty plasmids.
B) Cells transformed with plasmids containing different antibody fragments.
Fd single copy – Fd-fragment in p413Gal1 plasmid, Fd multi copy – Fd-fragment in p423Gal1 plasmid, LC single copy – light chain in p416Gal1 plasmid, LC multi copy – light chain in p426Gal1 plasmid, FAB single – Fd-fragment in p413Gal1 plasmid co-transformed with light chain in p416Gal1 plasmid, FAB multi – Fd-fragment in p423Gal1 plasmid co-transformed with light chain in p426Gal1 plasmid, WT – wild type (strain BY4147 MATa).

To be sure that the yeast cells are able to cope with antibody expression, the general "fitness" of the cultures expressing antibody fragments was also checked. For this, samples of yeast cells expressing different MAK33 fragments in different media were prepared according to section 4.4.4 and investigated with scanning electron microscopy (Figure 15). The expression of antibody fragments does not seem to have any visible harmful effect on the yeast cells, because no difference could be found between the induced and non-induced cells.

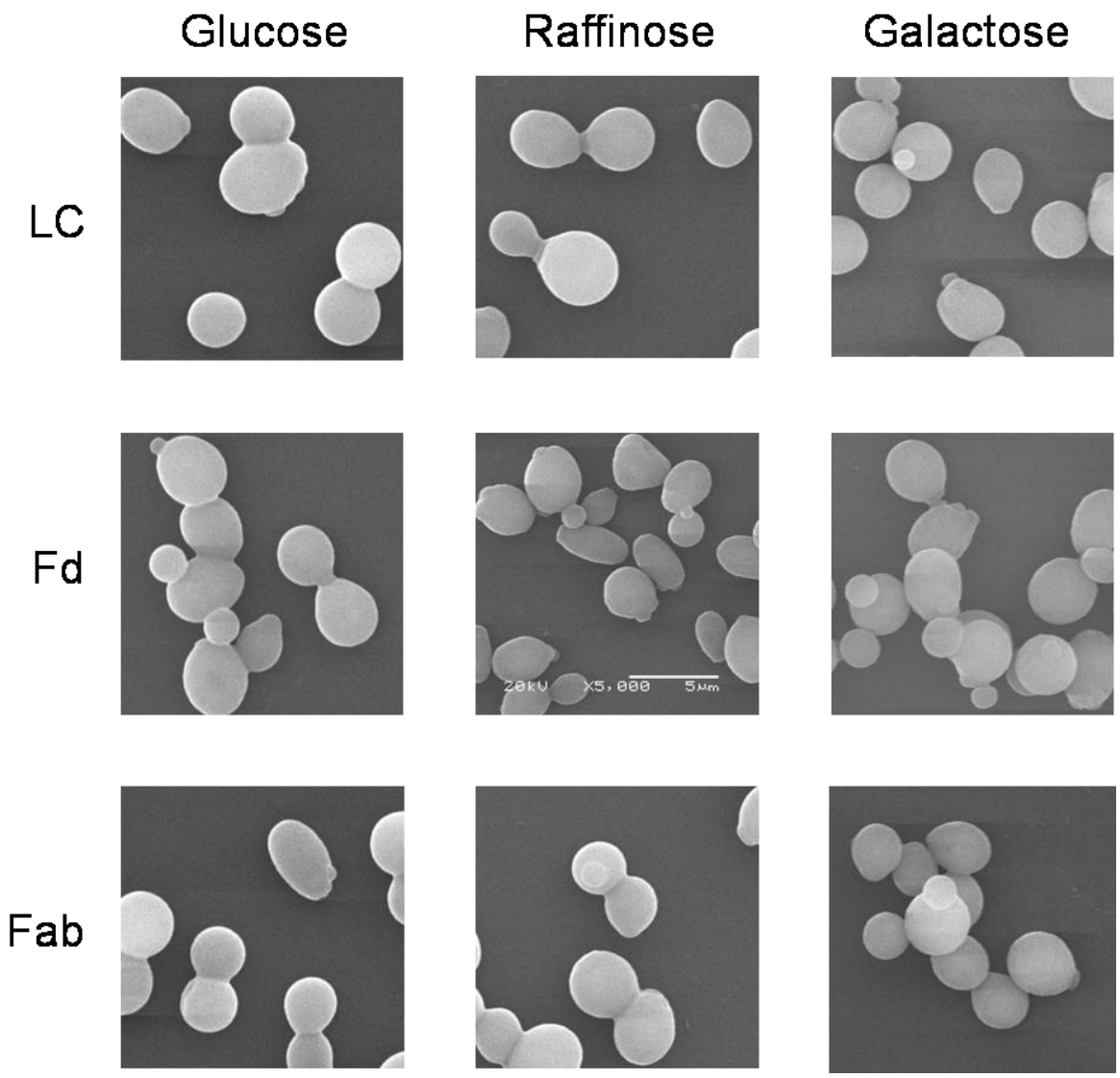

Figure 15: Scanning electron microscopy pictures of yeast cells expressing different MAK33 antibody fragments in CEN plasmids in different media.
LC – MAK33 light chain, Fd – MAK33 Fd-fragment, Fab – MAK33 Fab-fragment, Glucose – glucose medium, Raffinose – raffinose medium, Galactose – galactose medium.

2.1.1.3 Expression of antibody fragments

The expression of the antibody fragments was performed as depicted in the scheme in figure 16. Precultures of *S. cerevisiae* were cultivated in a glucose minimal medium at 30 °C over night. Subsequently, 100 ml of a glucose minimal medium was inoculated from the preculture and incubated at 30 °C. After transferring the cells into a raffinose minimal medium, the cultures were incubated further at room temperature (section 4.5.2). Induction with galactose was performed at room temperature as well, because it is known from the literature that

during antibody expression in yeast better yields could be achieved by lowering the cultivation temperature (Hackel et al., 2006; Potgieter et al., 2009). Samples were taken during the growth of each culture and cell pellets were stored (see section 4.5.2). Subsequently, cells were diluted to the same OD_{600}, (typically to OD_{600} 30, or 15-20 respectively), lysed and pull-downs were performed to analyze the expression of different antibody fragments.

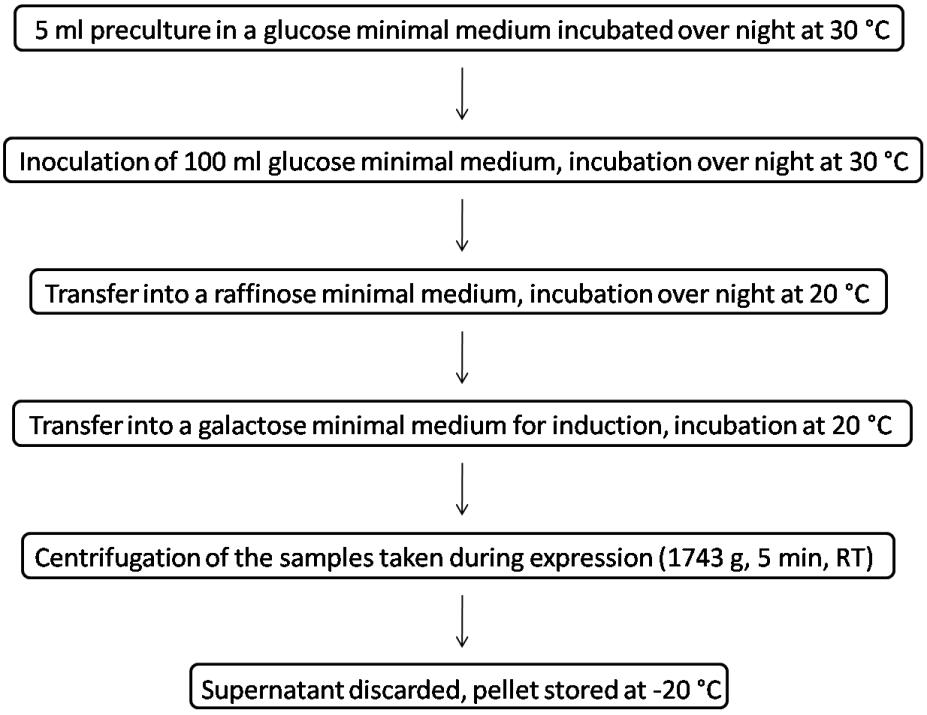

Figure 16: Scheme of the expression of MAK33 antibody fragments in *S. cerevisiae*.
RT – room temperature.

2.1.2 Pull-downs of antibody fragments

Depending on the respective experiments, pull-downs were performed in two different ways: either from a fractionated lysate or directly from a clear lysate as shown in figure 17 and described in detail in section 4.5.3. Briefly, for a pull-down from a clear lysate, cells were centrifuged at 1743 g, 8 °C for 15 min, the pellet was discarded and the pull-down was performed from the clear supernatant. After the elution from beads, the sample was labeled as a "clear lysate".

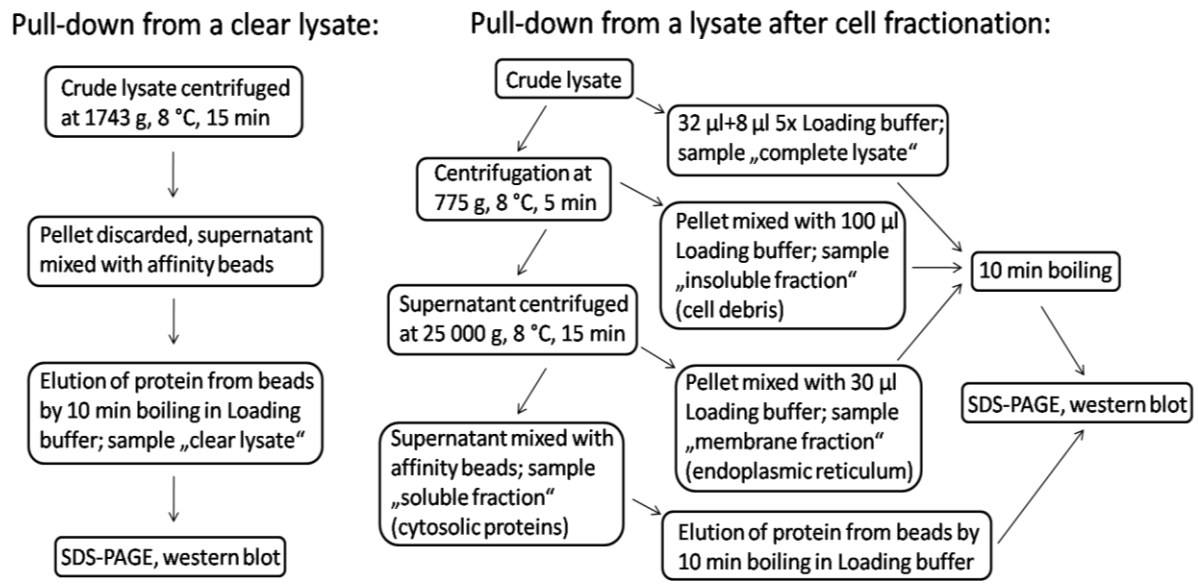

Figure 17: Scheme of different pull-down procedures from lysates of yeast cells expressing antibody fragments. Expected content of the respective samples obtained during the pull-down procedure from the lysate after fractionation is given in brackets.

For a pull-down after cell fractionation, a sample from the crude lysate was taken and labeled as a “complete lysate”. Subsequently, cells were centrifuged at 775 g, 8 °C for 5 min and the pellet which contained cell debris was resuspended in Loading buffer. This represents the “insoluble fraction”. The supernatant was centrifuged further (25 000 g, 8 °C, 15 min) and the pellet was resuspended in Loading buffer and labeled “membrane fraction”. The membrane fraction should contain endoplasmatic reticulum, peroxisomes and parts of Golgi membranes according to Spector et al. (1998). A pull-down was performed from the supernatant and after the elution form the beads, the sample was labeled as “soluble fraction”. All samples in Loading buffer were boiled and subsequently, SDS-PAGE and western blot analysis were performed (section 4.5.4).

Loading buffer contains SDS, but in contrast to reducing Loading buffer, it does not contain 2-mercaptoethanol (section 4.4.1.1). In this work, all samples of MAK33 antibody fragments loaded on the SDS gels were in Loading buffer. Loading buffer without 2-mercaptoethanol was used in order not to disturb the disulfide bond between the LC and the Fd-fragment within the Fab-fragment (Figure 18).

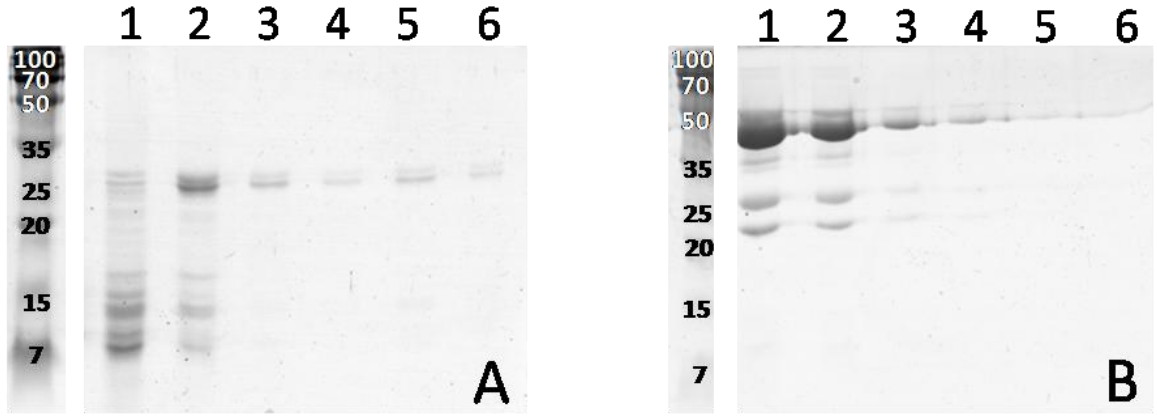

Figure 18: SDS gel of MAK33 Fab-fragment standard (Roche, Mannheim, Germany).
A) Fab-fragment in presence of 2-mercaptoethanol (in reducing Loading buffer).
B) Fab-fragment without 2-mercaptoethanol (in Loading buffer). 2-mercaptoethanol reduces the Fab-fragment (the band at ~50 kDa in figure B) to the LC and the Fd-fragment (the double band at ~27 kDa in figure A).
1-6 – numbers of the respective lanes corresponding to the following amounts of the Fab-Fragment: 1 – 10 µg, 2 – 5 µg, 3 – 1 µg, 4 – 0.5 µg, 5 – 0.1 µg, 6 – 50 ng.

In figure 18, Fab-fragment of different concentrations in either reducing Loading buffer or in Loading buffer was loaded to SDS-gels and SDS-PAGE was performed. In the presence of 2-mercaptoethanol (reducing Loading buffer), the Fab-fragment is reduced to the LC and the Fd-fragment (visible as a double band at ~27 kDa in figure 18A). Without 2-mercaptoethanol, the Fab-fragment remains intact (visible as a band at ~50 kDa in figure 18B).

2.1.3 Kar2 as an ER marker

It is known from the literature that antibodies accumulate in the ER during expression in yeast (e.g Gasser et al, 2006; Kauffman et al, 2002; Abdel-Salam, 2001). Therefore, the membrane fraction was tested on the presence of Kar2 in order to prove the presence of the ER. WT yeast cells were grown in YPD medium, samples of OD_{600} = 50 were lysed and the lysate was fractionated according to the protocol procedure summarized in figure 17. Subsequently, SDS-PAGE and western blot were performed (sections 4.4.1.2 and 4.4.1.3). After blocking of the membrane with 5% milk in PBS buffer, the membrane was detected with α-Kar2 antibody (produced in rabbit) and subsequently with secondary α-rabbit antibody conjugated with peroxidase.

In figure 19, samples of the complete lysate, the cytosolic and the membrane fraction detected with α-Kar2 antibody are shown. Kar2 (78 kDa) was predominantly detected in the membrane fraction. However, a small band corresponding to Kar2 was visible also in the cytosolic fraction. This means that the membrane fraction is either not completely separated from the soluble fraction or that a part of the ER brakes upon cell lysis with the glass beads and its content is released into the cytosolic fraction.

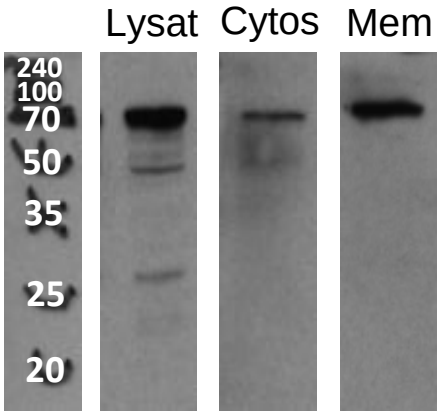

Figure 19: Western blot of the samples of the complete and fractionated lysate of *S. cerevisiae* WT cells detected with α-Kar2 antibody.
Lysat – sample of the complete lysate, Cytos – sample of the cytosolic fraction, Mem – sample of the membrane fraction

To investigate these options, WT cells were grown again in YPD medium. Afterwards, they were diluted to several different OD_{600} values with either usual cell lysis buffer or 1% Triton X-100 was added to the buffer to solubilize the membranes. Indeed, as shown in figure 20, upon Triton X-100 treatment the intensity of the Kar2 bands in the membrane fraction diminished or, in samples with lower OD_{600} values (OD_{600} = 1-10), the corresponding bands disappeared completely. In contrast, the intensity of the bands in the cytosolic fraction was not influenced by Triton X-100. The fact, that only the membrane, but not the cytosolic fraction, were influenced by Triton X-100 means that the ER is present only in the membrane fraction. Therefore, Kar2 bands detected in the cytosolic fraction are presumably a contamination from the ER which might had been damaged during the cell disruption rather than a signal coming from the intact ER which was not separated properly from the cytosolic fraction.

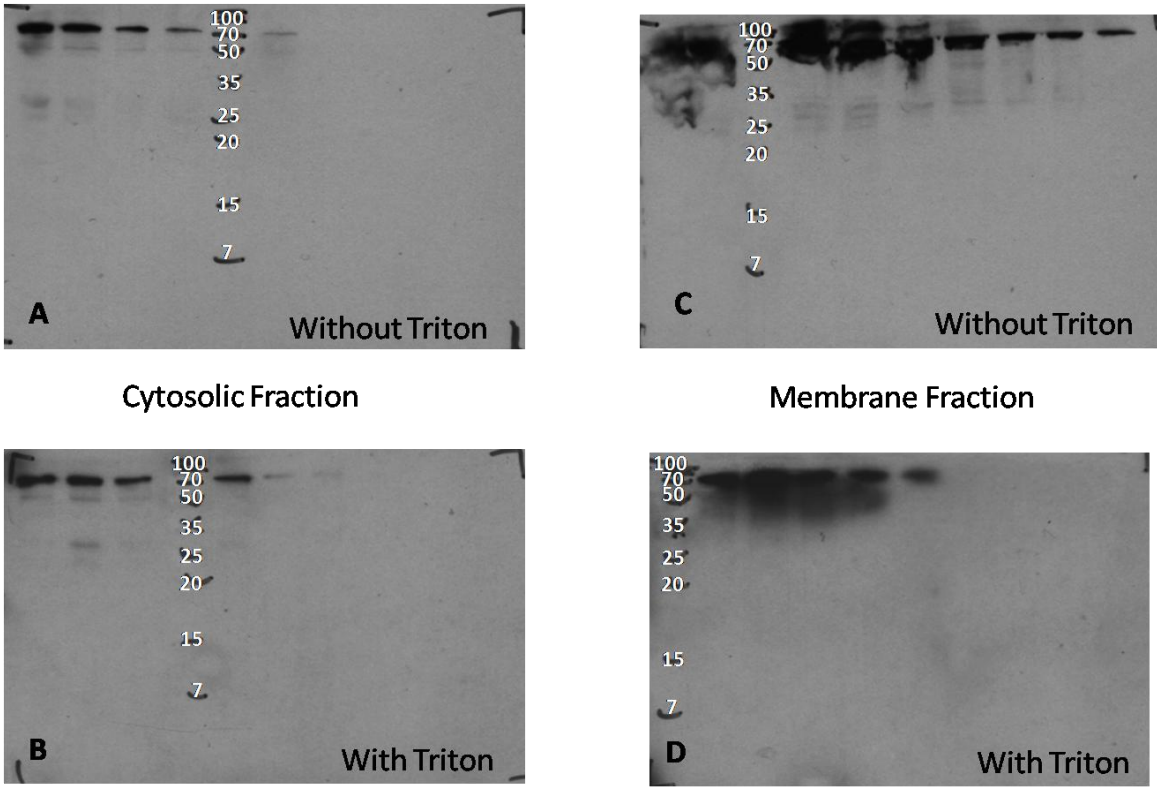

Figure 20: Western blots of the samples of the membrane and cytosolic fraction from *S. cerevisiae* WT cells detected with α-Kar2 antibody
A) Cytosolic fraction without Triton X-100 in the buffer.
B) Cytosolic fraction with Triton X-100 in the buffer.
C) Membrane fraction without Triton X-100 in the buffer.
D) Membrane fraction with Triton X-100 in the buffer.
Triton X-100 solubilizes membranes, therefore the intensity of the Kar2 bands in the membrane fraction is diminished in the presence of Triton X-100. The bands correspond to samples with OD_{600} values (60, 50, 40, 30, 20, 10, 5, 2.5, 1 from left to right).

2.1.4 Antibody expression from single-copy constructs (CEN plasmids)

Transformation with CEN plasmids results in one copy of a CEN plasmid per cell. This is advantageous especially for the co-expression of a light chain and Fd-fragment in one culture, because then the 1:1 ratio of both fragments in every cell is assured.

MAK33 HA-light chain and Flag-Fd-fragment were expressed from CEN plasmids as described in section 4.5.2. Samples were diluted to OD_{600} = 30 and pull-downs from the clear lysate were performed. After SDS-PAGE, samples were western blotted and detected with α-HA antibody for the LC and α-Flag antibody for the Fd-fragment. A signal could be detected only on the western blot of the LC (Figure 21).

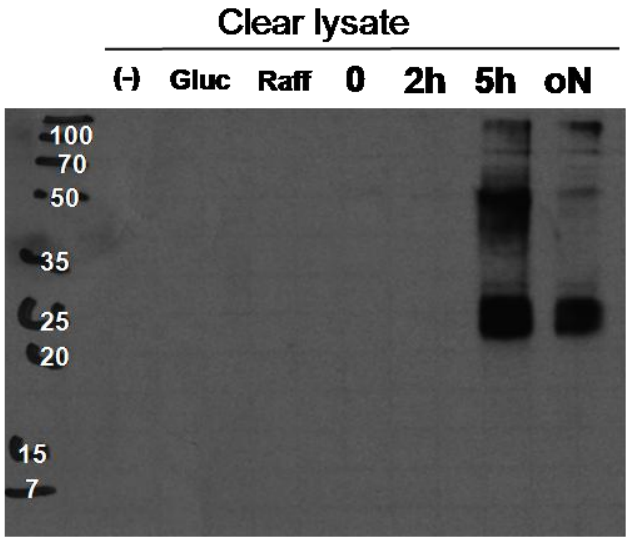

Figure 21: Pull-down from clear lysate and western blot of MAK33 HA-light chain (26.8 kDa).
(-) – negative control (buffer alone), Gluc – sample of *S. cerevisiae* grown in glucose medium, Raff – sample of *S. cerevisiae* grown in raffinose medium, 0-oN – samples of *S. cerevisiae* at different times after induction with galactose (0 – immediately after induction, 2h – 2 hours after induction, 5h – 5 hours after induction, oN – over night induction).

Because of the more complicated detection, the Fd-fragment was expressed alone and samples were diluted to higher OD (OD_{600} = 50) for more contrast. Besides the Fd-fragment, also the Fab-fragment was expressed and pull-downs with both α-Flag and α-HA beads from the clear lysate were performed. To prove the presence of the Fd-fragment, a cross-detection was performed, in which the samples from each type of beads were detected by both α-Flag and α-HA antibody. This should provide an evidence for the Fd-fragment because, for instance in the case of α-HA pull-down and α-Flag detection, there should be a signal for the Fab-fragment but not for the Fd-fragment. This and the other three cases of the cross-detection are for simplicity shown in figure 22. Corresponding to this scheme, four western blots are shown in figure 23.

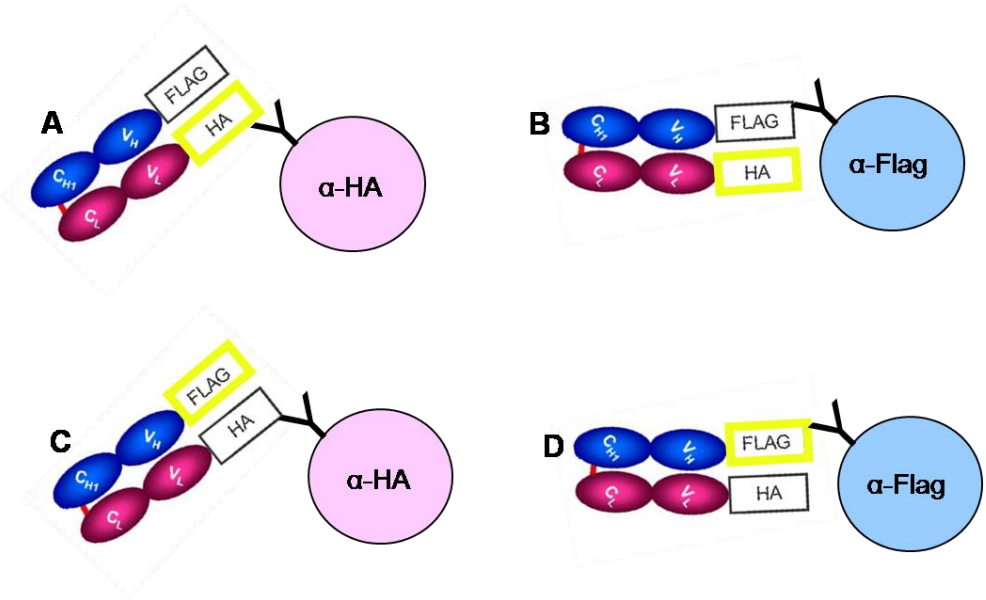

Figure 22: Scheme of the pull-downs and detections corresponding to figure 23.
Pale pink circles – α-HA affinity beads, pale blue circles – α-Flag affinity beads.
The Fab-Fragment consists of a light chain (dark pink) and an Fd-fragment (dark blue), connected together with an intermolecular disulfide bond (red). HA-tag and Flag-tag are represented by rectangles connected with the variable domains. For each case (A-D), one of the two rectangles is highlighted in yellow representing the tag detected in the western blot.

For the western blots A and B, the α-HA antibody was used for detection whereas the α-Flag antibody was used for detection of the western blots C and D. Samples on the western blots A and C were both pulled with α-HA beads, on western blots B and D with α-Flag beads. The results are as one would expect for the Fd-fragment and the Fab-fragment. On the western blots A and B, there are no bands for the Flag-Fd-fragment alone, because the detection was performed with α-HA antibody against HA-LC. However, there are quite strong bands for the Fab-fragment on both western blots A and B. On western blot A, the HA-LC was both pulled and detected, but on western blot B, the Flag-Fd-fragment was pulled and HA-LC detected, which actually proves the presence of both antibody fragments in a complex.

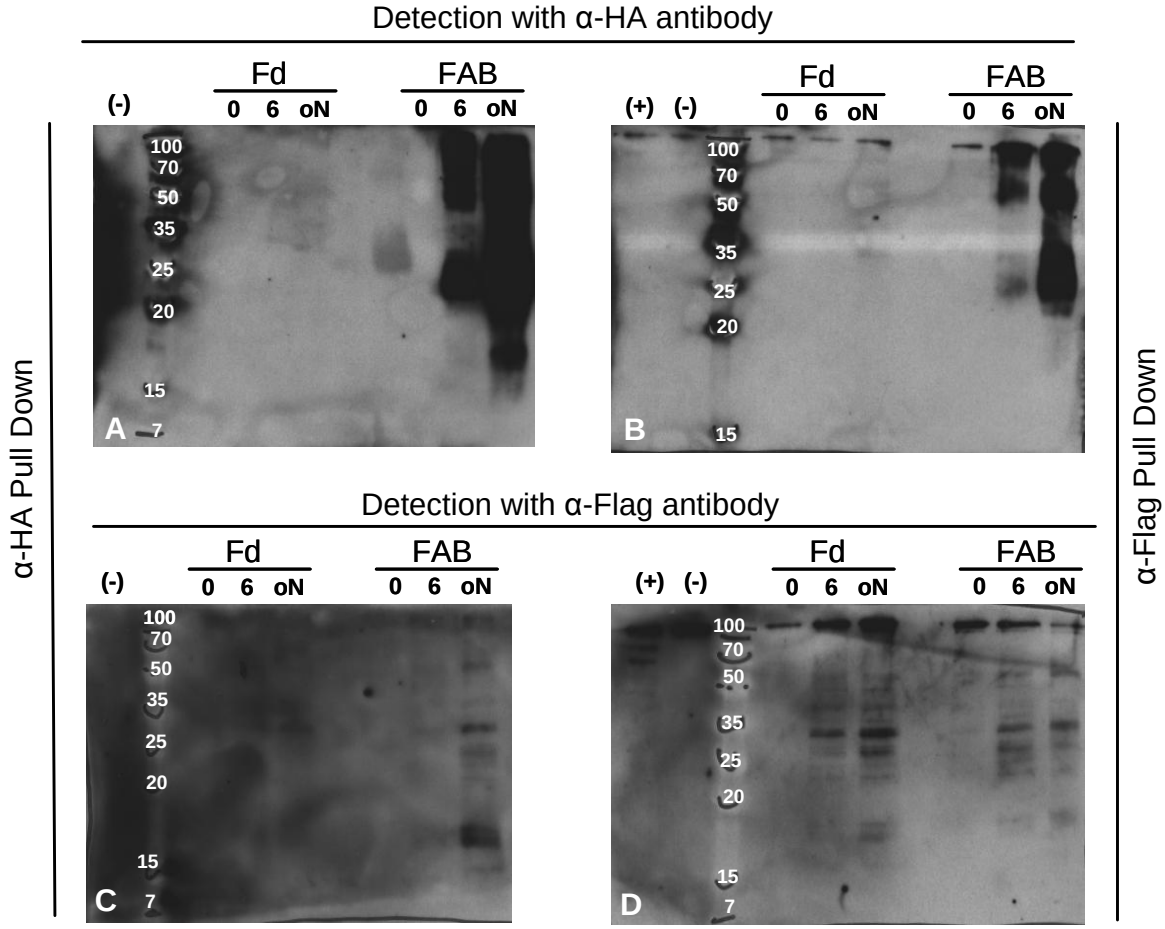

Figure 23: Pull-downs and western blots of MAK33 fragments from the clear lysate.
A) Pull-down with α-HA beads (against LC), detection with α-HA antibody (against LC).
B) Pull-down with α-Flag beads (against Fd-fragment), detection with α-HA antibody (against LC).
C) Pull-down with α-HA beads (against LC), detection with α-Flag antibody (against Fd-fragment).
D) Pull-down with α-Flag beads (against Fd-fragment), detection with α-Flag antibody (against Fd-fragment).
0 – sample taken immediately after induction with galactose , 6 – sample 6 hours after induction, oN – sample after induction over night.

The presence of both antibody fragments is shown also on the western blots C and D, where bands for the Fab-fragment could be detected. On western blot C, there are again no bands for the Flag-Fd-fragment alone, because the pull-down was performed with α-HA antibody against HA-LC. On western blot D, there are also bands from the Fd-fragment alone visible. In addition to that, on western blot D there are two bands in the area corresponding to the Fd-fragment which differ from each other by approximately a quarter of the distance of 10 kDa between the respective bands of the marker. This might be a hint on a processed and non

processed version of the Fd-fragment, because the cleavage of the invertase signal sequence (~2.3 kDa) would result in this difference in the molecular weight. Furthermore, for samples of the Fab-fragment, there are also bands at the height corresponding to the assembled Fab-fragment (54.3 kDa) on every western blot on the figure 23.

It should be noted that the detection with the α-HA antibody in general gives a much stronger signal compared to the detection with the α-Flag antibody.

2.1.5 Multi-copy constructs (2µ plasmids)

Since the detected signal on the western blots of antibody fragments expressed from the single-copy CEN plasmids was quite weak, even at OD_{600} = 50, both MAK33 HA-LC and Flag-Fd-fragment were also expressed from the multi-copy 2µ plasmids. During the expression from 2µ plasmids, the 1:1 ratio of both antibody fragments per cell might be destroyed, but, on the other hand, the detected signal should be stronger. To follow the expression of MAK33 fragments more precisely, the lysate was fractionated into the membrane and soluble fractions (section 4.5.3.2). In this way, it should be possible to localize the bottleneck of the antibody expression in yeast cells and also to distinguish between the processed and non-processed versions of the respective fragments.

First, the expression of MAK33 LC was tested. The expression of the HA-LC in 2µ plasmids (Figure 24) revealed a much stronger signal than the expression from the CEN plasmid (Figure 21). As shown in figure 24A, the expression of the light chain (26.8 kDa) can be followed nicely even in a small sample of the complete lysate. The second strong band could come from light chain dimers (53.6 kDa) and the signal at higher molecular weight could result from higher oligomers and aggregates.

In figure 24B, samples of the soluble fractions and the membrane fractions containing the ER were blotted next to each other. There are several bands visible in the membrane fraction already at time zero. The time span between the induction and freezing of the sample (i. e. transferring the yeast culture into the galactose medium, measuring the OD_{600}, taking out the sample, centrifugation and freezing of the pellet) is approximately 10-20 min. Therefore, it might be possible that the expression of the light chain is already detectible in the first sample taken immediately after induction (at time zero). The expression of the LC is clearly visible as the bands corresponding to the molecular mass of the light chain are getting more intensive. Dimers of the LC are formed again, which can be followed in the membrane fraction after 2

and 4 hours after expression. In addition to that, the double band on the position corresponding to the monomeric LC could represent the processed and non processed version of the LC (white arrows). The band of the non processed form of the LC is located higher than the band of the processed LC. After 4 h expression, bands corresponding to the LC are detectible also in the soluble fraction. In general, the data from figure 24B suggests that the LC is retained in the membrane fraction which corresponds to the literature, as summarized, e.g., by Gasser and Mattanovich (2007) and Joosten et al. (2003).

Although the data suggested that the LC is accumulated within the ER, its secretion into the medium was tested as well. For this, the LC was expressed in 50 ml galactose medium over night. Cells were spun down and proteins were precipitated from the medium with trichloroacetic acid (section 4.5.5). The pellets were resuspended in 100 µl Tris/Loading buffer and loaded on a SDS-gel. Subsequently, SDS-PAGE and western blot were performed (sections 4.4.1.2 and 4.4.1.3). However, no signal could be detected on the western blot (data not shown) which suggests, that no LC was secreted into the medium.

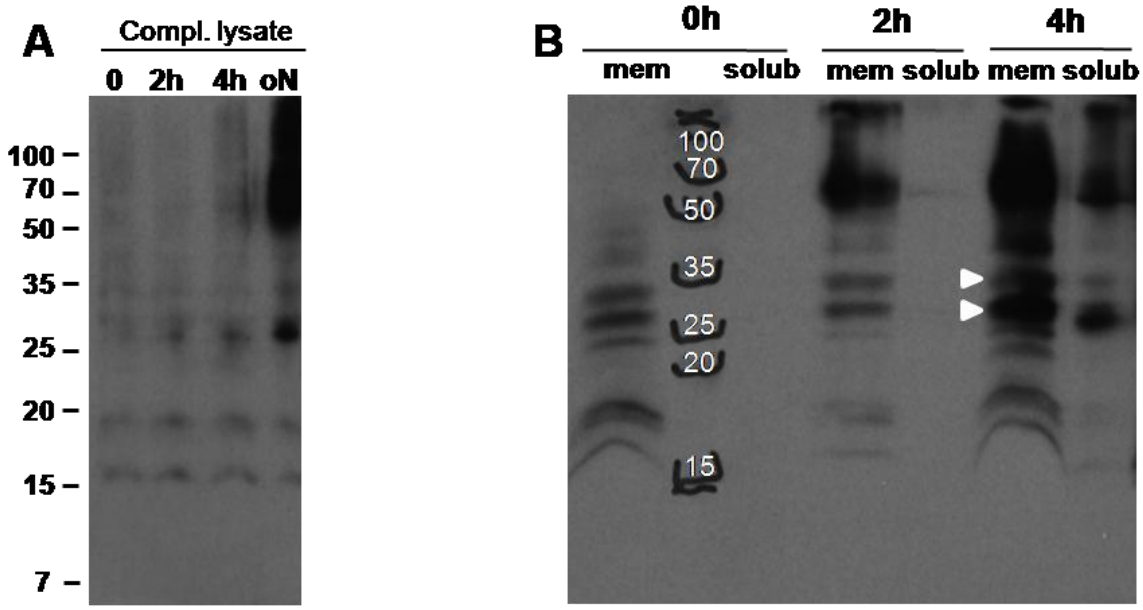

Figure 24: Western blots of MAK33 light chain expressed from 2µ plasmids.
A) Complete lysate.
B) Membrane fractions (mem) and soluble fractions (solub).
0h – immediately after the induction with galactose, 2h-4h – samples 2 hours and 4 hours after induction. White arrows represent the possible processed and non-processed version of the light chain.

Subsequently, the same procedure as for the LC was repeated with the Fab-fragment (Figure 25). The Fab-fragment was expressed from 2µ plasmid (4.5.2) and the cell lysate was fractionated (section 4.5.3.2). The western blots of the samples from complete lysate and membrane fraction detected with α-HA antibody are shown in figure 25A and B, detection with α-Flag antibody is shown in figure 25C and D.

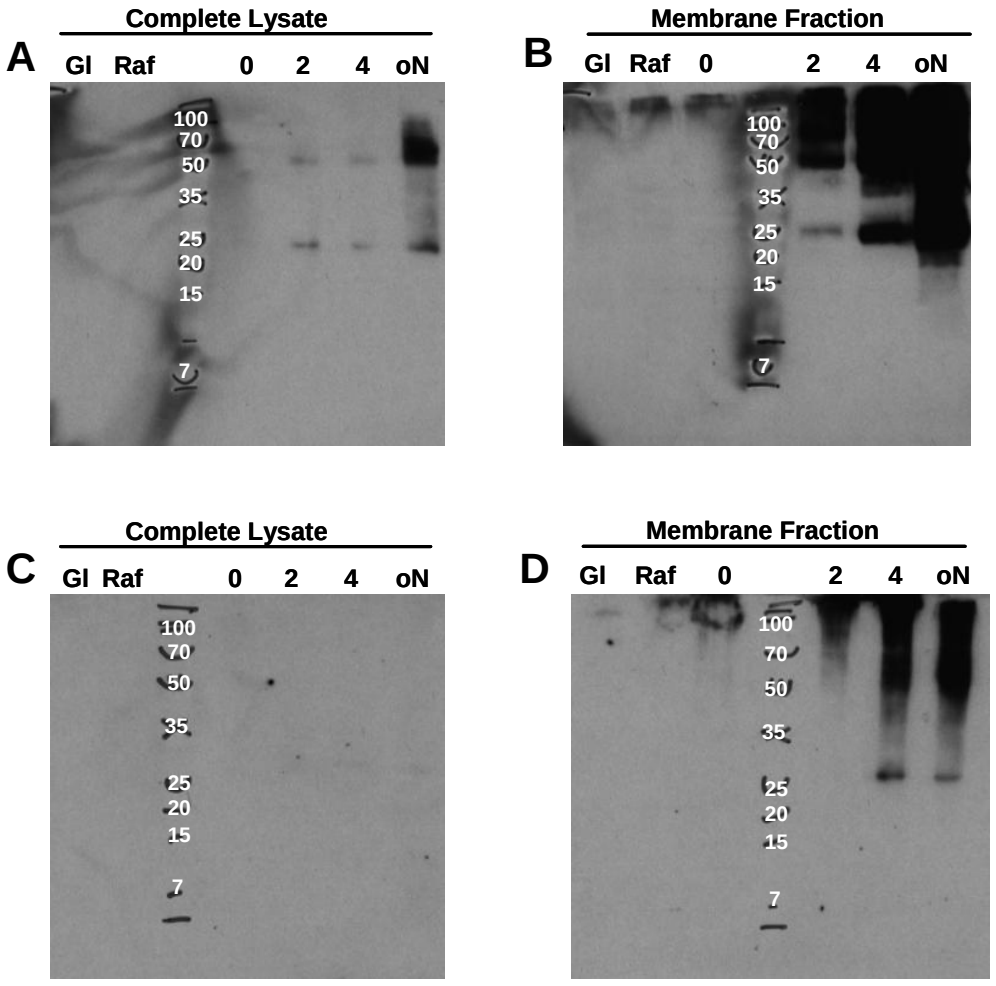

Figure 25: Western blots of MAK33 Fab-fragment expressed from 2µ plasmid.
A) Light chain in complete lysate detected with α-HA antibody.
B) Light chain in membrane fractions detected with α-HA antibody.
C) Fd-fragment in complete lysate detected with α-Flag antibody.
D) Fd-fragment in membrane fractions detected with α-Flag antibody.
Gl – samples grown in glucose medium, Raf – samples grown in raffinose medium, 0-oN – samples at different times after induction with galactose (0 – immediately after induction, 2 – 2 hours after induction, 4 – 4 hours after induction, oN – over night induction).

The expression of the Fab-fragment was detected in all cases with an exception of the complete lysate detected with α-Flag antibody (Figure 25). However, this is not unexpected.

The Fd-fragment alone is not stable (Lilie et al., 1995; Rothlisberger et al., 2005) and therefore it might be present in low amounts. Possibly, the concentration is so low that it is not enough to give a signal in a western blot. This theory is actually supported by the western blot in figure 25D, where concentrated membrane fractions are western blotted and detected with α-Flag antibody. However, the signal resulting from the membrane fractions detected with α-HA antibody (Figure 25B) is much stronger than the signal of the membrane fractions detected with α-Flag antibody. On the western blots A, B and D, an additional band at approximately 50 kDa was detected again, which could correspond to the assembled Fab-fragment. The bands at higher molecular weights could result from higher oligomers and aggregates.

Samples of the soluble fractions of MAK33 Fab-fragment are shown in figure 26. Samples pulled with α-HA beads were detected with α-HA antibody (Figure 26A) and samples pulled with α-Flag beads were detected with α-Flag antibody (Figure 26B). Expression of the Fab-fragment was detected in both cases, although the signal obtained after the detection with α-Flag antibody is again weaker than the signal obtained after the detection with α-HA antibody. Not only the bands for the Fab-fragment (54.3 kDa) but also for the respective monomers (26.8 kDa LC, 27.5 kDa Fd-fragment) could be detected in both cases. In order to distinguish between the LC and Fd-fragment dimers (55 kDa and 53.6 kDa) and the Fab-fragment (54.3 kDa), a cross detection was performed. The soluble fraction was pulled with α-HA beads and detected with α-Flag antibody (Figure 26C). Bands at the positions corresponding to the Fab-fragment were detected also in this case, confirming that both fragments are present in the lysate. On the western blot of the over-night sample in figure 26C, also a band around 27 kDa appeared which corresponds to the Fd-fragment alone. This could mean that there is also free, unassembled Fd-fragment present as a monomer in the sample.

A possible secretion of the Fab-fragment into the medium was tested as well. Proteins from the medium were precipitated with trichloroacetic acid, analogously as for the LC (see page 47). However, same as for the LC, no signal could be detected on the western blot (data not shown). This suggests that no antibody fragments were secreted into the medium.

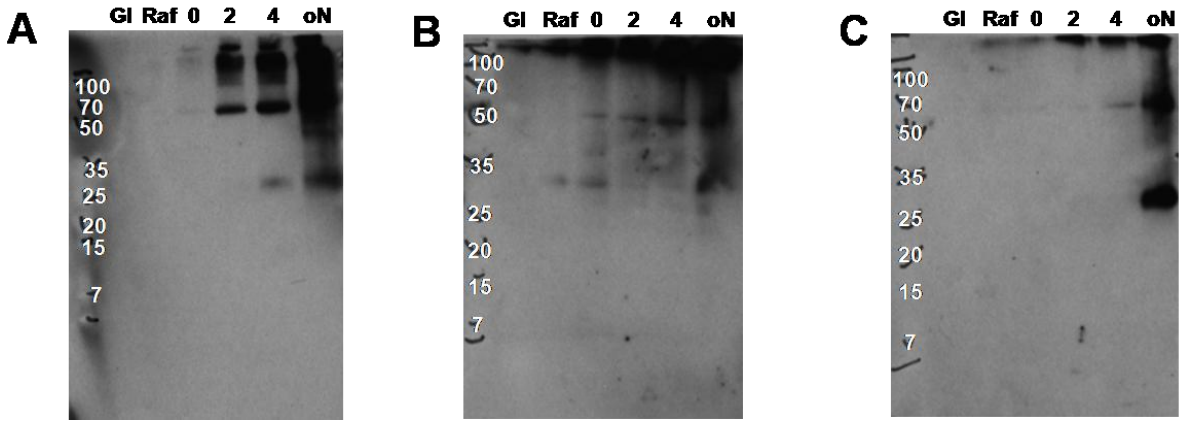

Figure 26: Pull-downs and western blots of the soluble fractions of MAK33 Fab-fragment.
A) α-HA pull-down detected with α-HA antibody.
B) α-Flag pull-down detected with α-Flag antibody.
C) α -HA pull-down detected with α-Flag antibody.
Gl – sample grown in glucose medium, Raf – sample grown in raffinose medium, 0-oN – samples at different times after induction with galactose (0 – immediately after induction, 2 – 2 hours after induction, 4 – 4 hours after induction, oN – induction over night).

Taken together, the data obtained from the expression of MAK33 antibody fragments in *S. cerevisiae* suggests that the antibody fragments are retained in the ER which corresponds to the data known from literature, summarized, e.g., by Gasser and Mattanovich (2007) and Joosten et al. (2003). One of the possible bottlenecks leading to the accumulation of the antibody fragments within the ER might be their improper folding due to the lack of some chaperones known to assist antibody folding in mammalian cells *in vivo*. One of these chaperones is the recently identified small ER resident protein pERp1 which was shown to play a role during antibody folding and assembly in B cells (Shimizu et al., 2009; van Anken et al., 2009). However, until today nothing has been known about pERp1 structure and stability. Therefore, the following studies were focused on elucidating these properties.

2.2 Biophysical analysis of pERp1

2.2.1 pERp1 proteins

To elucidate the structure and stability of pERp1, several pERp1 proteins were analyzed. We obtained glycerol stocks of pERp1 expressing *E. coli* cultures from the lab of Linda M. Hendershot, Memphis. All constructs were cloned in a pQE30 vector which harbors a ß-lactamase gene that enables a selective growth of transformed cells in the presence of

100 µg/mL ampicillin as a selection marker. Additionally, pQE30 contains a His_6-tag between the T5 promotor and the beginning of the multiple cloning site.

pERp1 (23 kDa) consists of 188 amino acids. It contains six cysteines connected via disulfide bonds in a specific pattern (Figure 11B) and three tryptophans located in the middle part of the amino acid sequence which enables fluorescence studies (Figure 27). Apart from the ER retention signal (REEL), pERp1 also contains a signal sequence targeting the ER (Figure 11A). This signal sequence was replaced by a His_6-tag from the pQE30 vector to make further pERp1 purification easier (Figure 27).

MRGS**HHHHHH**GSAIPGGLGDRAPLTATAPQLDDEEMYSAHMPAHLRCDACRAVAYQMWQNL
AKAETKLHTSNSGGRRELSELVYTDVLDRSCSRNWQDYGVREVDQVKRLTGPGLSEGPEPSISVM
VTGGPWPTRLSRTCLHYLGEFGEDQIYEAHQQGRGALEALLCGGPQGACSEKVSATREEL

Figure 27: pERp1 sequence, modified from Shimizu et al. (2009) and van Anken et al. (2009). Cysteines are marked in magenta, the CXXC and $C(X)_6C$ motifs are underlined. Tryptophans are marked in blue and the ER retention signal in green. The N-terminal signal sequence was replaced by the His_6-motif shown in bold.

Besides the pERp1 wild type (WT), also mutants in which certain cysteines were replaced by serines were analyzed. These mutants can be divided into two groups. The first group consists of “S” mutants, where the respective disulfide bond was mutated to serines. In the second group, there are “only” mutants in which all cysteines except of the mentioned disulfide bond were replaced by serines. A schematic example is shown in figure 28.

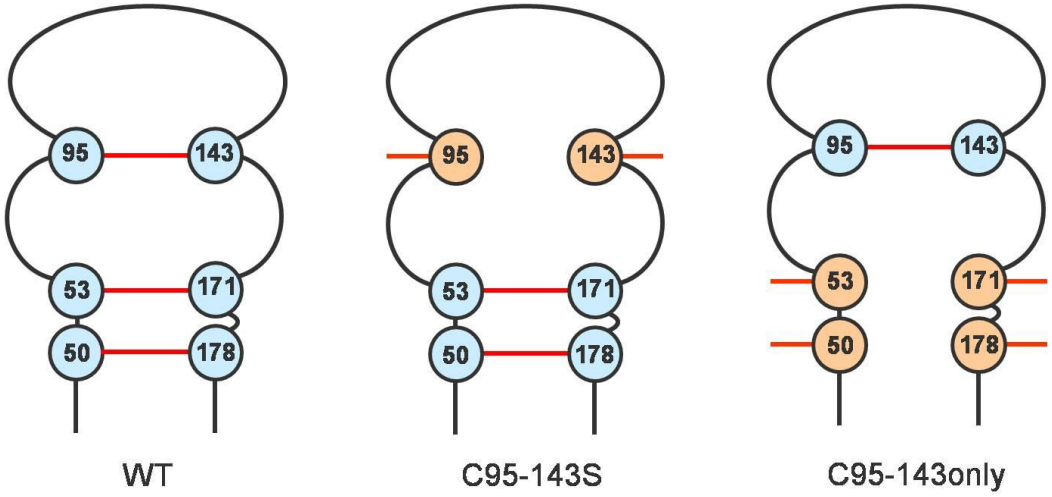

Figure 28: Schematic representation of pERp1 mutants.
WT – wild type with the typical disulfide bond pattern.
C95-143S – a representative from the group of "S" mutants. In C95-143S, the two cysteines at the positions 95 and 143 were replaced by serines.
C95-143only – a representative from the group of "only" mutants. In C95-143only, only the two cysteines at the positions 95 and 143 are maintained, all other cysteines were replaced by serines.

2.2.2 pERp1 expression and purification

2.2.2.1 Expression of pERp1 proteins

The expression of pERp1 proteins was performed in LB_0 medium upon induction with 1mM isopropyl-β-D-thiogalactopyranosid (IPTG). To obtain the soluble protein, pERp1 was induced and expressed for 3 h at 37 °C. However, the obtained expression yields were very low, therefore the expression conditions were changed and pERp1 was expressed after induction for 5 h at 30 °C. Nevertheless, the expression yields were still quite low. Finally, an optimal expression protocol was established as schematically shown in figure 29. Briefly, a 150 ml *E.coli* preculture was cultivated over night at 37 °C. Afterwards, a 15 l expression culture was inoculated from the preculture and cultivated at 37 °C until an OD_{600} ~ 0.8 was reached. After induction, cells were cultivated over night at 20 °C and harvested the next morning. For more details see section 4.3.1. Generally, the expression yield of pERp1 WT was much higher than the yields obtained from the expression of pERp1 mutants.

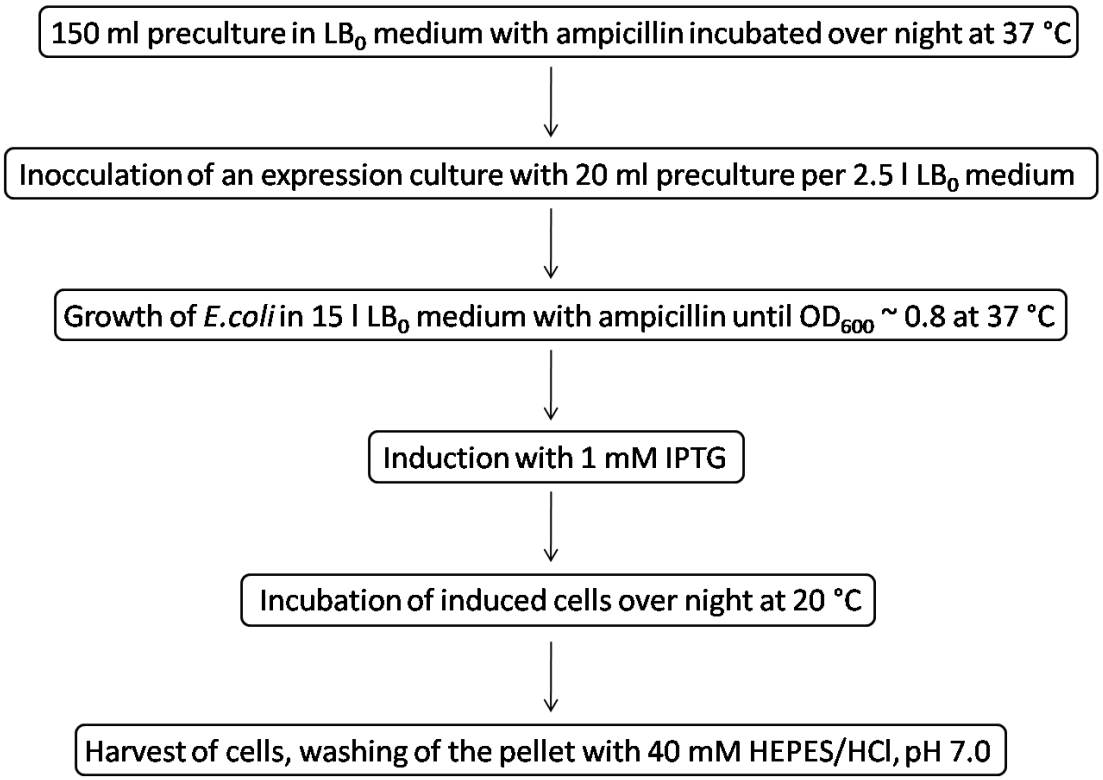

Figure 29: Scheme of the expression of pERp1 proteins in *E.coli*.
IPTG – isopropyl-β-D-thiogalactopyranosid.

2.2.2.2 Purification of pERp1 proteins

The over-night expression at 20 °C provided enough protein to develop a purification strategy. Several different purification procedures and conditions were tested until an optimal purification protocol was established. This protocol enabled to obtain pure pERp1 protein and it is schematically depicted in figure 30.

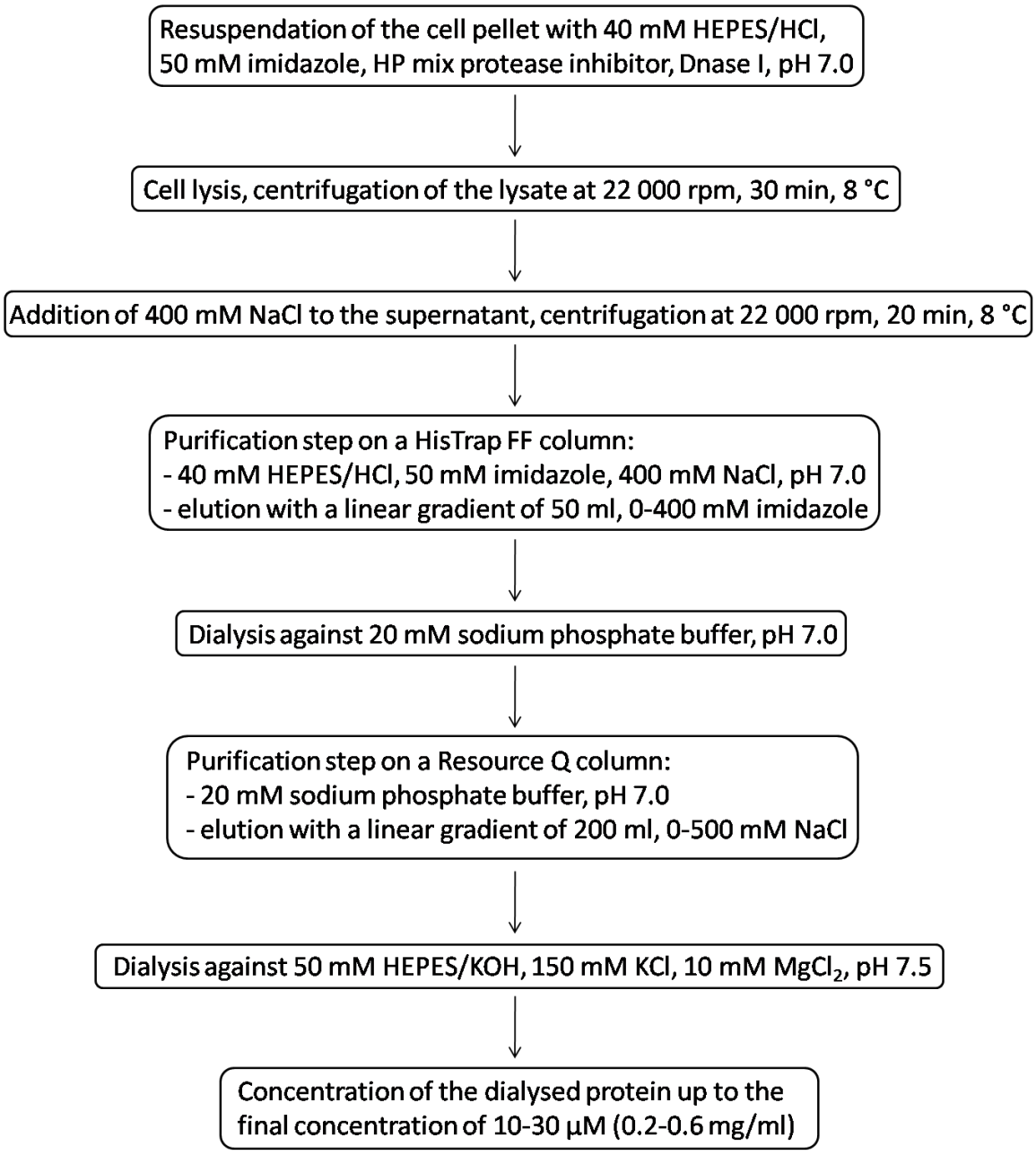

Figure 30: Scheme of the purification of pERp1 proteins from *E.coli*.

Briefly, harvested cells were lysed (section 4.3.2), NaCl was added to the supernatant until the final concentration of 400 mM and the lysate was loaded on a HisTrap FF column. Ni-affinity chromatography was performed in 40 mM HEPES/HCl, 50 mM imidazole, 400 mM NaCl, pH 7.0. pERp1, bound to the column, was eluted with a linear increasing concentration of imidazole in the running buffer up to 400 mM. Because there were some contaminating proteins in the fractions eluted form the HisTrap FF column, also different types of elution

were tested. An elution with a shallower gradient of imidazole concentration (from 40 to 400 mM over 100-200 ml) was tried as well as a "jump-elution", during which the imidazole concentration was increased step-wise from 40 to 400 mM in 40-50 ml steps. However, none of these modifications resulted in a purer protein preparation. Therefore, for the standard pERp1 purification, the elution with a linear gradient from 40 to 400 mM imidazole over 50 ml was used (Figure 30).

Typically, all fractions eluted from the HisTrap FF column were collected and dialyzed against 20 mM sodium phosphate buffer. Occasionally, part of the protein precipitated in the dialysis tube. In this case, an additional centrifugation step (22 000 rpm, 20 min, 8 °C) was introduced. Subsequently, the protein solution was loaded on a Resource Q column and anion exchange chromatography was performed in 20 mM sodium phosphate buffer. pERp1, which bound to the column, was eluted with a linearly increasing concentration of NaCl from 0-500 mM over 200 ml. This shallow gradient turned out to be necessary in order to get rid of the impurity at a molecular weight of ~25 kDa (Figure 31, black arrows). With steeper gradients, pERp1 co-eluted together with the impurity in the same fractions. Generally, the purification step on the Resource Q column resulted in pure pERp1 protein, which was collected and dialysed either against PBS buffer or against 50 mM HEPES/KOH, 150 mM KCl, 10 mM $MgCl_2$, pH 7.5. Finally, the protein was concentrated up to the final concentration of 10-30 µM (0.2-0.6 mg/ml), shock frozen in liquid nitrogen and stored at –80 °C.

The purification protocol shown in figure 30 was applied for all pERp1 mutants; representative SDS-gels of the fractions eluted from the respective columns are shown in figure 31. The presence of pERp1 in the respective bands was verified by mass spectroscopy.

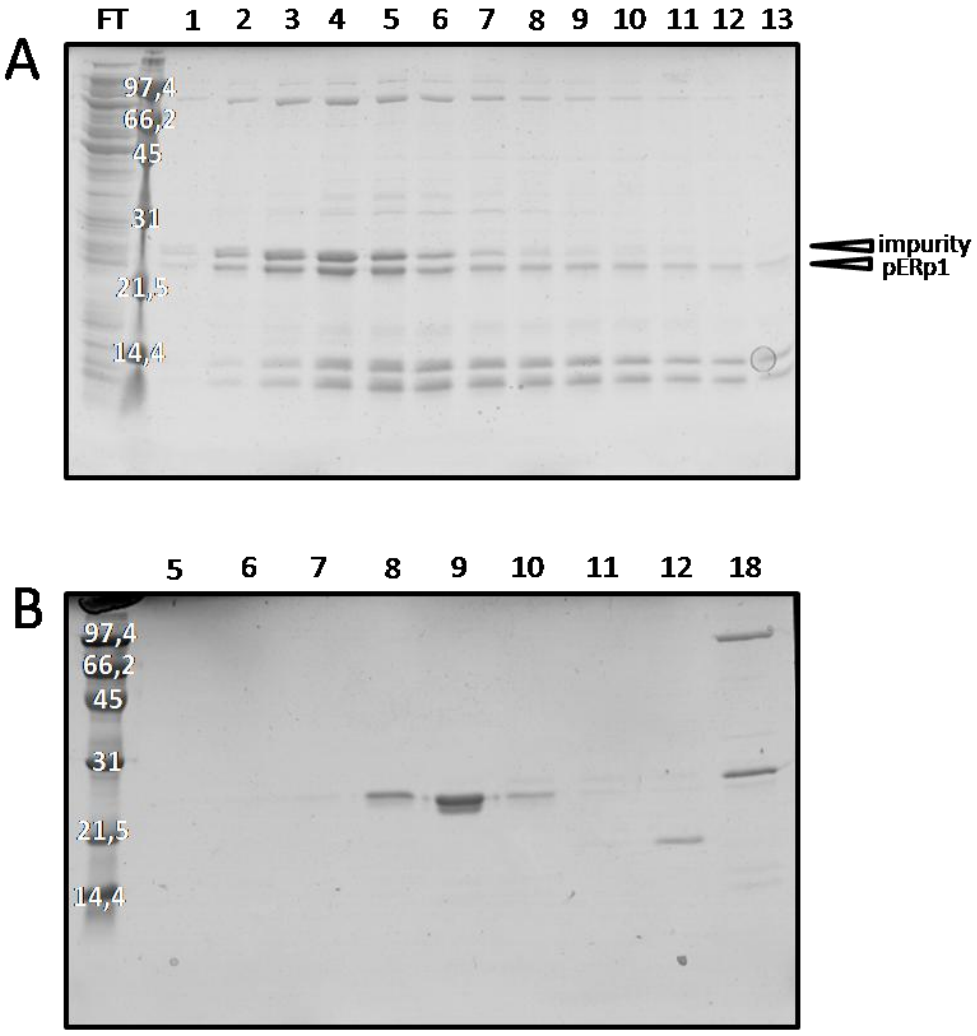

Figure 31: Representative SDS gels of pERp1 after respective purification steps.
A) C50-158S after the HisTrap FF column. Elution was performed over 50 ml, fraction volume was 4 ml.
1-13 – numbers of the respective fractions. For the next purification step, all fractions were pooled.
B) C50-178S after the Resouce Q column. Elution was performed over 200 ml, fraction volume was 4 ml.
5-18 – numbers of the respective fractions. Fractions 7-10 containing the pure pERp1 mutant C50-178S were pooled and concentrated to the final concentration of 26 µM.
FT – flow through.

In case of pERp1 wild type, which typically provided much higher expression yield than pERp1 mutants, the purification protocol in figure 30 was not sufficient. In order to get pure pERp1 wild type protein, an additional step after the anion exchange chromatography had to be performed. Collected fractions eluted from the Resource Q column were concentrated down to the volume of 5 ml and a gel filtration on a Superdex 75 column was performed ei-

ther in PBS buffer or in 50 mM HEPES/KOH, 150 mM KCl, 10 mM $MgCl_2$, pH 7.5. A representative gel of the pERp1 WT after the gel filtration is shown in figure 30.

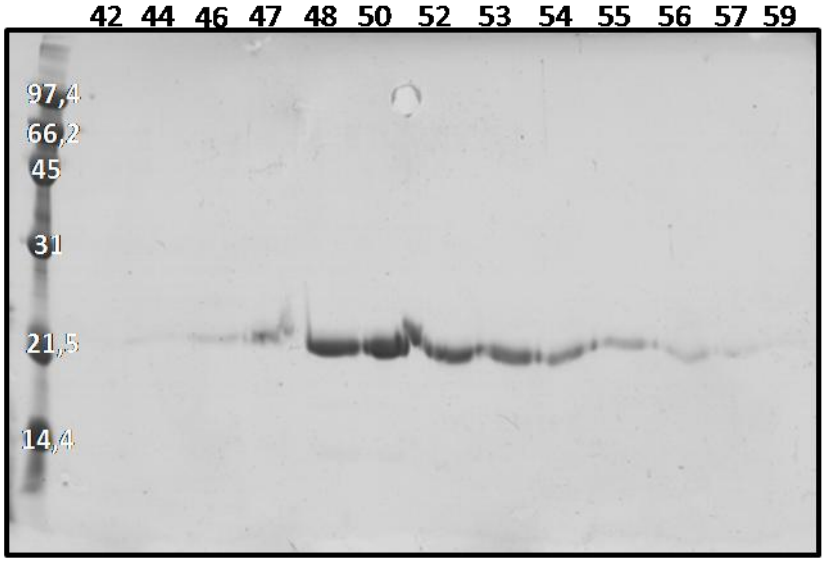

Figure 32: Representative gel of the pERp1 wild type after gel filtration on a Superdex 75 column. 42-59 – numbers of respective fractions (4 ml), fractions 43-59 containing the pure pERp1 wild type were pooled and concentrated to the final concentration of 28 µM.

2.2.3 Oligomeric state of pREp1

To elucidate the oligomeric state of pERp1 proteins, an analytical size exclusion chromatography was performed on a high performance liquid chromatography (HPLC) system (section 4.4.2). pERp1 samples were injected on a Superdex 75 column and chromatograms were recorded (Figure 33). Except of the C50-178only mutant, pERp1 proteins were eluted in a single peak between 14-17 min with a slight shift in the maximum, which might be caused by structural differences due to the missing disulfide bonds (Figure 33A). The chromatogram of the C50-178only mutant indicates that, in contrast to other pERp1 proteins, this mutant was degraded and aggregated (peak at 13 min) during the analysis (Figure 33B).

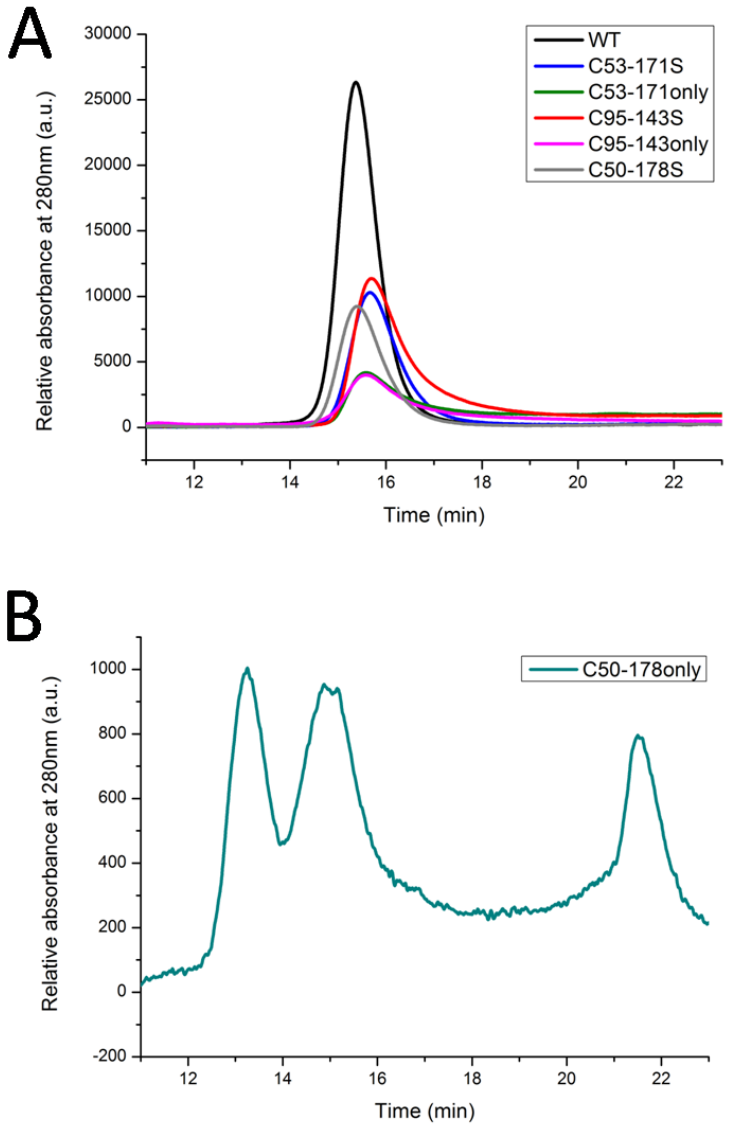

Figure 33: Analytical size exclusion chromatography of pERp1 proteins.
A) Chromatograms of the WT and five different mutants.
B) Chromatogram of the C50-178only mutant.

In order to estimate the oligomeric state of pERp1 proteins, chromatograms of HPLC standard proteins of defined molecular weights were recorded and a calibration curve was estimated (Figure 34B), see section 4.4.2. According to the calibration curve, the elution time of pERp1 is located between the theoretical molecular mass of a monomer and a dimer, with a slight shift towards the monomer as shown for the WT in figure 30.

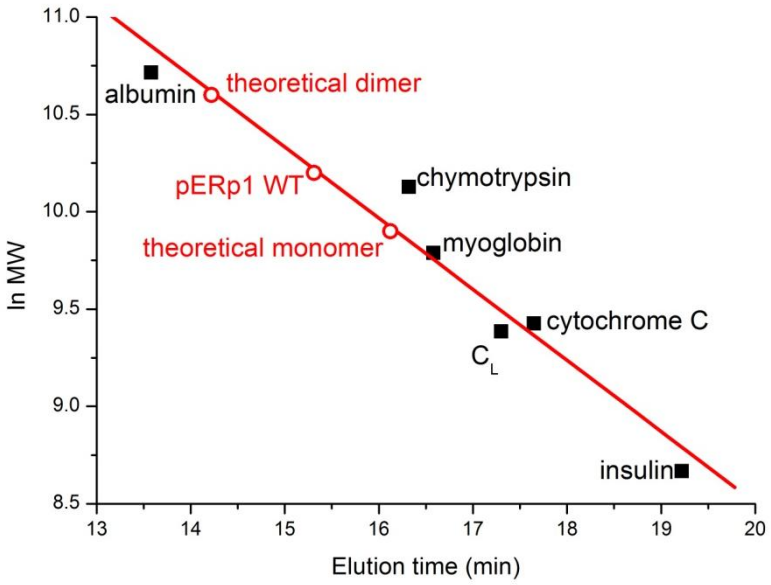

Figure 34: HPLC calibration curve.
C_L – constant domain of the MAK33 light chain, WT – wild type, MW – molecular weight.

To confirm the indication from HPLC data that pERp1 is a monomer, an analytical ultracentrifugation (aUC) analysis of pERp1 proteins was performed (section 4.4.5). In equilibrium sedimentation runs and sedimentation velocity runs, the absorption at 230 nm and 280 nm of 5 µM pERp1 was measured against a reference buffer. An example of the equilibrium sedimentation experiment for pERp1 WT is shown in figure 35. For all samples, the molecular mass of 20 kDa was determined, which corresponds to a monomer. In summary, the aUC experiments confirmed that pERp1 is a monomer.

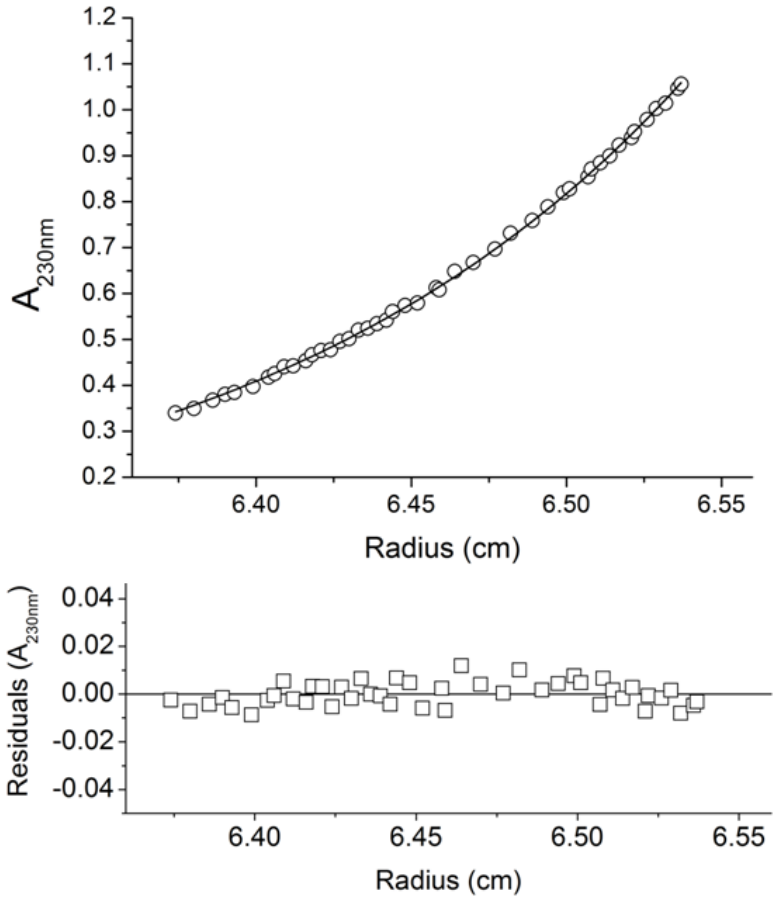

Figure 35: Equilibrium sedimentation ultracentrifugation run of 5 µM pERp1 wild type in 0.1 M Tris buffer, pH 7.5 at 20 °C.

2.2.4 pERp 1 structure and stability

2.2.4.1 pERp1 structure

Circular dichroism (CD) spectroscopy was used to analyze the secondary structure of pERp1 proteins. CD spectra of all proteins were recorded (Figure 36A) as described in section 4.4.3.1. Except of the mutant C50-178only, all pERp1 proteins show a spectrum typical for α-helical proteins. The content of the respective secondary structure elements was estimated with CDNN program (http://gerald-boehm.de) and is summarized in the table (Figure 36B). Together with the HPLC data, the C50-178only mutant seems to be unfolded and/or degraded. Therefore, this mutant was not considered in the further analysis.

A

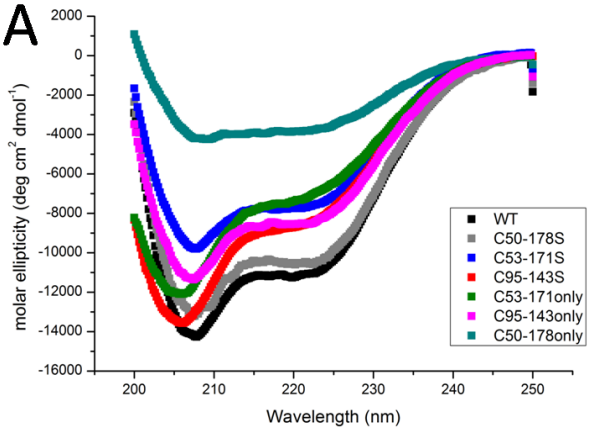

B

pERp1 variant	α-helical structure (%)	β-sheet structure (%)	random coil (%)
WT	40.8	30.1	29.1
C50-178S	37.6	31.6	30.8
C53-171S	27.2	36.6	36.2
C95-143S	33.4	33.7	32.9
C53-171only	30.7	34.8	34.5
C95-143only	28.6	35.9	35.5
C50-178only	15.3	42.9	41.8

Figure 36: Analysis of pERp1 structure by CD spectroscopy. All proteins show α-helical structure except of the C50-178only mutant which seems rather unfolded.
A) CD spectra of pERp1 proteins.
B) Content of the respective secondary structure elements within the pERp1 variants.

2.2.4.2 Thermal stability of pERp1variants

To investigate the thermal stability of pERp1, temperature transitions were recorded (Figure 37A) as described in section 4.4.3.1. pERp1 WT is stable until approximately 55 °C and then melts cooperatively with the melting temperature of 71 °C. Other pERp1 proteins also melt cooperatively with melting temperatures (Tm) summarized in the table (Figure 37B). Interestingly, the Tm of the C95-143S mutant which lacks the 95-143 disulfide bond is 10 °C higher than the Tm of the wild type with all disulfide bonds. In accordance with this, the C95-143only mutant which contains only the 95-143 disulfide bond is the least stable mutant of all pERp1 proteins with a Tm of 30 °C.

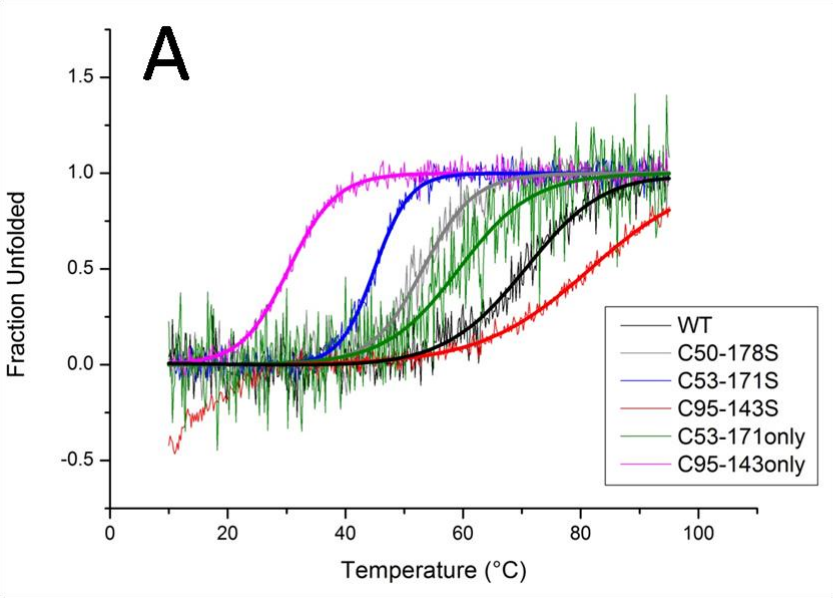

B

pERp1 variants	Tm (°C)
C95-143S	81
WT	71
C53-171only	59
C50-178S	53
C53-171S	45
C95-143only	30

Figure 37: Temperature transitions of pERp1 proteins.
A) Temperature transition curves of pERp1 proteins. The most stable protein is the C95-143S mutant, the least stable mutant is the C95-143only mutant.
B) Melting temperatures of the respective pERp1 proteins.

To investigate the surprising effect of the C95-143S disulfide bond further, pERp1 WT was reduced over night and the CD spectrum was recorded (Figure 38A). Since pERp1 contains three disulfide bridges, 10 mM TCEP was used to reduce the protein before temperature transition in order to assure that the TCEP concentration was high enough to reduce all disulfide bonds. Upon reduction with 10 mM TCEP, the CD signal is quite noisy below 215 nm because of the absorption of the reducing agent. However, the reduced protein still shows an α-helical structure, particularly upon reduction with 3 mM TCEP. The thermal transition was measured at the wavelength of 222 nm (Figure 38B) as described in section 4.4.3.1. The destabilizing effect of the 95-143 disulfide bond was confirmed, because the C95-143only mutant containing the disulfide bond is less stable than the reduced wild type lacking all disulfide bonds. The melting temperature of the reduced wild type (40 °C) is 10 °C higher than the melting temperature of the C95-143only mutant.

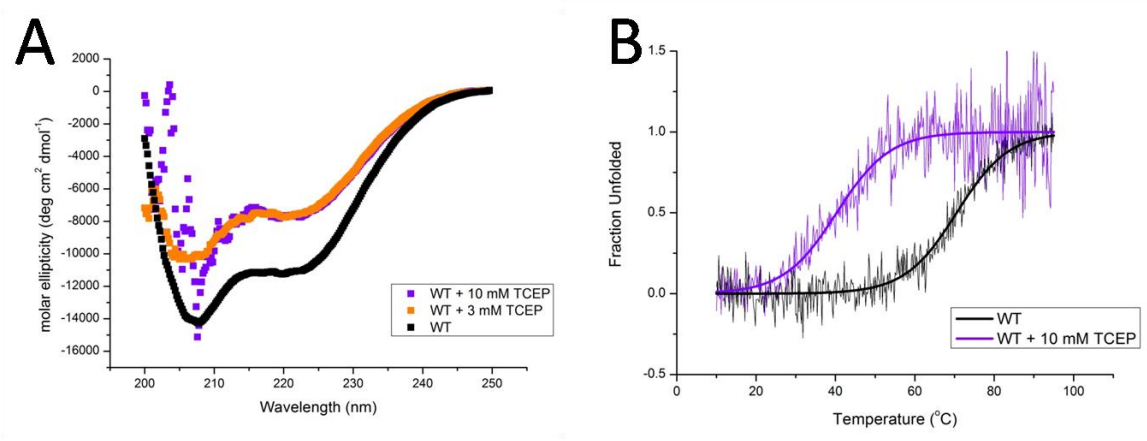

Figure 38: CD analysis of the reduced pERp1 wild type (WT).
A) CD spectra of the WT and of the WT reduced with different TCEP concentrations.
B) Thermal transition of the WT and WT reduced with 10 mM TCEP.
The melting temperature of the WT is 71 °C, the melting temperature of the reduced WT is 40 °C.

In accordance with the destabilizing effect of the 95-143 disulfide bond are also the thermal transitions of the pERp1 wild type and the C95-143S mutant lacking the 95-143 disulfide bond. The transition of the WT is partially reversible (Figure 39A) and the CD spectrum after the transition is not completely identical with the spectrum before the transition, although it still shows an α-helical structure (Figure 39B). In contrast, the transition of the C95-143S mutant is reversible to a large extend (Figure 39C) and the CD spectra before and after the transition are nearly identical (Figure 39D).

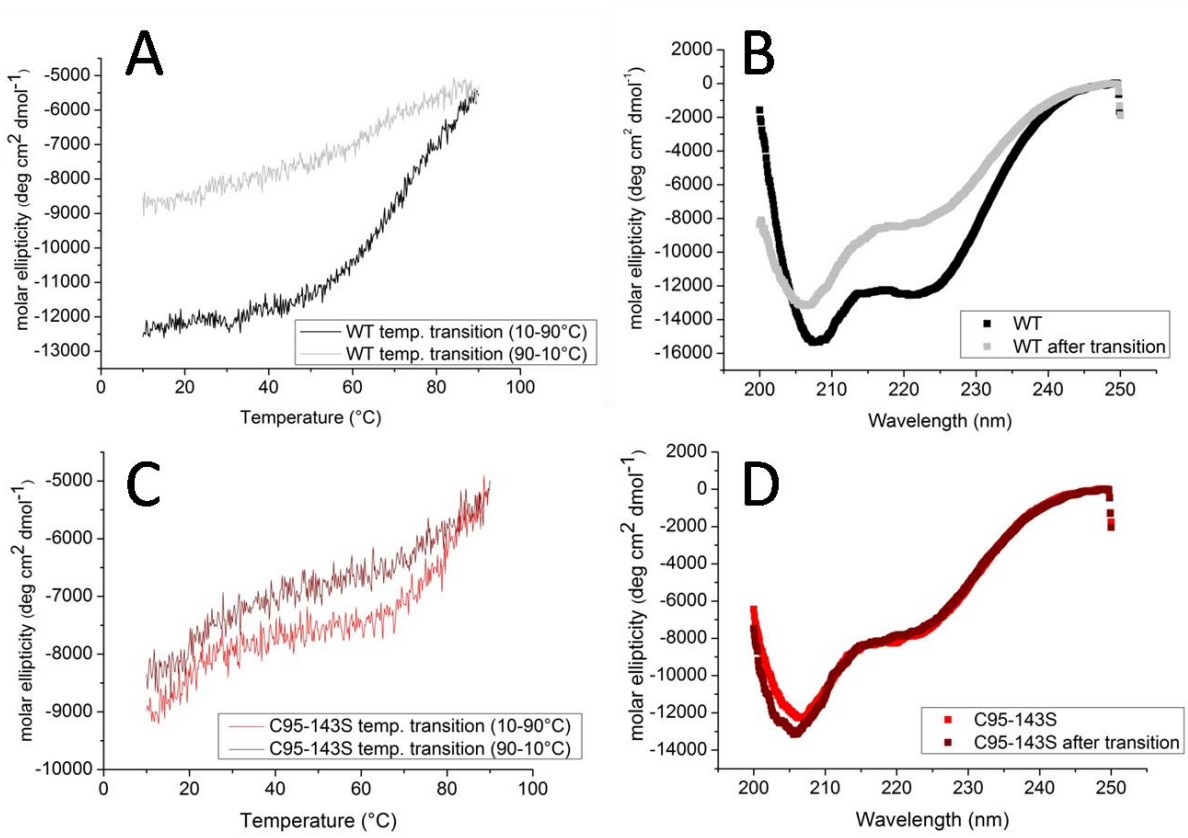

Figure 39: Temperature transitions of pERp1 wild type and C95-143S mutant.
A) The temperature transition of the WT.
B) CD spectra of the WT before and after the temperature transition.
C) The temperature transition of the C95-143S mutant.
D) CD spectra of the C95-143S mutant before and after the temperature transition.

2.2.4.3 Chemical stability of pERp1

pERp1 contains three intramolecular tryptophans (Figure 27) which allows to follow the unfolding of the protein by fluorescence as shown in figure 40. pERp1 wild type was either reduced with 10 mM TCEP or unfolded with 6 M guanidine hydrochloride (GdmHCl) or both reduced and unfolded over night and the fluorescence spectra were recorded as described in section 4.4.3.2. The fluorescence maximum decreases and shows a slight shift in a wave-length upon unfolding and reduction.

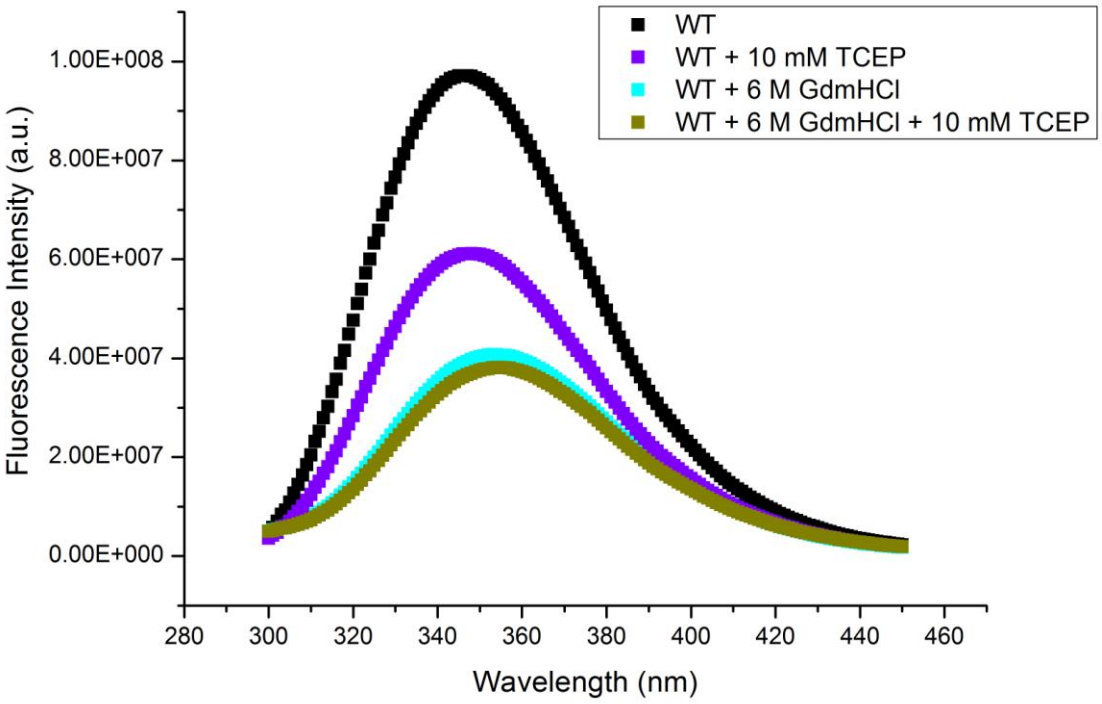

Figure 40: Fluorescence spectra of the pERp1 wild type (WT). Fluorescence of 1 µM pERp1 was measured either directly or the protein was unfolded (with 6 M GdmHCl) or reduced (with 10 mM TCEP) or both unfolded and reduced over night before the measurement.

The decrease in fluorescence upon reduction and unfolding was used to investigate the chemical stability of pERp1. Transition curves of all pERp1 proteins were measured as described in section 4.4.3.2 and are shown in figure 30A. In contrast to the thermal stability, the wild type with all disulfide bonds is the most stable and the reduced wild type lacking all disulfide bonds is the least stable protein of all pERp1 proteins. The transition points $[D]_{1/2}$ are shown in the table (Figure 41B).

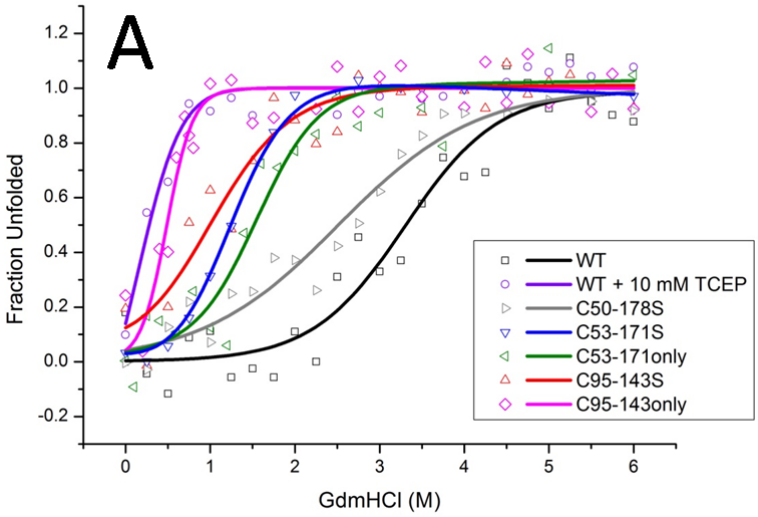

B

pERp1 variants	$[D]_{1/2}$ GdmHCl (M)
WT	3.3
C50-178S	2.5
C53-171only	1.6
C53-171S	1.2
C95-143S	0.92
C95-143only	0.49
WT + 10 mM TCEP	0.28

Figure 41: Chemical stability of pERp1.
A) Transition curves of pERp1 during unfolding with guanidine hydrochloride (GdmHCl). Wild type is the most stable and reduced wild type the least stable protein.
B) Transition points $[D]_{1/2}$ of the respective pERp1 proteins.

2.2.5 pERp1 binding to BiP is nucleotide-dependent

As it is known that pERp1 binds to BiP *in vivo* (Shimizu et al., 2009), the binding was investigated by surface plasmon resonance (section 4.4.3.4) *in vitro*. BiP-pERp1 binding turned out to be nucleotide-dependent. Without nucleotides, no binding could be observed. However, upon addition of 1 mM ATP, BiP bound to pERp1 with K_D=1.89 +/– 0.37 µM and with 1mM ADP with K_D=1.09 +/– 0.38 µM (Figure 42).

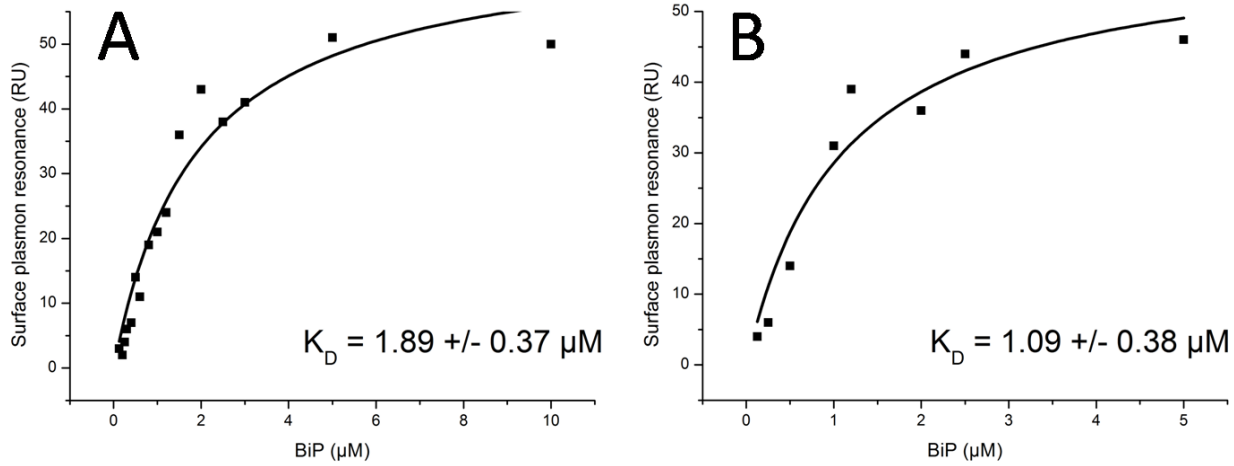

Figure 42: Binding of BiP to pERp1 is nucleotide-dependent.
A) Binding in the presence of 1 mM ATP.
B) Binding in the presence of 1 mM ADP.
Without nucleotides, no binding could be observed.

Subsequently, an ATPase assay was performed to test whether pERp1 has an effect on the ATPase activity of BiP. Different BiP and pERp1 concentrations and their ratios were tested (Figure 43). The assay was performed at 37 °C as described in section 4.4.6. However, no effect of pERp1 on the ATPase activity of BiP could be observed (Figure 43).

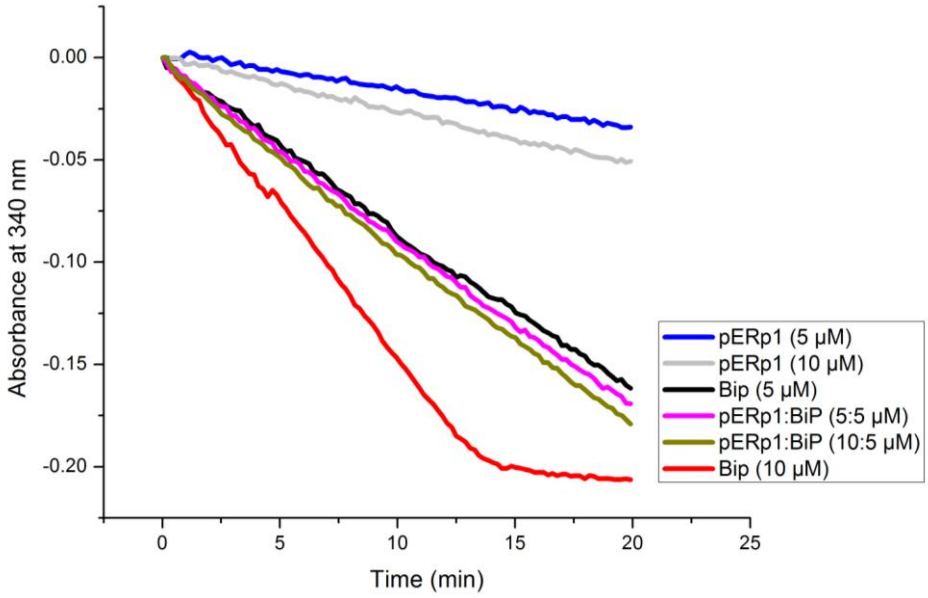

Figure 43: ATPase assay with BiP and pERp1. pERp1 does not have an effect on the ATPase activity of BiP.

3 *Discussion*

3.1 Antibody Expression in yeast

The importance of antibodies has been continuously growing over the past years. Consequently, the demand for antibodies increased significantly. Currently, therapeutic antibodies are preferentially produced in mammalian cell cultures which causes high production costs (Farid, 2007). Therefore, the production of antibodies in microorganisms would be more useful since they can be cultivated up to high densities with cheap media and the expression time is shorter in comparison to mammalian cells.

Yeast combines the advantages of microorganisms with the eukaryotic ability of adding the correct post-translational modifications. However, the expression of antibodies in yeast was shown to cause cellular stress and activate the unfolded protein response which hampers the cell growth and leads to a decrease in amount of the expressed antibody (Kauffman et al., 2002). One of the main obstacles during expression of antibodies and their fragments in yeast seems to be their retention within the ER and their improper folding and assembly. LC and HC expressed in *H. polymorpha* were shown to be intracellularly retained (Abdel-Salam et al., 2001). Also Fab-fragment expressed in *P. pastoris* (Gasser et al., 2006) and scFv-fragment expressed in *S. cerevisiae* (Kauffman et al., 2002) accumulated within the ER as shown in western blot and by confocal microscopy, respectively. Additionally, only 30% of the Fab-fragment expressed in *P. pastoris* was shown to be correctly assembled into heterodimers (Lange et al., 2001). In several studies, it was shown that it is possible to increase the expressed antibody amount by co-expression of chaperones responsible for antibody folding such as BiP and/or PDI (Damasceno et al., 2007; Gasser et al., 2006; Hackel et al., 2006; Kauffman et al., 2002; Shusta et al., 1998). Therefore, because of the intracellular accumulation of expressed antibodies and the positive effect of chaperone co-expression, the antibody expression in yeast is generally considered to lead to an overload of the secretory pathways (Gasser and Mattanovich, 2007; Joosten et al., 2003).

Currently, the methylotrophic yeast *P. pastoris* is the most preferred strain for antibody production in yeast (Jeong et al., 2011). However, in contrast to *S. cerevisiae, P. pastoris* does not possess the GRAS (generally regarded as safe) status. This would make *S. cerevisiae* more advantageous for antibody expression. But the antibody levels achieved from expression

in *S. cerevisiae* are quite low with 50 µg/l (Horwitz et al., 1988) to 0.5 mg/l (Hackel et al., 2006). By optimizing the temperature and co-expression of BiP and PDI, the expressed amounts of scFv-fragment could be increased to 20 mg/l (Gasser and Mattanovich, 2007; Shusta et al., 1998). Several examples of antibodies and antibody fragments expressed in yeast are given in table 3 on the next page.

In this work, an antibody expression system in *S. cerevisiae* was established. MAK33, a mouse antibody against creatine kinase from a human heart muscle, was used as a model antibody. MAK33 light chain (LC) and Fd-fragment were expressed separately or co-expressed (Fab-fragment) from either single-copy (CEN) or multi-copy (2µ) vectors. At the C-terminus, every construct contains an invertase signal sequence which targets the ER as well as an affinity tag (Figure 12). The LC was fused with a HA-tag, whereas the Fd-fragment was fused with a Flag-tag.

In a glucose medium, all transformed cultures grew well until they reached the stationary phase (Figure 14). However, compared to the wild type strain, the transformed cultures were growing slower and also reached lower OD_{600} values. This was the case for strains expressing antibody fragments as well as for strains transformed with empty plasmids. Therefore, the worse growth of the transformed cells seems to be caused by the transformation in general, not by the expression of antibodies itself. Nevertheless, the antibody expression does not seem to have any harmful effect on the general fitness of the cells as shown by scanning electron microscopy (Figure 15).

Construct	Host	Promoter	Signal Sequence	Expr. Temp.	Maximal yield	Comments	Reference
Chimeric Fab-fragment (mouse-human)	*S. cerevisiae*	PGK-promoter, constitutive expression	Invertase signal sequence	30 °C	100-200 ng/ml light chain	Secreted	Horwitz et al., 1988
scFv-fragment (mouse)	*S. cerevisiae*	Gal1-10 promoter, plasmid integrated within the chromosome	Synthetic pre-pro signal sequence	20 °C	20 mg/ml	Secreted, overexpression of BiP and PDI	Shusta et al., 1998
scFv-fragment (rat)	*S. cerevisiae*	Gal1-10 promoter, plasmid integrated within the chromosome	Synthetic pre-pro signal sequence	20 °C	0.5 mg/ml	Secreted, overexpression of BiP and PDI	Hackel et al., 2006
V_{HH} fragment (llama)	*S. cerevisiae*	Gal7 promoter	*SUC2* signal sequence	30 °C	≥ 2.5 mg/ml	Secreted	Frenken et al., 2000
Co-expression of LC and HC (mouse)	*H. polymorpha*	AOX1 promoter	α-mating factor signal sequence	37 °C	LC and HC not assembled into functional heterodimeric form	LC and HC intracellularly retained	Abdel-Salam et al., 2001
Co-expression of LC and HC (mouse)	*P. pastoris*	AOX1 promoter	α-mating factor signal sequence	30 °C	36 mg/l *	secreted	Ogunjimi et al., 1999
scFv-fragment and Fab-fragment (human)	*P. pastoris*	GAP-promoter, constitutive expression	α-mating factor signal sequence	28 °C	41 mg/ml (fermentation)	Secreted; Fd-fragment accumulated in the membrane fraction	Gasser et al., 2006
Co-expression of LC and HC (human)	glycoengineered *P.pastoris*	AOX1 promoter	n. a.	24 °C	≥ 1 g/l (fermentation)	secreted	Potgieter et al., 2009
Fab-fragment (human)	*P. pastoris*	AOX1 promoter, plasmid integrated within the chromosome	n. a.	30 °C	458 mg/ml (fermentation)	secreted	Ning et al., 2005

Table 3: Examples of antibodies and antibody fragments expressed in yeast.
GAP – glyceraldehyde-3-phosphate dehydrogenase, PGK – phosphoglycerate kinase, LC – light chain, HC – heavy chain, Expr. Temp. – expression temperature, * – according to Gasser and Mattanovich (2007) and Lange et al. (2001), a significant fraction of the secreted antibody is believed not to be intact, but LC-HC heterodimers.

The advantage of the co-expression of the LC and Fd-fragment from CEN plasmids is that the 1:1 ratio of both fragments per cell is assured which is favorable for the assembly of the Fab-fragment. First of all, MAK33 LC and Fd-fragment were expressed separately from the CEN plasmids. However, only expression of the LC could be detected (Figure 21). On the western blots of the Fd-fragment, no signal was visible. Therefore, the Fd-fragment and the Fab-fragment were expressed again from CEN plasmids up to higher densities. In the cross-detection, Fd-fragment could be detected in the lysate (Figure 23). Also a signal at the position of the Fab-fragment (54.3 kDa) was visible which means that there have to be both LC and Fd-fragment present in the lysate. Additionally, the bands corresponding to the respective monomers (26.8 kDa LC, 27.5 kDa Fd-fragment) were detected on all western blots. Besides the band of the monomeric Fd-fragment, another band corresponding to possible Fd-fragment dimers (55 kDa) is visible on the western blot in figure 23C. Finally, also bands corresponding to higher oligomers are present on all westernblots. The presence of the monomeric antibody fragments suggests that the Fab-fragment might not be assembled correctly or covalently and breaks during the elution from the affinity beads.

The signal detected after the expression of the antibody fragments from CEN plasmids was quite weak. Therefore, the LC and the Fd-fragment were also expressed from 2µ plasmids. The 1:1 ratio of the antibody fragments per cell is not assured in this way but the detected signal should be stronger. Additionally, the lysate was fractionated after the cell lysis in order to localize the bottleneck of the antibody expression. Again, only the expression of the LC could be detected (Figure 24), no signal was visible for the Fd-fragment. In figure 24A, the expression of the light chain can be followed in a small amount of the complete lysate. In figure 24B, the membrane and the cytosolic fraction are blotted next to each other. Despite some unspecific bands in the sample of the membrane fraction taken immediately after the induction, the expression of the LC is clearly visible. Additionally, also a possible processed and non processed form of the LC could be distinguished (Figure 24, white arrows). In the processed form of the LC, the invertase signal sequence (2.3 kDa) is cleaved. Apart from the LC monomers, bands corresponding to the possible LC dimers and higher oligomers were detected as well. In general, LC was found to accumulate in the endoplasmic reticulum.

In figure 25, the same experiment was repeated with the Fab-fragment. Samples of the complete lysate and the membrane fraction were detected with both α-HA (against the LC) and α-Flag (against the Fd-fragment) antibody. Signals for the Fab-fragment as well as for the

monomeric LC/Fd-fragment and higher oligomers could be detected. The expression of the LC was visible also in the complete lysate (Figure 25A). In contrast, no Fd-fragment was detectible in this sample (Figure 25C). *In vivo*, both antibody chains are synthesized independently from each other (Burrows et al., 1979) and, in contrast to unpaired light chains, which can be secreted from the ER alone, heavy chains can be secreted only if they are assembled together with light chains in form of a correctly folded antibody molecule. It is also known from the literature that the Fd-fragment is not stable *in vitro* (Lilie et al., 1995; Rothlisberger et al., 2005). The C_H1 domain of heavy chains is intrinsically disordered *in vitro* (Feige et al., 2009a) and bound to BiP which retains the heavy chain in ER until it becomes assembled with the LC. The V_H domain, which aggregates above 30 °C *in vitro*, is the least stable of the structured antibody domains (Feige et al., 2010b). These might be some of the reasons why it was not possible to detect any signal for the Fd-fragment alone. The concentration of the Fd-fragment might be so low that it is not sufficient to be visible on a western blot.

Soluble fractions of the Fab-fragment are shown in figure 26. A cross detection was performed again and the presence of both the LC and the Fd-fragment in the lysate could be shown. Besides the Fab-fragment, a signal for the monomeric LC/Fd-fragment and higher oligomers was detected again. The Fab-fragment (54.3 kDa) has a very similar molecular weight as the LC dimers (53.6 kDa) and the Fd-fragment dimers (55 kDa). In some cases, e.g. in figure 23, figure 25 and figure 26, the band at the position around 54 kDa corresponds to both LC/Fd-fragment dimers and the Fab-fragment. A method which could distinguish between the LC/Fd-fragment dimers and the Fab-fragment is the mass spectroscopy (MS). In addition, MS would be also a useful method to prove if the two bands in the Figure 9B (white arrows) are really the processed and non processed version of the LC. Unfortunately, in case of MAK33 expression in *S. cerevisiae*, this protocol could not be used as the expressed antibody amounts were so low that no bands were visible on the SDS-gels and the detection of the respective bands was possible only via western blots.

However, it is possible to estimate the amount of the expressed antibody fragments. On an SDS gel, amounts of 50 ng of the Fab-fragment are still visible (Figure 18). On a western blot detected with the anti-Flag antibody, amounts of up to 2 ng should be detectible according to the manufacturer. Therefore, the amounts of the expressed antibody fragments should be somewhere in this interval (2-50 ng). Given that the expressed amount would be 20 ng in a sample of 20 µl and $OD_{600} = 50$, which was the maximal OD_{600} loaded on the SDS-gels. Then,

it would be necessary to have a culture of 1 l and OD_{600} = 50 to achieve 1 mg of the desired antibody fragment. Or, in other words, to achieve the expression yield of 1 mg of the desired antibody fragment, it would be necessary to have at least 7 l culture of OD_{600} = 7 which is the averaged OD_{600} value reached by yeast cells in the stationary phase (Figure 14). The concentration of the antibody fragment in such a culture would correspond to ~100-150 µg/ml.

In conclusion, an expression system for antibody fragments in *S. cerevisiae* was established, expressing both, the LC and the Fd-fragment. These were found to accumulate in the membrane fraction, suggesting that they are retained within the ER and are not released into the medium. This is in accordance with the literature, as summarized by Gasser and Mattanovich (2007), and Joosten et al. (2003). It remains an open question, whether the expressed MAK33 fragments are within the ER aggregated or soluble. This might be addressed in an experiment, where the membrane fraction is solubilized with a detergent.

Below, several possible reasons for the accumulation of antibody fragments within the ER are discussed together with some suggestions for potential further investigations focused on the improvement of the antibody expression in yeast.

First, optimization of the promoter could lead to the better expression results. *P. pastoris* is the yeast strain most frequently used for antibody expression in yeast (Jeong et al., 2011). In *P. pastoris*, antibodies are mostly produced under the control of the strong inducible alcohol oxidase (AOX1) promoter which can lead to cellular stress due to the accumulation of over-expressed protein. Gasser and coworkers studied the effect of the different promoters on the expression of antibody fragments in *P. pastoris* and found that the expression of both, Fab- and scFv-fragment was better under the weaker, constitutive glyceraldehyde-3-phosphate dehydrogenase (GAP) promoter (Gasser et al., 2006). Therefore, it might be useful to test different promoters such as an inducible Cu^{2+} promoter or a constitutive GAP promoter also for *S. cerevisiae*.

Second, different signal sequences might be worth of testing because the correct processing (cleavage of the signal sequence) is essential for further antibody folding and secretion. Besides the invertase signal sequence, which was successfully used in several studies (Horwitz et al., 1988; Kies, 2001), the *S. cerevisiae* α-mating factor signal sequence is one of the most used signal sequences (Abdel-Salam et al., 2001; Damasceno et al., 2007; Gasser et al., 2006; Hackel et al., 2006; Ogunjimi et al., 1999). Recently, a library of the mutant α-

mating factor leader peptides was screened for an enhanced antibody secretion in *S. cerevisiae* (Rakestraw et al., 2009). In this study, a significant improvement was achieved in the secretion of not only scFv-fragment but also full-length, glycosylated, functional human IgG. For the expression of antibody fragments in *P. pastoris* , also human leader sequences were tested, but they turned out not to be suitable for antibody secretion (Gasser et al., 2006).

Third, the major problem during the expression of antibodies in yeast seems to be the accumulation of the expressed antibody fragments in the folding/secretion apparatus. Generally, accumulation of unfolded proteins within the cell activates the unfolded protein response (UPR) which leads to the enhanced expression of the molecular chaperones and activation of the ERAD pathway (section 1.3). The UPR is activated by the transcription factor Hac1. Therefore, it might be possible to increase the amount of needed chaperones by additional over-expression of Hac1. The higher amounts of available chaperones could increase the chances of the expressed antibody fragments to fold properly. The effect of Hac1 on the secretion of invertase, α-amylase and endoglucanase in *S. cerevisiae* has already been investigated (Valkonen et al., 2003). It was shown, that the over-expression of Hac1 led to the increased protein secretion, whereas Hac1 disruption decreased the secretion of expressed proteins in *S. cerevisiae*. However, the over-expression of Hac1 showed no effect on the expression of antibody fragments in *S. cerevisiae* (Kies, 2001) and exhibited only moderate effect on the expression of Fab-fragment in *P. pastoris* (Gasser et al., 2006). Therefore, the over-expression of Hac1 does not seem to be suitable for improving the antibody expression in yeast.

The UPR activates the ERAD pathway, in which terminally unfolded proteins are retrotranslocated through the ER membrane back to the cytosol where they are degraded in a proteasome (section 1.3.2). In *S. cerevisiae*, besides BiP also the Hsp40s Scj1p and Jem1p maintain the solubility of the ERAD substrates which enables their retrotranslocation from the ER and degradation (Nishikawa et al., 2001). The UPR also leads to the enhanced expression of molecular chaperones. A direct over-expression of chaperones known to assist antibody folding was shown to improve antibody expression in yeast. Especially BiP and protein disulfide isomerase (PDI) positively influenced the expression of scFv and Fab-fragments in *P. pastoris* (Damasceno et al., 2007; Gasser et al., 2006) as well as the expression of scFv-fragments in *S. cerevisiae* (Hackel et al., 2006; Kauffman et al., 2002; Shusta et al., 1998).

Kar2, the yeast homologue of BiP, functions as a chaperone and it also plays a role in the translocation of secretory proteins across the ER membrane (Nguyen et al., 1991). Additionally, Kar2 dissociates upon ER stress from Ire1 which leads to the activation of the UPR (Okamura et al., 2000). However, neither the over-expression of BiP nor the over-expression of Kar2 showed an effect on the expression of antibody fragments (LC, HC and Fd-fragment) in *S. cerevisiae* (Kies, 2001).

Unfolded substrates bound to Kar2 are released upon ATP-hydrolysis. In *S. cerevisiae*, the nucleotide exchange factors Lhs1p and Sil1p are responsible for the exchange of ADP for ATP which makes Kar2 available for another unfolded substrate. Therefore, also over-expression of Lhs1p and Sil1p could be favorable with respect to antibody expression. Especially Lhs1 might be worth testing as it represents the yeast homologue of the mammalian Grp170. The glucose regulated protein Grp170 is an Hsp110 homologue that acts as an ER chaperone. Grp170 was shown to bind immunoglobulin chains and was proposed to play a role in antibody folding and assembly (Lin et al., 1993).

Thiol oxidoreductases are also needed for antibody folding and assembly. As already mentioned, the over-expression of protein disulfide isomerase (PDI) was shown to positively influence the expression of antibody fragments in yeast. Additionally, PDI also plays a role in the ERAD pathway responsible for the degradation of the terminally misfolded proteins. Yeast Pdi1p was shown to associate with Mnl1p, ER mannosidase-like protein, which is involved in the ERAD-L pathway in *S. cerevisiae* and the Pdi1p-Mnl1p complex was proposed to initiate the degradation of unfolded proteins (Gauss et al., 2011). Besides PDI, also the expression of other thiol oxidoreductases might be advantageous for antibody production in yeast. One such example is ERdj5, a mammalian disulfide reductase, which has been shown to accelerate ERAD through association with EDEM and BiP (Ushioda et al., 2008). Another example of a potential favorable thiol oxidoreductase in *S. cerevisiae* is Mpd1p which was proposed to act as a homologue of mammalian ERp57 in yeast (Kimura et al., 2005). Mpd1p was shown to interact with Cne1p, a homologue of mammalian calnexin in yeast. Calnexin is a lectin chaperone which is, together with calreticulin, responsible for the folding of gylcoproteins in mammalian cells (Ou et al., 1993). Calnexin and calreticulin associate with ERp57, a ER thiol oxidoreductase, which is involved in the folding of disulfide-bonded, glycosylated substrates (Molinari and Helenius, 1999). Antibodies represent glycosylated, disulfide bonded proteins, therefore the over-expression of both calnexin/calreticulin (or the yeast

homologue Cne1p) and/or ERp57 (or the yeast thiol oxidoreductase Mpd1p) might have a positive effect on antibody expression in yeast. However, all mentioned proteins (calnexin, calreticulin, Cne1p, Mn1p, ERp57, Mpd1p) interact with glycoproteins. Since in this work only Fab-fragment was expressed, consisting of the LC and the Fd-fragment only (V_H and C_H1 domains), it should be emphasized that this concerns only full length antibodies glycosylated at the C_H2 domain.

Generally, an over-expression of proteins that are known to assist antibody folding but do not have homologues in yeast might improve the antibody expression in *S. cerevisiae*. One of these proteins is the ER chaperone Grp94 (glucose regulated protein 94), a member of the Hsp90 family that interacts with unassembled antibody chains. It was shown that in contrast to BiP, which interacts with an early disulfide intermediate of a light chain and dissociates within few minutes, Grp94 associates with late, fully oxidized folding intermediates of the LC which are handed over from BiP (Melnick et al., 1994). The lack of Grp94 might be one of the possible reasons why folding and assembly of antibodies is not correctly performed in yeast.

Another protein that promotes antibody folding and secretion in B cells is the small ER resident protein pERp1 (Shimizu et al., 2009; van Anken et al., 2009). pERp1, also known as Mzb1, associates in innate-like B cells in Ca^{2+}-dependent manner with BiP and Grp94 as well as with ERp57 and the Mzb1-ERp57 interaction leads to an exchange of calnexin and calreticulin (Flach et al., 2010). Although up to now only three studies have been published about pERp1 and therefore not much is known about this protein, the data suggests that pERp1 plays a very important role in antibody folding. Since nothing has been known about pERp1 structure and stability, in this work these issues were elucidated and are discussed in detail in the next section.

3.2 Biophysical analysis of pERp1

To elucidate the structure and stability of pERp1, the wild type (WT) and six mutants were expressed (Figure 29, section 2.2.2.1), purified (Figure 30, section 2.2.2.2) and analyzed with size exclusion chromatography, circular dichroism (CD) spectroscopy and fluorescence spectroscopy. pERp1 harbors six cysteines connected in a typical pattern (Figure 11B). In the studied pERp1 mutants, some of these cysteines are mutated into serines which abolishes the

respective disulfide bonds. Depending on which cysteines were mutated to serines, pERp1 mutants can be divided into two groups referred to as “S” and “only” (Figure 28).

In the size exclusion chromatography, all pERp1 proteins eluted in a single peak (Figure 33A) with an exception of the C50-178only mutant which seemed to be degraded (Figure 33B). The elution times of the pERp1 proteins were between the elution times for a theoretical monomer and a theoretical dimer with a slight shift towards the monomer (Figure 34). Subsequent analytical centrifugation confirmed that pERp1 is a monomeric protein (Figure 35). According to CD spectroscopy, all pERp1 proteins have predominantly an α-helical structure with the exception of the C50-178only mutant which seems rather unfolded (Figure 36). Since the C50-178only mutant seems to be unfolded and/or degraded, it was not regarded in subsequent experiments.

The stability of the pERp1 proteins was investigated by thermal transitions (Figure 37) which revealed an interesting effect of the 95-143 disulfide bond on the stability of the protein. pERp1 WT is stable up to ~55 °C and then melts cooperatively with the melting temperature (Tm) of 71 °C. However, if the disulfide bond 95-143 is removed (C95-143S mutant) the protein is even more stable with the Tm of 81 °C. The other way round, the C95-143only mutant which contains only the 95-143 disulfide bond is with the Tm of 30 °C less stable than the reduced WT lacking all disulfide bonds (Tm 40 °C). Therefore, the C95-143S mutant (lacking the 95-143 disulfide bond) is the most stable of all pERp1 proteins and the C95-143only mutant (containing only the 95-143 disulfide bond) is the least stable protein of all pERp1 proteins. Melting temperatures of all pERp1 proteins are listed in the table in figure 37B. For better illustration, the effect of the 95-143 disulfide bond is depicted in the figure 44 on the next page.

The destabilizing effect of the 95-143 disulfide bond was also confirmed by a comparison of the reversibility of the thermal transitions of the WT and the 95-143S mutant. For the WT, the thermal transition is only partly reversible whereas the transition of 95-143S is reversible to a large extent. In addition, the CD spectra of the 95-143S mutant before and after the thermal transition are nearly identical in contrast to the WT (Figure 39).

The stability of the pERp1 proteins was also investigated upon unfolding with guanidine hydrochloride (GdmHCl). Transition curves and corresponding transition points $[D]_{1/2}$ are shown in figure 41. Upon GdmHCl unfolding, in contrast to the thermal stability, the most

stable pERp1 protein is the WT possessing all disulfide bonds with $[D]_{1/2}$ = 3.3 M GdmHCl and the least stable is the reduced WT lacking all disulfide bonds with $[D]_{1/2}$ = 0.28 M GdmHCl.

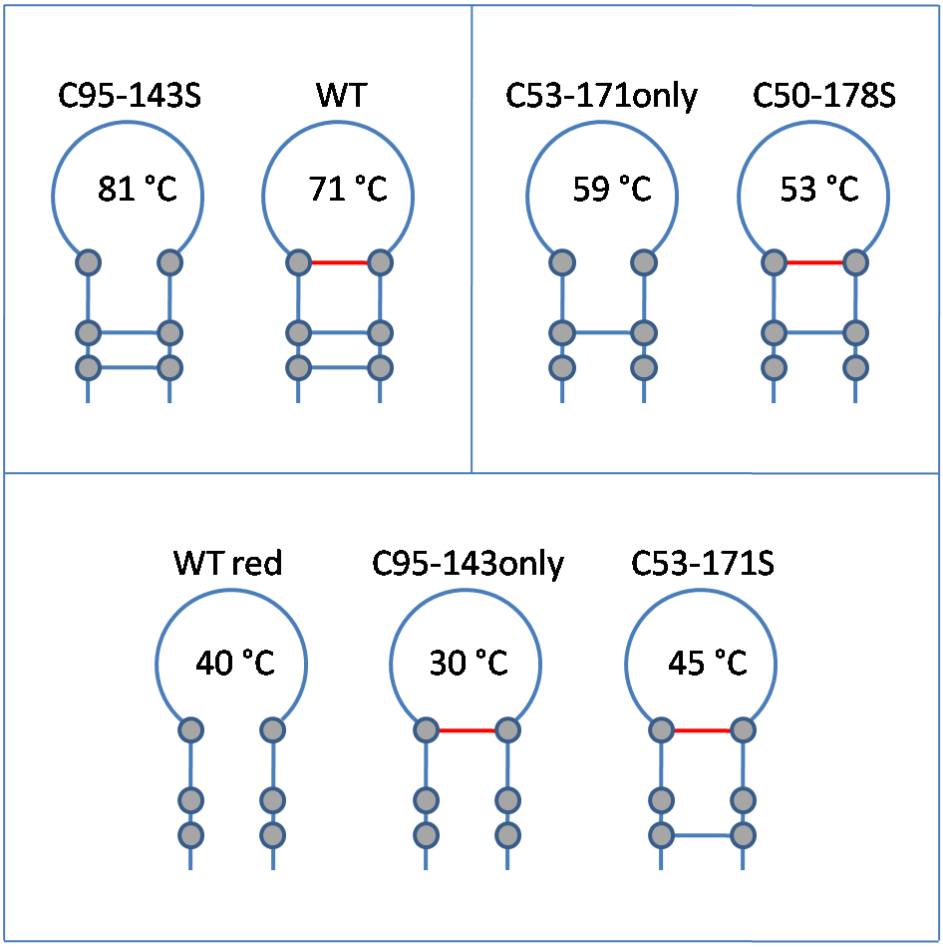

Figure 44: Effect of the 95-143 disulfide bond on the thermal stability of pERp1 proteins. The schematic structure of the respective proteins corresponds to the structure shown in figure 28. The 50-178 and 53-171 disulfide bonds present in the respective pERp1 proteins are depicted as blue lines, the 95-143 disulfide bond is depicted as a red line. Melting temperatures are given for the respective proteins. The presence of the 95-143 disulfide bond destabilizes the protein and lowers the melting temperature by about 5-10 °C in comparison with the proteins lacking the 95-143 disulfide bond.

pERp1 was also shown to bind to BiP (Shimizu et al., 2009) and in this work the pERp1-BiP binding was shown to be nucleotide dependent (Figure 42). Surface plasmon resonance measurements did not show any binding without nucleotides. However, BiP bound to pERp1 with K_D = 1.89 +/– 0.37 µM and K_D = 1.09 +/– 0.38 µM in presence of ATP and ADP, re-

spectively. It is known from the literature that the dissociation constant of the C_H1 antibody domain, representing the natural substrate of BiP, is 7.4 +/– 0.2 µM (Marcinowski et al., 2011). In contrast, the dissociation constant of ERdj3, which is the main BiP co-chaperone in antibody folding in mammalian cells (Shen and Hendershot, 2005), is 0.9 +/– 0.1 µM (Marcinowski et al., 2011). In this regard, the K_D of pERp1 is rather similar to the dissociation constant of a co-chaperone than to the constant of a substrate. However, in contrast to ERdj3 which stimulates the ATPase activity of BiP, pERp1 does not seem to have any effect on the ATPase activity of BiP (Figure 43).

3.3 Conclusion

In this work, an expression system for antibody fragments was established which provides the opportunity for further studies on improvements of antibody expression in yeast. An important issue would be to identify the bottlenecks of the expression that leads to the accumulation of the antibody fragments in yeast. Some options that should be considered are, e.g., testing of different ER targeting sequences, testing of different promoters, eventually integration of the antibody sequence into the chromosome. Co-transformation of yeast cells with chaperones that are known to assist protein folding in both yeast and mammalian cells (such as BiP and PDI) should also promote antibody folding. Finally, co-expression of chaperones which occur in mammalian cells but not yeast (such as Grp94 and pERp1) might have a positive effect on the antibody expression in yeast as well. Processes important for the antibody expression in yeast, including the possibilities concerning further investigations, are schematically depicted in figure 45 on the next page.

One of the chaperones whose effect might be favorable for antibody expression in yeast is pERp1. In this work, it was shown that pERp1 is a monomeric, α-helical protein which binds to BiP in a nucleotide dependent manner. pERp1 contains six cysteins connected to a specific pattern via disulfide bonds (Figure 11B). In this work, studies of the thermal stability of the pERp1 mutants missing defined disulfide bonds were performed and an interesting destabilizing effect of the 95-143 disulfide bond was shown. The Tm of the pERp1 mutant missing the 95-143 disulfide bond is 10 °C higher than the Tm of the WT with all disulfide bonds. Similarly, the pERp1 mutant containing only the 95-143 disulfide bond is the least stable pERp1 protein with Tm = 30 °C which is 10 °C lower than the Tm of the reduced WT missing all disulfide bonds.

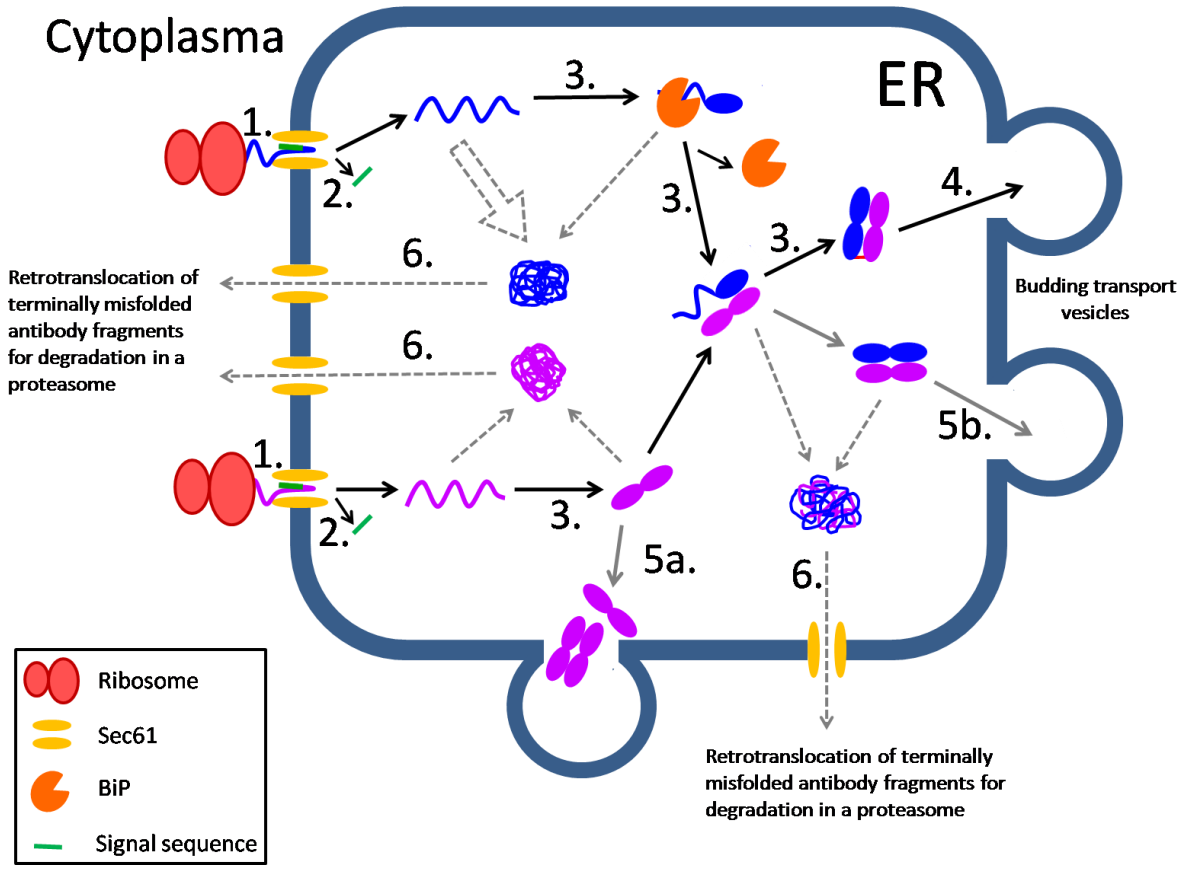

Figure 45: Processes important for folding of the antibody fragments within the yeast ER. Productive folding pathways leading to the secretion of the proper folded antibody fragments are depicted with black solid arrows. Grey solid arrows represent the secretion of monomeric or incorrectly assembled antibody fragments. Unsuccessful folding pathways leading to protein aggregation and degradation are depicted with grey dashed arrows. The free Fd-fragment, i.e. not bound to BiP or LC, is not stable. Therefore, it might be assumed that the free Fd-fragment would aggregate to a large extend as indicated by a large arrow. The respective processes and their suggested improvements are as followed:

1. Transcription: testing of different promoters.
2. Processing (cleavage of the signal sequence): testing of different signal sequences.
3. Folding: co-expression of yeast ER chaperones and folding enzymes (Pdi1, Kar2 etc.) as well as co-expression of mammalian ER chaperones and folding enzymes involved in antibody folding (Grp94, pERp1, Bip, PDI, etc).
4. Secretion of the correctly folded and assembled antibody fragments from the ER.
5. Secretion of the incorrectly assembled antibody fragments such as monomeric or dimeric light chains (5a) or non-covalently linked heterodimers (5b).
6. Quality control: co-expression of the proteins involved in the ERAD pathway to promote the degradation of the misfolded or aggregated proteins in order to prevent their accumulation in the ER and the subsequent overload of the secretory pathway.

4 Material and Methods

4.1 Material

4.1.1 Chemicals

Acrylamide solution (38% acrylamide, 2% bisacrylamide)	Serva, Heidelberg, Germany
Adenosine-5´-diphosphate (ADP)	Sigma-Aldrich, St. Louis, USA
Adenosine-5´-triphosphate (ATP)	Roche, Mannheim, Germany
Agarose, ultra pure	Serva, Heidelberg, Germany
Ammoniumperoxodisulfate (APS)	Roth, Karlsruhe, Germany
Ampicillin	Roth, Karlsruhe, Germany
Bradford reagent	Serva, Heidelberg, Germany
Bromphenol blue sodium salt	Merck, Darmstadt, Germany
Dodecylsulfate-Na-salt (SDS)	Serva, Heidelberg, Germany
Ethanol p.a.	Merck, Darmstadt, Germany
Ethylendinitrilotetraacetic acid (EDTA)	Merck, Darmstadt, Germany
Glycerol	Roth, Karlsruhe, Germany
Guanidine hydrochloride	Sigma-Aldrich, St. Louis, USA
4-(2-hydroxyethyl)-1-piperazineethanesulfonic acid (HEPES)	Roth, Karlsruhe, Germany
Imidazol	Sigma-Aldrich, St. Louis, USA
Isopropyl β-D-1-thiogalactopyranoside (IPTG)	Serva, Heidelberg, Germany
Magnesium chloride	Roth, Karlsruhe, Germany
2-Mercaptoethanol	Sigma-Aldrich, St. Louis, USA

Milk powder	Roth, Karlsruhe, Germany
N,N,N´,N´-Tetramethylethylenediamine (TEMED)	Roth, Karlsruhe, Germany
Potassium chloride	Roth, Karlsruhe, Germany
Protease inhibitor mix (HP)	Serva, Heidelberg, Germany
Sodium chloride	Merck, Darmstadt, Germany
Stain G	Serva, Heidelberg, Germany
Titriplex® (Ethylendinitrilotetraacetic acid)	Merck, Darmstadt, Germany
Tris(2-carboxyethyl)phosphine hydrochloride (TCEP)	Sigma-Aldrich, St. Louis, USA
Tris-(hydroxymethyl)-aminomethane (Tris)	Roth, Karlsruhe, Germany
Triton® X-100 detergent	Merck, Darmstadt, Germany
Tween® 20 detergent	Merck, Darmstadt, Germany

All other used chemicals were purchased from Merck (Darmstadt, Germany) and were of grade p.a. All buffers and solutions were prepared with double distilled water.

4.1.2 Proteins

Alkaline phosphatase	Roche, Mannheim, Germany
DNase I	Roche, Mannheim, Germany
Go-Taq-DNA-Polymerase	Promega, Madison, USA
Pfu-DNA-Polymerase	Promega, Madison, USA
Pwo-DNA-Polymerase	Roche, Mannheim, Germany
Restriction endonucleases	Promega, Madison, USA
T4-Ligase	Promega, Madison, USA

4.1.2.1 Antibodies

Anti-Flag (developed in rabbit)	Sigma-Aldrich, St. Louis, USA
Anti-HA (developed in rabbit)	Sigma-Aldrich, St. Louis, USA
Anti-rabbit-peroxidase (developed in goat)	Sigma-Aldrich, St. Louis, USA
Anti-Kar2 (developed in rabbit)	Santa Cruz Biotechnology, Santa Cruz, USA

4.1.3 Standards and Kits

BiaCore amine coupling kit	BiaCore Inc., Uppsala, Sweden
Calibration proteins for HPLC	Sigma-Aldrich, St. Louis, USA
ECL Plus Western Blotting Detection System	GE Healthcare, Munich, Germany
High Pure PCR Product Purification Kit	Promega, Madison, USA
peqGOLD 1 kb Ladder	Peqlab, Erlangen, Germany
SDS-PAGE Standard Low Range	BioRad, München, Germany
SERVAChrom Protein Standard III	Serva, Heidelberg, Germany
Wizard® Plus SV Mini-Preps DNA purification kit	Promega, Madison, USA

4.1.4 Chromatographic Columns and Affinity Gels

Anti-Flag® M2 Affinity Gel	Sigma-Aldrich, St. Louis, USA
EZview™ Red Anti-HA Affinity Gel	Sigma-Aldrich, St. Louis, USA
HisTrap™ FF (1 ml)	GE Healthcare, Munich, Germany
Resource™ Q (6 ml)	GE Healthcare, Munich, Germany
Superdex™ 75	GE Healthcare, Munich, Germany

4.1.5 Additional materials

Amicon® Ultra Centrifugal Filter Units (10 000 MWCO)	Millipore, Billerica, USA
Glass beads (0.25-0.5 mm)	Roth, Karlsruhe, Germany
Millex®-GS Sterile Filter (0.22 µm)	Millipore, Billerica, USA
Plastibrand® disposable cuvettes	VWR, Munich, Germany
Roti®-NC Nitrocellulose Membrane	Roth, Karlsruhe, Germany
Slide-A-Lyzer Dialysis Cassette (10 000 MWCO)	Thermo Scientific, Rockford,USA
Spectra/Por® Dialysis Membrane (MWCO: 6-8000)	Spectrumlabs, Rancho Dominguez, USA
Ultrafiltration Membrane (10 000 NMWL)	Millipore, Billerica, USA
Whatman® Chromatography Paper	GE Healthcare, Munich, Germany
Kodak Biomax XAR film	Sigma-Aldrich, St. Louis, USA

4.1.6 Biological materials

4.1.6.1 Microbial strains

Microbial strain	**Genotype**	**Origin**
E. coli Mach1-T1^{R}	*lac*ZΔM15 *hsd*R *lac*X74 *rec*A *end*A *ton*A	Invitrogen, Darmstadt, Germany
E. coli M15	*nal*S *str*S *rif*S *thi- lac- ara- gal+ mtl-*. F- *rec*A+ *uvr*+ *lon*+ *Kan*R	Qiagene, Hilden, Germany
E.coli XL 1 Blue	*rec*A1 *end*A1 *gyr*A96 *thi*-1 *hsd*R17 *sup*E44 *rel*A *lac* [F´proAB *lac*IqZDM15 Tn10 (*Tet*R)]	Stratagene, La Jolla, USA
S. cerevisiae BY4741	MATa; his3Δ 1; leu2Δ 0; met 15Δ 0; ura3Δ 0	Euroscarf, Frankfurt, Germany

4.1.6.2 Plasmids

Plasmid	Promotor	Selection marker	Origin
pQE30	T5	Ampicillin	(Shimizu et al., 2009)
p413Gal1	Gal1	Ampicillin, HIS	American Type Culture Collection, Manassas, USA
p416Gal1	Gal1	Ampicillin, URA	American Type Culture Collection, Manassas, USA
p423Gal1	Gal1	Ampicillin, HIS	American Type Culture Collection, Manassas, USA
p426Gal1	Gal1	Ampicillin, URA	American Type Culture Collection, Manassas, USA

4.1.7 Media for microorganism cultivation

LB_0 and YPD media were prepared according to the manufacturer instructions by mixing 20 g/l LB_0 (Serva, Heidelberg, Germany) or 50 g/l YPD (Roth, Karlsruhe, Germany) with dd H_2O and autoclaved. For agar plates, 20 g/l agar was added before autoclaving.

For 1 liter of the minimal medium following substances were mixed: 6.7 g Difco™ (Yeast Nitrogen Base w/o Amino Acids, BD, Franklin Lakes, USA), 2 g “drop-out mix”, 20 g sugar and 1 ml 1 M NaOH, filled up with dd H_2O and autoclaved. For agar plates, 20 g/l agar was added before autoclaving.

Depending on the respective media, the used sugar varied between glucose (Merck, Darmstadt, Germany), raffinose (Merck, Darmstadt, Germany) and galactose (VWR, Munich, Germany).

For the “drop-out mix”, following substances were mixed and the mixture was thoroughly homogenized in the mixer mill by shaking for 15 min x 30 s^{-1}.

Adenine	0.5 g	Methionine	2.0 g
Arginine	2.0 g	Phenylalanine	2.0 g
Aspartic acid	2.0 g	Threonine	2.0 g
Histidine	2.0 g	Tryptophan	2.0 g
Leucine	10.0 g	Tyrosine	2.0 g
Lysine	2.0 g	Uracil	2.0 g

All substances used for the “drop-out mix” were obtained from Sigma-Aldrich, St. Louis, USA. The substance(s) corresponding to the selection marker of the desired plasmid were left out.

4.1.8 Equipment

Balances	
Analytical balance SI-234	Denver Instrument, Bohemia, USA
Halfmicro balance BL 1500	Satorius, Göttingen, Germany
Centrifuges	
Avanti™ J-25 Centrifuge	Beckman Coulter, Krefeld, Germany
Beckman XL-I analytical ultracentrifuge	Beckman Coulter, Krefeld, Germany
Eppendorf 5418 table-top centrifuge	Eppendorf, Hamburg, Germany
Eppendorf 5418R table-top coolable centrifuge	Eppendorf, Hamburg, Germany
Optima™ MAX-E Ultracentrifuge	Beckman Coulter, Krefeld, Germany
Rotina 420R	Hettich, Tuttlingen, Germany
Chromatography	
FPLC System with LKB Frac 100 and UV detector	AmershamPharmacia, Uppsala, Sweden

LC-20AT liquid chromatography system with UV/VIS and fluorescence detector	Shimadzu, Columbia, USA
Circular dichroism	
Jasco J-715 with PTC Peltier temperature unit	Jasco, Groß-Umstadt, Germany
Fluorescence	
FluoroMax-2 Fluorescence Spectrophotometer	Horiba Jobin Yvon, Unterhaching, Germany
FluoroMax-4 Spectrophotometer	Horiba Jobin Yvon, Unterhaching, Germany
Electrophoresis and Westernblots	
Fastblot B44 western blot apparatus	Biometra, Göttingen, Germany
Power Supply EPS 601	AmershamPharmacia, Uppsala, Sweden
SE 250 Mighty Small II gel electrophoresis unit	Hoefer, Holliston, USA
Surface Plasmon Resonance	
Biacore® X	BiaCore, Uppsala, Sweden
UV/VIS Spectrophotometers	
NanoDrop 2000	Thermo Scientific, Rockford,USA
VarianCary50 Bio	Agilent Technologies, Böblingen, Germany
Ultrospec 1100 pro	GE Healthcare, Munich, Germany

4.1.8.1 Additional Equipment

Biometra TI3 UV lamp	Biometra, Göttingen, Germany
Brunswick Ultra Low Temperature Freezer	Eppendorf, Hamburg, Germany
Centromat® S culture shaker	Braun Biotech, Melsungen, Germany
Constant Cell Disruption System	Constant Systems, Daventry, UK

Diaphragm Vacuum Pump	Vacuumbrand, Wertheim, Germany
Haake F6/G40 water bath	Hakke, Karlsruhe, Germany
Heidolph MR Hei-Standard magnetic stirrer	Heidolph, Schwabach, Germany
Image Scanner III	GE Healthcare, Munich, Germany
Image Quant 300	GE Healthcare, Munich, Germany
Incubator Mytron	Eppendorf, Hamburg, Germany
Leica Mark II, ABBE Refractometer	Leica, Solms, Germany
Mixer mill MM 400	Retsch, Haan, Germany
Optimax X-Ray Fil Processor	Protec Medizintechnik, Oberstenfeld, Germany
pH meter	WTW, Weilheim, Germany
T-7 test tube roller	Eppendorf, Hamburg, Germany
Thermomixer comfort	Eppendorf, Hamburg, Germany
Vortex mixer	Heidolph, Schwabach, Germany

4.1.9 Computer programs

Biacore X Control Software	BiaCore, Uppsala, Sweden
CDNN	http://gerald-boehm.de
CD Spectra Manager	Jasco, Groß-Umstadt, Germany
ClustalW2	http://www.ebi.ac.uk/Tools/msa/clustalw2/
Chromas 2.32	Technelysium, Brisbane, Australia
ExPASy Tools	http://www.expasy.org
FluorEssence	Horiba Jobin Yvon, Unterhaching, Germany
DataMax	Horiba Jobin Yvon, Unterhaching, Germany

Gimp 2.6	http://www.gimp.org
Image Quant	GE Healthcare, Munich, Germany
LabScan 6.0	GE Healthcare, Munich, Germany
LCsolution	Shimadzu, Columbia, USA
Microsoft Office 2007	Microsoft, Unterschleißheim, Germany
Origin 8.0	OriginLab, Northampton, USA

4.2 Methods of molecular biology

4.2.1 Cultivation and storage of **E. coli**

E. coli cultures were prepared from glycerol stocks or by adding a single colony of XL1-Blue or M15 *E. coli* cells from a LB_0 agar plate into LB_0 medium containing 100 µg/ml ampicillin. Cultures with volumes up to 10 ml were incubated in a test tube roller, cultures with volume above 10 ml were incubated in an incubator upon orbital shaking. Liquid cultures were incubated at 37 °C, pERp1 expressing *E. coli* cultures were inoculated from over-night cultures and incubated at 37 °C, 30 °C or at room temperature (see section 4.3.1). Agar plates were incubated at least 16 hours at 37 °C.

Growth of *E. coli* cells was determined photometrically by measuring optical density at 600 nm (OD_{600}). An $OD_{600} \sim 1$ corresponds to approximately 10^9 cells.

For short-time storage, *E. coli* cultures were kept in a fridge at 4 °C. For long-term storage, glycerol stocks were prepared by mixing 600 µl *E. coli* culture with 300 µl 50 % glycerol. The mixture was shock-frozen in liquid nitrogen and kept at -80 °C.

4.2.2 Cultivation and storage of **S. cerevisiae**

S. cerevisiae liquid cultures were prepared by transferring a single colony from a corresponding agar plate into liquid YPD or minimal medium and incubated at 30 °C. As for *E. coli* cultures, volumes up to 10 ml were incubated in a test tube roller, cultures with volumes above 10 ml were incubated in an incubator upon orbital shaking. Agar plates were incubated at 30 °C for at least 40 hours.

Growth of *S. cerevisiae* cells was determined photometrically by measuring the OD_{600}, analogously to *E. coli*.

S. cerevisiae cultures were stored at 4 °C and regularly inoculated into fresh medium every 3-4 weeks, followed by incubation at 30 °C for at least 20 hours.

4.2.3 DNA digestion, dephosphorylation and ligation

4.2.3.1 Digestion of DNA by restriction endonucleases

Both analytical and preparative DNA digestions were performed. For analytical digestion, a final volume of 6 µl was used, consisting of 5 µl DNA and 1µl of the "pre-mix" containing one or two restriction enzyme(s) in 10x reaction buffer. For preparative digestion, 50 µl DNA were mixed with 2 µl of one or two restriction enzyme(s) and 6 µl of 10x reaction buffer. Restriction digest samples were incubated at 37 °C for at least 4 hours and afterwards analyzed by agarose gel electrophoresis. Preparative digests were purified with the PCR Product Purification kit.

4.2.3.2 Dephosphorylation of DNA

Digested plasmids were dephosphorylated in order to prevent the self-ligation. 50 µl of the digested plasmid were mixed with 6 µl of 10x dephosphorylation buffer and 4 µl alkaline phosphatase and incubated at 37 °C for 1 h. Subsequently, the sample was purified with the PCR Product Purification kit.

4.2.3.3 Ligation of DNA

A digested and dephosphorylated plasmid was mixed with a digested insert DNA in a concentration ratio of 1:3 in a final volume of 16 µl to which 2 µl of 10x ligation buffer and 2 µl of T4 DNA ligase were added. DNA ligation was performed either 4 h at room temperature or at 4 °C over night. Subsequently, XL1-Blue *E. coli* cells were transformed with the ligated DNA.

4.2.4 DNA isolation and purification

4.2.4.1 Solutions and buffers used for DNA isolation and purification

Solution for 1% agarose gels	1 g agarose 100 ml TAE buffer (1x) 3 µl Stain G or ethidiumbromide solution
50x TAE Puffer	2 M Tris/Acetate, pH 8 50 mM EDTA
10x Agarose gel loading buffer	Glycerol 50% (v/v) Bromphenole blue 0.025% (w/v) Xylencyanole 0.025% (w/v)

4.2.4.2 Agarose gel electrophoresis

DNA fragments were separated in 1% agarose gels which were prepared by heating a 1% agarose solution (see section 4.2.4.1) until agarose dissolved. After cooling down to a temperature of ~50 °C, 3 µl of "Stain G" were added. DNA samples were mixed with 1/10 volume of a loading buffer (see section 4.2.4.1) and electrophoresis was performed in 1x TAE buffer for 20 min upon constant voltage of 125 V. Subsequently, gels were analyzed in the "Image Quant 300". As a molecular weight standard, the "peqGOLD 1 kb ladder" was used.

4.2.4.3 Isolation of DNA from agarose gels

After electrophoresis, agarose gels were illuminated by UV light and the respective bands were excised from the gels. Subsequently, DNA was purified with the PCR Product Purification kit and stored at -20 °C for further usage.

4.2.5 Preparation of chemical competent E. coli cells

100 ml of *E. coli* culture were grown at 37 °C until an OD_{600} ~ 0.8. After addition of 2 ml sterile 1 M $MgCl_2$, the culture was incubated for further 10 min at 37 °C and afterwards for 60 min on ice. After centrifugation (4500 rpm, 5 min, 4 °C), cells were resuspended in 20 ml sterile solution A and incubated for additional 60 min on ice. After another centrifugation (4500 rpm, 5 min, 4 °C), cells were resuspended in 2 ml of solution A with 15% glycerol (v/v) and divided into 200 µl aliquots which were shock-frozen in liquid nitrogen and stored at -80 °C for further usage.

Solution A	
3 M sodium acetate, pH 5.5	13 ml
1 M $CaCl_2$	100 ml
2.8 M $MnCl_2$	25 ml
H_2O	862 ml

4.2.6 Transformation of E. coli

An aliquot of competent *E. coli* cells (see section 4.2.5) was defrosted on ice and mixed with either 1 µl of plasmid DNA or 20 µl of fresh ligated DNA (see section 4.2.3.3). After 15 min of incubation on ice, samples were heat-shocked at 42 °C for 60 s and subsequently cooled on ice for 2 min. Afterwards, 1 ml of sterile LB_0 medium was added and the samples were incubated at 37 °C for 30 min. Then, the cells were spun down (1 min, 5000 rpm, RT), the supernatant was discarded, cells were resuspended in the remaining media and plated out to LB_0 agar plates containing 100 µg/ml ampicillin.

4.2.7 Transformation of S. cerevisiae

1 ml of a fresh over-night *S. cerevisiae* culture was spun down for 5 s at room temperature and the supernatant was discarded. After addition of 2 µl of 10 mg/ml "carrier DNA" (single stranded DNA from salmon testes, Sigma-Aldrich, St. Louis, USA), cells were resuspended in the remaining liquid. Subsequently, 5-7 µl plasmid DNA, 0.5 ml sterile "plate-mix" and 40 µl sterile 1 M dithiothreitol were added one after another with vortexing after each step. Cells were incubated at least 6 hours (typically over night) at room temperature and then subjected to a heat shock at 42 °C for 10 min. Finally, cells were plated out to agar plates with corresponding minimal medium and left at least 36 h at 30 °C.

Plate Mix	
45% polyethylene glycol	90 ml
1 M LiOAc	10 ml
1 M Tris, pH 7.5	1 ml
0.5 M EDTA	0.2 ml

4.3 Protein expression and purification

All described procedures were used for expression and purification of pERp1 proteins.

4.3.1 Protein expression, harvest and storage of cells

pERp1 proteins were expressed from glycerol stocks of *E. coli* cultures. A small amount of a corresponding glycerol stock was inoculated into 150 ml LB_0 medium with 100 µg/ml ampicillin and the preculture was grown at 37 °C over night. Protein expression was performed in 15 l of LB_0 medium, divided into 6 flasks à 2.5 l where each was inoculated with 20 ml of the over-night preculture. Cells were grown at 37 °C until they reached an OD_{600} ~ 0.8 and protein expression was subsequently induced by addition of 1/1000 culture volume of 1 M IPTG. Times and temperatures of further incubation varied between 3-5 h at 37 °C or 30 °C and over night at room temperature.

Cells were harvested by centrifugation (7000 rpm, 10 min, 8 °C) and washed with 40 mM HEPES/HCl, pH 7.0. Afterwards, cells were either directly disrupted or the cell pellet was frozen for short term storage at -20 °C.

4.3.2 Cell disruption

Cells were resuspended in "cell lysis buffer" (40 mM HEPES/HCl, 50 mM imidazol, pH 7.0 containing protease inhibitor and Dnase I) and lysed in a cell disruption system at the pressure of 1.8 kbar. Afterwards, the cell lysate was centrifuged for 40 min at 22 000 rpm, 8 °C. The pellet was discarded and NaCl was added to the clear supernatant until the final concentration of 400 mM. Another centrifugation at 22 000 rpm, 8 °C for at least 20 min was performed if the supernatant got cloudy after the addition of NaCl and the supernatant was loaded on the HisTrap FF column.

4.3.3 Affinity chromatography

Affinity chromatography is a very useful method for protein purification which enables the separation of a desired protein from a protein mixture. Affinity chromatography is based on the interaction of the desired protein with a particular ligand that is covalently linked to the column matrix. For this purpose, some characteristics of the desired protein such as the isoelectric point (pI) can be used as well as particular affinity tags that can be artificially introduced to the N- or C-terminus of the desired protein in order to facilitate its purification. The

desired protein, which bound to the matrix, can be released from the column by competitive replacement or by changing buffer conditions such as pH, ionic strength etc.

4.3.3.1 Ni-affinity chromatography

Ni-affinity chromatography on a HisTrap FF column was used in this work as the first method in the purification procedure of pERp1 proteins. Binding the protein to the column is based on the interaction between Ni^{2+} ions which are linked to the column matrix and an N-terminal affinity His_6-tag of the pERp1 proteins. Imidazol rings of the six histidines bind to the nickel ions and the bound protein can be eluted by increased imidazol concentration in the running buffer.

4.3.3.2 Ion exchange chromatography

The principle of this method is based on the interaction between oppositely charged proteins and column matrix. Proteins possess a particular net charge consisting of the charges of the N- and C- termini and the side chains. Above their pI, proteins are negatively charged whereas under their pI, they are positively charged. In the anion exchange chromatography, a positively charged column matrix binds negatively charged proteins, whereas in the cation exchange chromatography, positively charged proteins bind to a negatively charged column matrix. Matrix bound proteins are released from the column by increasing the ionic strength in the buffer which weakens the electrostatic interactions between the protein and the column matrix.

Anion exchange chromatography on a Resource Q column was the second protein purification method used in this work to purify pERp1 proteins.

4.3.4 Gel filtration

Gel filtration (or size exclusion chromatography) allows separating of proteins according to their size. For this purpose, a protein mixture is loaded on a column with a matrix that consists of a three-dimensional network with defined pore size. Proteins whose hydrodynamic radius is smaller than the pores diameter of the column matrix can penetrate into these pores and are thereby retained on the column. Larger proteins are not able to penetrate into the pores of the column matrix and are eluted within the void volume of the column.

Gel filtration on Superdex 75 column was used in this work as a final purification method for pERp1 proteins.

4.3.5 Protein dialysis

During purification of pERp1 proteins in this work, a change of buffer was necessary between particular purification steps. Therefore, dialysis was performed at 4 °C against 100-1000-fold of the original volume either in dialysis tubes (MWCO 6-8000) or, for smaller volumes, in a Slide-A-Lyzer dialysis cassette (MWCO 10 000).

4.3.6 Concentration of proteins

Before gel filtration and as the very last step of a protein purification procedure, protein solutions had to be concentrated. To concentrate pERp1 solutions in this work, ultrafiltration was performed during which pERp1 proteins were pressed through an ultrafiltration membrane (MWCO 10 000). For volumes under 15 ml, Amicon Ultra Centrifugal Filter Units were used and centrifuged at 3700 rpm, 4 °C until the desired volume or the desired concentration were reached. For larger volumes, Amicon cells with corresponding ultrafiltration membranes (MWCO 10 000) were used.

4.4 Bioanalytical methods

4.4.1 SDS-polyacrylamide electrophoresis and western blot

4.4.1.1 Solutions and buffers used for SDS-PAGE and Western blot

SDS-PAGE running buffer	25 mM Tris/HCl, pH 8.3 0.2 M glycine 0.1% SDS (w/v)
5x reducing Loading buffer	300 mM Tris/HCl, pH 6.8 10% SDS (w/v) 50% glycerol (v/v) 0.05% bromphenol blue (w/v) 5% 2-mercaptoethanol (v/v)

5x Loading buffer	300 mM Tris/HCl, pH 6.8 10% SDS (w/v) 50% glycerol (v/v) 0.05% bromphenol blue (w/v)
Fairbanks A	25% isopropanol (v/v) 10% acetic acid (v/v) 0.05% Comassie Blue R (w/v)
Fairbanks D	10% acetic acid (v/v)
Western blot transfer buffer	25 mM Tris/HCl, pH 8.3 0.2 M glycine 20% methanol (v/v) 0.037% SDS (w/v)
PBS buffer	137 mM NaCl 2.7 mM KCl 8 mM Na_2HPO_4 1.8 mM KH_2PO_4
PBST buffer	PBS buffer + 0.05% Tween 20 (v/v)

4.4.1.2 SDS-polyacrylamide electrophoresis (SDS-PAGE)

In order to separate cell lysates or protein mixtures by protein size, samples were prepared by mixing 20 µl of the protein mixture with 5 µl 5x reducing Loading buffer or Loading buffer. SDS-PAGE was performed on 15% polyacrylamide gels with “SDS-PAGE Low Range Standard” as a molecular weight standard or with “SERVAChrom Protein Standard III” if a western blot followed the SDS-PAGE. SDS-PAGE was carried out at a constant current of 40 mA per gel for 45 min. After SDS-PAGE, gels were either western blotted on a nitrocellulose membrane (see section 4.4.1.3) or stained. For staining, gels were boiled in Fairbanks A solution for a few seconds and then incubated for another 5 min. Subsequently, gels were destained in hot Fairbanks D solution and scanned with “Image Scanner III”.

4.4.1.3 Western blot

Western blots were performed by a semi-dry method on a nitrocellulose membrane. For this, six Whatman filter papers, the nitrocellulose membrane and the SDS-gels after SDS-PAGE were incubated in the "Western blot transfer buffer" for 5 min and then transferred into a western blot apparatus with 3 Whatman filter papers on the bottom, the membrane, the gel and 3 Whatman filter papers on the top. Western blotting was carried out at a constant current of 80 mA per gel for 45 min. Subsequently, the membrane was blocked by incubatinon upon gentle shaking in PBS buffer with 5% milk (w/v) for 1 h at room temperature. After 3x 5 min washing with PBST buffer, the membrane was incubated upon gentle shaking with the primary antibody either in PBST buffer or in PBS buffer with 1% milk (w/v) for either 2 h at room temperature or at 4 °C over night. Afterwards, the membrane was washed again 3x 5 min with PBST and then incubated upon gentle shaking with the secondary "anti-rabbit" antibody conjugated with peroxidase in PBST buffer for 1.5 h at room temperature. Subsequently, the membrane was washed again 4x 5 min with PBST and then detected with "ECL Plus Western Blotting Detection System". The detection method is based on chemoluminiscence which is caused by oxidation of diacyl hydrazine catalyzed by peroxidase in presence of H_2O_2. Emitted chemoluminiscence light was recorded on a "Kodak Biomax XAR" film which was finally developed in the "Optimax X-Ray" film processor.

4.4.2 Analytical size exclusion chromatography (SEC)

Analytical SEC is a method used to separate and analyze protein mixtures. Similar to the gel filtration (section 4.3.4), proteins are separated by size during analytical SEC. However, in contrast to the gel filtration, protein volumes injected on a column are smaller and the running buffer is pumped through the column with a higher pressure. Analytical SEC was performed in this work in order to estimate the oligomeric state of pERp1 proteins. For this, 100 µl of 10 µM pERp1 solution was injected on a Superdex 75 column and SEC was performed in PBS buffer with a flow of 0.5 ml/min. Before pERp1 analysis, chromatograms of HPLC calibration proteins with defined molecular weights (MW) were recorded. A calibration curve was obtained by plotting of the logarithms of the respective molecular weights (ln MW) against the respective elution times.

4.4.3 Spectroscopic methods

For all spectroscopic measurements, a reference sample containing the respective buffer or medium with all components except of the protein was measured first.

4.4.3.1 Circular dichroism spectroscopy

Optical active molecules, such as amino acids in proteins, absorb left and right circularly polarized light in a different manner which is used in the circular dichroism (CD) spectroscopy. CD spectroscopy is commonly used to determine the protein secondary (far-UV CD spectroscopy) and tertiary (near-UV CD spectroscopy) structure. Far-UV CD spectra of α-helical proteins show a double minimum at 208 and 222 nm, whereas proteins consisting of β-sheets have only one minimum at 218 nm. Spectra of unfolded proteins (random coil) show also only one minimum at 195 nm.

In this work, far-UV CD spectroscopy was used to determine the secondary structure of pERp1 proteins. All spectra were recorded in PBS buffer at 25 °C with the following parameters:

Wavelength	200-250 nm
Speed	20 nm/min
Response time	4 sec
Band width	1 nm
Accumulation	16
Cuvette thickness	1 mm
Sample concentration	10 µM
Sample volume	300 µl

The measured CD signal was recorded in ellipticity (θ, mdeg), a concentration dependent parameter, which was converted to molar ellipticity ([θ], deg cm^2 $dmol^{-1}$) to allow the comparison between different samples. The conversion followed according to the equation (Creighton, 1997)

$$[\Theta] = \frac{\Theta * 100 * Mr}{c * l * N_A},$$

where *Mr* is the protein molecular weight, *c* is the protein concentration (mg/ml), *l* is the path length of the cuvette (cm) and N_A is the number of amino acids per protein. The concen-

tration of each sample was estimated spectroscopically by measuring of the absorbance at 280 nm (see section 4.4.3.3).

Thermal transitions were measured at 222 nm between 10 and 90 °C and the sample was heated with 20 °C/h. The midpoint analysis of the thermal transition curves was performed with a Boltzmann fit.

4.4.3.2 Fluorescence spectroscopy

Electrons of substances which are excited by light at a certain wavelength change their ground state to the energetically higher excited state. During their return back to the ground state, fluorescence (emission of light) might be observed. Proteins contain three amino acids (tryptophan, tyrosine and phenylalanine) with intrinsic fluorescence properties. In protein folding studies, tryptophan fluorescence is used to monitor protein (un)folding. In native proteins, tryptophan is commonly buried within the protein hydrophobic core. During protein unfolding, buried tryptophan residues get exposed which contributes to the change in fluorescence.

In this work, fluorescence spectroscopy was used to monitor the stability of pERp1 proteins during unfolding with guanidine hydrochloride (GdmHCl). For this, a stock solution of 8 M GdmHCl in HKM buffer (50 mM HEPES/KOH, 150 mM KCl, 10 mM $MgCl_2$, pH 7.5) was prepared. HKM buffer and GdmHCl stock solution were mixed in different proportions to obtain the desired GdmHCl concentration in a sample of 150 µl containing 1 µM pERp1 protein. Samples were excited at a constant wavelength of 280 nm and emission spectra were recorded at 20 °C between 300 and 450 nm. Fluorescence intensity at 350 nm (y) was plotted against corresponding GdmHCl concentration (x) and the data points were fitted according to the equation

$$y = \frac{(y_n + m_n x) + (y_u + m_u x) * (\exp(-\frac{-\Delta G - mx}{RT})}{1 + \exp(-\frac{\Delta G - mx}{RT})},$$

where y_n and y_u stand for intercepts on the axis and m_n and m_u are the slopes of the native and unfolded baselines, respectively. ΔG (J mol^{-1}) represents the change of the free energy upon protein unfolding, m is the constant of proportionality ($=-\Delta\Delta G/\Delta y$), R is the molar gas constant (8.314 kJ mol^{-1} K^{-1}) and T is the temperature (293.15 K).

To enable the comparison between pERp1 proteins, data was converted to a fraction unfolded f_u according to the equation

$$f_u = \frac{y - y_n}{y_u - y_n}.$$

Midpoints of the transitions $[D]_{1/2}$ were calculated according to the equation

$$[D]_{1/2} = \frac{\Delta G}{m}.$$

4.4.3.3 UV absorption spectroscopy

UV absorption spectroscopy makes use of the fact that proteins absorb UV light at several wavelengths. Peptide bond absorbs light at wavelengths of 190-230 nm whereas aromatic residues tryptophan and tyrosine absorb light at 280 nm and 274 nm, respectively. Commonly, UV absorption spectroscopy is used to determine the protein concentration. Protein concentration is directly proportional to the absorption according to the Lambert-Beer law

$$A = \varepsilon * l * c,$$

where A represents the absorbance, ε is the molar extinction coefficient (mol l^{-1} cm^{-1}), l is the cuvette thickness and c is the protein concentration (mol l^{-1}).

In this work, UV absorption spectroscopy was used to determine the protein concentration. All measurements were performed in a cuvette with the width of 1 cm and all spectra were recorded from 200 to 400 nm. All samples were diluted to an absorbance of less than 1 which ensures the linearity of the Lambert-Beer law. Protein concentration was calculated according to the absorbance at 280 nm and molar extinction coefficient calculated on the basis of the protein's amino acid sequence using the program ProtParam (http://web.expasy.org/protparam/).

4.4.3.4 Surface plasmon resonance spectroscopy

Surface plasmon resonance spectroscopy (SPR) is a method used for the determination of protein interactions. SPR is based on the change of the refractive index of the media caused by interaction of proteins, one of which is fixed on a sensor chip and the second one is in the mobile phase (running buffer). The measured signal (expressed in response units, RU) is directly proportional to the amount of the bound protein.

In this work, SPR spectroscopy was used to investigate the binding of pERp1 to BiP. The CM5 sensor chip (Biacore, Uppsala, Sweden) was coupled with pERp1 in HKM buffer (50 mM HEPES/KOH, 150 mM KCl, 10 mM $MgCl_2$, pH 7.5) up to 550 RU. Measurements were performed at 25 °C in HKM buffer with or without nucleotides with a flow of 30 µl/min and the injected volume of BiP samples was 35 µl. The linear relationship between the amount of bound BiP (*c*) and the increase in resonance signal (*RU*) was used to determine the binding constant (K_D) according to the equation (Wegele et al., 2003)

$$RU = RU_{max} * \frac{c}{c+K_D},$$

where RU_{max} is the maximal resonance signal at which all pERp1 molecules on the chip are saturated with BiP.

4.4.4 Scanning electron microscopy (SEM)

SEM was used in this work to investigate *S. cerevisiae* cells expressing different antibody fragments. For the preparation of SEM samples, 1 ml of the over-night *S. cerevisiae* culture was harvested by centrifugation at 5000 rpm, room temperature for 5 min. The supernatant was discarded and the pellet was washed with PBS buffer. Subsequently, cells were resuspended in 270 µl PBS buffer with 30 µl of 25% glutaraldehyde solution (Merck, Darmstadt, Germany) and incubated upon gentle shaking for 1 h at room temperature. After washing with PBS buffer, cells were resuspended in 300 µl of the same buffer, dispersed on a sample slide and left for 1 h at room temperature. Finally, the sample slide was washed several times with 10 ml ethanol solution with increasing ethanol concentration starting from 50% ethanol, then 70% ethanol, 80% ethanol, 95% ethanol and finishing with 3x washing with 100% ethanol p.a. Sample slides were dried over night and SEM analysis was performed with a JEOL 5900 LV microscope (Jeol, Eching, Germany) at a constant voltage of 20 kV at different magnifications.

4.4.5 Analytical ultracentrifugation

In this work, analytical ultracentrifugation (aUC) was used to determine the exact molecular mass of pERp1 proteins. For this, samples of 5 µM pERp1 in 0.1 M Tris buffer, pH 7.5 were prepared and the aUC runs were performed at 20 °C in a Beckman XL-I analytical centrifuge with a TI-60 rotor. Equilibrium sedimentation experiments were carried out at 20 000 rpm, sedimentation velocity experiments at 42 000 rpm. Absorption was monitored at 230 nm and

280 nm every 2 min (for the sedimentation velocity runs) or every 6 h (for equilibrium sedimentation runs). Data was analyzed by Klaus Richter with the program Ultrascan, module c(s).

4.4.6 ATPase assay with an ATP-regenerating system

This assay, which measures the rate of ATP hydrolysis, was used in to investigate the effect of pERp1 proteins on the ATPase activity of BiP. The generated ADP is rapidly converted to ATP in a reaction with phosphoenolpyruvate (PEP) catalyzed by pyruvate kinase (PK). The generated pyruvate is subsequently reduced by NADH to lactate in a reaction catalyzed by lactate dehydrogenase (LDH). The conversion of NADH to NAD^+ can be followed by measuring the absorption at 340 nm. Before measurement, 3 ml of the premix were prepared consisting from the following reagents: 80 µl PEP (100 mM), 16 µl NADH (50 mM), 4 µl PK suspension (Roche, Mannheim, Germany), 14.7 µl LDH (Roche, Mannheim, Germany) and 2885.3 µl HKM buffer (50 mM HEPES/KOH, 150 mM KCl, 10 mM $MgCl_2$, pH 7.5). 126.8 µl of the premix was preincubated in the cuvette for 5 min. Then, 15 µl ATP (50 mM) and BiP and/or pERp1 were added until the final volume of 150 µl and the measurement was started immediately. The absorption at 340 nm was continuously monitored at 37 °C for 20 min.

4.5 Expression of antibody fragments in yeast

4.5.1 Buffers and solutions used for antibody fragments expression in yeast

Cell lysis buffer	50 mM Tris/HCl, pH 7.4 150 mM NaCl 1 mM EDTA
TBS buffer	10 mM Tris/HCl, pH 8.0 150 mM NaCl

4.5.2 Antibody fragments expression

S. cerevisiae culture (100 ml) was grown in a glucose medium at 30 °C over night. On the next day, the culture was transferred into a raffinose medium and was incubated over night at room temperature. On the third day, yeast cells were induced by transferring the cultures into

a galactose medium and grown further at room temperature. During growth and expression, samples were taken out, the OD_{600} was measured and samples were centrifuged for 5 min at 4500 rpm at room temperature. The supernatant was discarded and the pellets were frozen for further use.

4.5.3 Pull-downs from yeast lysates

After defrosting the cell pellets, cells were diluted with "cell lysis buffer" to the same OD_{600}, typically to OD_{600} = 30 (or 15-20 respectively). Afterwards, 1.5 ml was taken out and mixed with 750 µl glass beads (0.25-0.5 mm). Cells were lysed by shaking in the mixer mill 5x 2 min by 30 s^{-1} with 2 minutes pause in between and cell lysis was checked by microscopy. Depending on the respective experiment, pull-downs were performed either directly from the clear lysate or after the cell lysate was fractionated.

4.5.3.1 Pull-down from the clear lysate

The crude lysate was centrifuged at 1743 g, 8 °C for 15 min. The pellet was discarded and the supernatant was mixed with the corresponding affinity beads (see section 4.5.3.2.1). Samples were incubated for the respective times and labelled as "clear lysate" after elution from the beads. After boiling for 10 min at 95 °C, the samples were loaded onto an SDS-gel and SDS-PAGE and western blot were performed (see section 4.4.1.3).

4.5.3.2 Pull-down after cell lysate fractionation

From the crude lysate, a sample was taken out (32 µl + 8 µl 5x Loading buffer) and labeled as "complete lysate". The Loading buffer does not contain 2-mercaptoethanol in order to keep possible disulfide bridges between antibody chains intact. From the remaining lysate, 1 ml was transferred into a fresh tube and was centrifuged for 5 min at 775 g and 8 °C. The pellet was mixed with 100 µl of 1x Loading buffer to obtain the "insoluble fraction" sample. The supernatant was centrifuged further for 15 min at 25 000 g and 8 °C. 30 µl of 1x Loading buffer was added to the pellet and the sample was labeled as "membrane fraction". The supernatant was mixed with the corresponding affinity beads and incubated for the respective times (see section 4.5.3.2.1). After the elution from the beads, samples were labeled as "soluble fraction". All samples ("complete lysate", "insoluble fraction", "membrane fraction" and "soluble fraction") were boiled at 95 °C for 10 min and SDS-PAGE and western blot were performed (see section 4.4.1.3).

4.5.3.2.1 Pull-down with affinity-beads

According to the respective antibody fragment, pull-downs were performed either with α-HA or α-Flag affinity beads.

4.5.3.2.1.1 Pull-down with α-HA beads

α-HA beads (30 µl beads per 1 ml clear yeast lysate) were washed twice with 750 µl "cell lysis buffer" and centrifuged in between for 30 s at 10 000 rpm and 8 °C. To the washed beads, 1 ml of the clear lysate was added and incubated upon gentle shaking for 2 h at 8 °C. Subsequently, the samples were centrifuged for 30 s at 10 000 rpm and 8 °C, the supernatant was discarded and the beads were washed with 3x 750 µl "cell lysis buffer" with centrifugation for 30 sec at 10 000 rpm, 8 °C in between. Antibody fragments were eluted from the beads by adding of 40 µl 2x Loading buffer and boiled at 95 °C for 10 min. Finally, the samples were centrifuged for 1 min at 10 000 rpm, 8 °C and the supernatant was transferred into a fresh tube.

4.5.3.2.1.2 Pull-down with α-Flag beads

α-Flag beads (40 µl beads per 1 ml clear yeast lysate) were washed twice with 500 µl TBS buffer and centrifuged in between for 30 s at 7500 rpm and 8 °C. 1 ml of the clear lysate was added to the washed beads and the samples were incubated upon gentle shaking over night at 8 °C. Afterwards, the samples were centrifuged for 30 s at 7500 rpm, 8 °C and the supernatant was discarded. The beads were washed with 3x 500 µl TBS buffer and centrifuged in between for 30 s at 7500 rpm, 8 °C. For the elution of the antibody fragments from the beads, 40 µl of 2x Loading buffer was added and samples were boiled at 95 °C for 10 min. Subsequently, the samples were centrifuged for 1 min at 7500 rpm, 8 °C and the supernatant was transferred into a fresh tube.

4.5.4 SDS-PAGE and western blot of antibody fragments

Following volumes of the prepared samples (section 4.5.3) were loaded onto a 15% SDS-gel for further analysis: 10 µl of "insoluble fraction", 20-30 µl of "complete lysate", "membrane fraction" and "soluble fraction". SDS-PAGE was performed with 40 mA per gel for 45 min (see section 4.4.1.2). All gels were western blotted on a nitrocellulose membrane with 80 mA per gel for 45 min (see section 4.4.1.3). After blocking and washing the membrane, different primary antibodies were used according to the respective antibody fragment. α-HA antibody in PBST buffer was added to detect MAK33 HA-light chain and incubated upon

gentle shaking for 2 h at room temperature. For detection of MAK33 Flag-Fd-fragment, α-Flag antibody in PBS buffer containing 1% milk (w/v) was added and incubated at 4 °C over night. After washing the membrane, the secondary antibody was added and the membrane was developed (see section 4.4.1.3).

4.5.5 Precipitation of proteins from a medium with trichloroacetic acid

To investigate whether the antibody fragments were secreted, proteins contained in the medium were precipitated. For this, 1/1000 volume of 10% sodium deoxycholate (w/v) was added to the medium which was then incubated for 20 min on ice. Afterwards, 1/15 volume of ice cold trichloroacetic acid was added and the mixture was incubated for another 30 min on ice. Subsequently, centrifugation was performed for 45 min at 14 000 rpm and 8 °C. The supernatant was discarded and the pellet was resuspended in 1:4 of 5x Loading buffer: 1 M Tris buffer without adjusted pH.

5 *References*

Abdel-Salam, H.A., El-Khamissy, T., Enan, G.A., and Hollenberg, C.P. (2001). Expression of mouse anticreatine kinase (MAK33) monoclonal antibody in the yeast Hansenula polymorpha. Appl Microbiol Biotechnol *56*, 157-164.

Anfinsen, C.B., Haber, E., Sela, M., and White, F.H., Jr. (1961). The kinetics of formation of native ribonuclease during oxidation of the reduced polypeptide chain. Proc Natl Acad Sci U S A *47*, 1309-1314.

Arvan, P., Zhao, X., Ramos-Castaneda, J., and Chang, A. (2002). Secretory pathway quality control operating in Golgi, plasmalemmal, and endosomal systems. Traffic *3*, 771-780.

Augustine, J.G., de La Calle, A., Knarr, G., Buchner, J., and Frederick, C.A. (2001). The crystal structure of the fab fragment of the monoclonal antibody MAK33. Implications for folding and interaction with the chaperone bip. J Biol Chem *276*, 3287-3294.

Awad, W., Estrada, I., Shen, Y., and Hendershot, L.M. (2008). BiP mutants that are unable to interact with endoplasmic reticulum DnaJ proteins provide insights into interdomain interactions in BiP. Proc Natl Acad Sci U S A *105*, 1164-1169.

Baumal, R., Potter, M., and Scharff, M.D. (1971). Synthesis, assembly, and secretion of gamma globulin by mouse myeloma cells. 3. Assembly of the three subclasses of IgG. J Exp Med *134*, 1316-1334.

Bergman, L.W., and Kuehl, W.M. (1979). Formation of an intrachain disulfide bond on nascent immunoglobulin light chains. J Biol Chem *254*, 8869-8876.

Bertolotti, A., Zhang, Y., Hendershot, L.M., Harding, H.P., and Ron, D. (2000). Dynamic interaction of BiP and ER stress transducers in the unfolded-protein response. Nat Cell Biol *2*, 326-332.

Better, M., and Horwitz, A.H. (1989). Expression of engineered antibodies and antibody fragments in microorganisms. Methods Enzymol *178*, 476-496.

Bole, D.G., Hendershot, L.M., and Kearney, J.F. (1986). Posttranslational association of immunoglobulin heavy chain binding protein with nascent heavy chains in nonsecreting and secreting hybridomas. J Cell Biol *102*, 1558-1566.

Bork, P., Holm, L., and Sander, C. (1994). The immunoglobulin fold. Structural classification, sequence patterns and common core. J Mol Biol *242*, 309-320.

Braakman, I., and Bulleid, N.J. (2011). Protein folding and modification in the mammalian endoplasmic reticulum. Annu Rev Biochem *80*, 71-99.

Brodsky, J.L., Goeckeler, J., and Schekman, R. (1995). BiP and Sec63p are required for both co- and posttranslational protein translocation into the yeast endoplasmic reticulum. Proc Natl Acad Sci U S A *92*, 9643-9646.

Bukau, B., Weissman, J., and Horwich, A. (2006). Molecular chaperones and protein quality control. Cell *125*, 443-451.

Burrows, P., LeJeune, M., and Kearney, J.F. (1979). Evidence that murine pre-B cells synthesise mu heavy chains but no light chains. Nature *280*, 838-840.

Buschhorn, B.A., Kostova, Z., Medicherla, B., and Wolf, D.H. (2004). A genome-wide screen identifies Yos9p as essential for ER-associated degradation of glycoproteins. FEBS Lett *577*, 422-426.

Carvalho, P., Goder, V., and Rapoport, T.A. (2006). Distinct ubiquitin-ligase complexes define convergent pathways for the degradation of ER proteins. Cell *126*, 361-373.

Chantret, I., Kodali, V.P., Lahmouich, C., Harvey, D.J., and Moore, S.E. (2011). Endoplasmic reticulum-associated degradation (ERAD) and free oligosaccharide generation in Saccharomyces cerevisiae. J Biol Chem *286*, 41786-41800.

Chen, K., and Cerutti, A. (2011). The function and regulation of immunoglobulin D. Curr Opin Immunol *23*, 345-352.

Chen, K., Xu, W., Wilson, M., He, B., Miller, N.W., Bengten, E., Edholm, E.S., Santini, P.A., Rath, P., Chiu, A., *et al.* (2009). Immunoglobulin D enhances immune surveillance by activating antimicrobial, proinflammatory and B cell-stimulating programs in basophils. Nat Immunol *10*, 889-898.

Chen, X., Easton, D., Oh, H.J., Lee-Yoon, D.S., Liu, X., and Subjeck, J. (1996). The 170 kDa glucose regulated stress protein is a large HSP70-, HSP110-like protein of the endoplasmic reticulum. FEBS Lett *380*, 68-72.

Christis, C., Lubsen, N.H., and Braakman, I. (2008). Protein folding includes oligomerization - examples from the endoplasmic reticulum and cytosol. FEBS J *275*, 4700-4727.

Chumley, M.J., Dal Porto, J.M., and Cambier, J.C. (2002). The unique antigen receptor signaling phenotype of B-1 cells is influenced by locale but induced by antigen. J Immunol *169*, 1735-1743.

Clerc, S., Hirsch, C., Oggier, D.M., Deprez, P., Jakob, C., Sommer, T., and Aebi, M. (2009). Htm1 protein generates the N-glycan signal for glycoprotein degradation in the endoplasmic reticulum. J Cell Biol *184*, 159-172.

Connolly, T., and Gilmore, R. (1986). Formation of a functional ribosome-membrane junction during translocation requires the participation of a GTP-binding protein. J Cell Biol *103*, 2253-2261.

Cox, J.S., Chapman, R.E., and Walter, P. (1997). The unfolded protein response coordinates the production of endoplasmic reticulum protein and endoplasmic reticulum membrane. Mol Biol Cell *8*, 1805-1814.

Cox, J.S., Shamu, C.E., and Walter, P. (1993). Transcriptional induction of genes encoding endoplasmic reticulum resident proteins requires a transmembrane protein kinase. Cell *73*, 1197-1206.

Cox, J.S., and Walter, P. (1996). A novel mechanism for regulating activity of a transcription factor that controls the unfolded protein response. Cell *87*, 391-404.

Craven, A.R., Tyson, J.R., and Stirling, C.J. (1997). A novel subfamily of Hsp70s in the endoplasmic reticulum. Trends Cell Biol *7*, 277-282.

Credle, J.J., Finer-Moore, J.S., Papa, F.R., Stroud, R.M., and Walter, P. (2005). On the mechanism of sensing unfolded protein in the endoplasmic reticulum. Proc Natl Acad Sci U S A *102*, 18773-18784.

Creighton, T.E. (1990). Protein folding. Biochem J *270*, 1-16.

Creighton, T.E. (1997). Protein Structure: A Practical Approach. Oxford University Press, New York.

Damasceno, L.M., Anderson, K.A., Ritter, G., Cregg, J.M., Old, L.J., and Batt, C.A. (2007). Cooverexpression of chaperones for enhanced secretion of a single-chain antibody fragment in Pichia pastoris. Appl Microbiol Biotechnol *74*, 381-389.

Deisenhofer, J. (1981). Crystallographic refinement and atomic models of a human Fc fragment and its complex with fragment B of protein A from Staphylococcus aureus at 2.9- and 2.8-A resolution. Biochemistry *20*, 2361-2370.

Deshaies, R.J., Sanders, S.L., Feldheim, D.A., and Schekman, R. (1991). Assembly of yeast Sec proteins involved in translocation into the endoplasmic reticulum into a membrane-bound multisubunit complex. Nature *349*, 806-808.

Deshaies, R.J., and Schekman, R. (1987). A yeast mutant defective at an early stage in import of secretory protein precursors into the endoplasmic reticulum. J Cell Biol *105*, 633-645.

Dill, K.A., and Chan, H.S. (1997). From Levinthal to pathways to funnels. Nat Struct Biol *4*, 10-19.

Dolk, E., van der Vaart, M., Lutje Hulsik, D., Vriend, G., de Haard, H., Spinelli, S., Cambillau, C., Frenken, L., and Verrips, T. (2005). Isolation of llama antibody fragments for prevention of dandruff by phage display in shampoo. Appl Environ Microbiol *71*, 442-450.

Dul, J.L., Aviel, S., Melnick, J., and Argon, Y. (1996). Ig light chains are secreted predominantly as monomers. J Immunol *157*, 2969-2975.

Farid, S.S. (2007). Process economics of industrial monoclonal antibody manufacture. J Chromatogr B Analyt Technol Biomed Life Sci *848*, 8-18.

Feige, M.J., Groscurth, S., Marcinowski, M., Shimizu, Y., Kessler, H., Hendershot, L.M., and Buchner, J. (2009a). An unfolded CH1 domain controls the assembly and secretion of IgG antibodies. Mol Cell *34*, 569-579.

Feige, M.J., Hagn, F., Esser, J., Kessler, H., and Buchner, J. (2007). Influence of the internal disulfide bridge on the folding pathway of the CL antibody domain. J Mol Biol *365*, 1232-1244.

Feige, M.J., and Hendershot, L.M. (2011). Disulfide bonds in ER protein folding and homeostasis. Curr Opin Cell Biol *23*, 167-175.

Feige, M.J., Hendershot, L.M., and Buchner, J. (2010a). How antibodies fold. Trends Biochem Sci *35*, 189-198.

Feige, M.J., Nath, S., Catharino, S.R., Weinfurtner, D., Steinbacher, S., and Buchner, J. (2009b). Structure of the murine unglycosylated IgG1 Fc fragment. J Mol Biol *391*, 599-608.

Feige, M.J., Simpson, E.R., Herold, E.M., Bepperling, A., Heger, K., and Buchner, J. (2010b). Dissecting the alternatively folded state of the antibody Fab fragment. J Mol Biol *399*, 719-730.

Feldheim, D., Rothblatt, J., and Schekman, R. (1992). Topology and functional domains of Sec63p, an endoplasmic reticulum membrane protein required for secretory protein translocation. Mol Cell Biol *12*, 3288-3296.

Fersht, A. (1999). Structure and mechanism in protein science: a guide to enzyme catalysis and protein folding. W H Freeman and Company.

Flach, H., Rosenbaum, M., Duchniewicz, M., Kim, S., Zhang, S.L., Cahalan, M.D., Mittler, G., and Grosschedl, R. (2010). Mzb1 protein regulates calcium homeostasis, antibody secretion, and integrin activation in innate-like B cells. Immunity *33*, 723-735.

Flynn, G.C., Pohl, J., Flocco, M.T., and Rothman, J.E. (1991). Peptide-binding specificity of the molecular chaperone BiP. Nature *353*, 726-730.

Frand, A.R., and Kaiser, C.A. (1999). Ero1p oxidizes protein disulfide isomerase in a pathway for disulfide bond formation in the endoplasmic reticulum. Mol Cell *4*, 469-477.

Frenken, L.G., Hessing, J.G., Van den Hondel, C.A., and Verrips, C.T. (1998). Recent advances in the large-scale production of antibody fragments using lower eukaryotic microorganisms. Res Immunol *149*, 589-599.

Frenken, L.G., van der Linden, R.H., Hermans, P.W., Bos, J.W., Ruuls, R.C., de Geus, B., and Verrips, C.T. (2000). Isolation of antigen specific llama VHH antibody fragments and their high level secretion by Saccharomyces cerevisiae. J Biotechnol *78*, 11-21.

Gardner, B.M., and Walter, P. (2011). Unfolded proteins are Ire1-activating ligands that directly induce the unfolded protein response. Science *333*, 1891-1894.

Gasser, B., and Mattanovich, D. (2007). Antibody production with yeasts and filamentous fungi: on the road to large scale? Biotechnol Lett *29*, 201-212.

Gasser, B., Maurer, M., Gach, J., Kunert, R., and Mattanovich, D. (2006). Engineering of Pichia pastoris for improved production of antibody fragments. Biotechnol Bioeng *94*, 353-361.

Gauss, R., Kanehara, K., Carvalho, P., Ng, D.T., and Aebi, M. (2011). A complex of Pdi1p and the mannosidase Htm1p initiates clearance of unfolded glycoproteins from the endoplasmic reticulum. Mol Cell *42*, 782-793.

Graham, B.M., Porter, A.J., and Harris, W.J. (1995). Cloning, expression and characterization of a single-chain antibody fragment to the herbicide paraquat. J Chem Technol Biotechnol *63*, 279-289.

Green, N., Fang, H., and Walter, P. (1992). Mutants in three novel complementation groups inhibit membrane protein insertion into and soluble protein translocation across the endoplasmic reticulum membrane of Saccharomyces cerevisiae. J Cell Biol *116*, 597-604.

Haas, I.G., and Wabl, M. (1983). Immunoglobulin heavy chain binding protein. Nature *306*, 387-389.

Hackel, B.J., Huang, D., Bubolz, J.C., Wang, X.X., and Shusta, E.V. (2006). Production of soluble and active transferrin receptor-targeting single-chain antibody using Saccharomyces cerevisiae. Pharm Res *23*, 790-797.

Hale, S.J., Lovell, S.C., de Keyzer, J., and Stirling, C.J. (2010). Interactions between Kar2p and its nucleotide exchange factors Sil1p and Lhs1p are mechanistically distinct. J Biol Chem *285*, 21600-21606.

Hamers-Casterman, C., Atarhouch, T., Muyldermans, S., Robinson, G., Hamers, C., Songa, E.B., Bendahman, N., and Hamers, R. (1993). Naturally occurring antibodies devoid of light chains. Nature *363*, 446-448.

Harrison, S.C., and Durbin, R. (1985). Is there a single pathway for the folding of a polypeptide chain? Proc Natl Acad Sci U S A *82*, 4028-4030.

Hendershot, L., Bole, D., Kohler, G., and Kearney, J.F. (1987). Assembly and secretion of heavy chains that do not associate posttranslationally with immunoglobulin heavy chain-binding protein. J Cell Biol *104*, 761-767.

High, S. (1995). Protein translocation at the membrane of the endoplasmic reticulum. Prog Biophys Mol Biol *63*, 233-250.

Hirsch, C., Gauss, R., Horn, S.C., Neuber, O., and Sommer, T. (2009). The ubiquitylation machinery of the endoplasmic reticulum. Nature *458*, 453-460.

Horwitz, A.H., Chang, C.P., Better, M., Hellstrom, K.E., and Robinson, R.R. (1988). Secretion of functional antibody and Fab fragment from yeast cells. Proc Natl Acad Sci U S A *85*, 8678-8682.

Hoseki, J., Ushioda, R., and Nagata, K. (2010). Mechanism and components of endoplasmic reticulum-associated degradation. J Biochem *147*, 19-25.

Huyer, G., Piluek, W.F., Fansler, Z., Kreft, S.G., Hochstrasser, M., Brodsky, J.L., and Michaelis, S. (2004). Distinct machinery is required in Saccharomyces cerevisiae for the endoplasmic reticulum-associated degradation of a multispanning membrane protein and a soluble luminal protein. J Biol Chem *279*, 38369-38378.

Jakob, C.A., Bodmer, D., Spirig, U., Battig, P., Marcil, A., Dignard, D., Bergeron, J.J., Thomas, D.Y., and Aebi, M. (2001). Htm1p, a mannosidase-like protein, is involved in glycoprotein degradation in yeast. EMBO Rep *2*, 423-430.

Jakob, C.A., Burda, P., Roth, J., and Aebi, M. (1998). Degradation of misfolded endoplasmic reticulum glycoproteins in Saccharomyces cerevisiae is determined by a specific oligosaccharide structure. J Cell Biol *142*, 1223-1233.

Jakob, U., Muse, W., Eser, M., and Bardwell, J.C. (1999). Chaperone activity with a redox switch. Cell *96*, 341-352.

Janeway, C., Murphy, K.P., Travers, P., and Walport, M. (2008). Immunobiology. Garland Science, New York

Jeong, K.J., Jang, S.H., and Velmurugan, N. (2011). Recombinant antibodies: engineering and production in yeast and bacterial hosts. Biotechnol J *6*, 16-27.

Joosten, V., Lokman, C., Van Den Hondel, C.A., and Punt, P.J. (2003). The production of antibody fragments and antibody fusion proteins by yeasts and filamentous fungi. Microb Cell Fact *2*, 1.

Karplus, M., and Weaver, D.L. (1994). Protein folding dynamics: the diffusion-collision model and experimental data. Protein Sci *3*, 650-668.

Kauffman, K.J., Pridgen, E.M., Doyle, F.J., 3rd, Dhurjati, P.S., and Robinson, A.S. (2002). Decreased protein expression and intermittent recoveries in BiP levels result from cellular stress during heterologous protein expression in Saccharomyces cerevisiae. Biotechnol Prog *18*, 942-950.

Khatri, N.K., Gocke, D., Trentmann, O., Neubauer, P., and Hoffmann, F. (2011). Single-chain antibody fragment production in Pichia pastoris: Benefits of prolonged pre-induction glycerol feeding. Biotechnol J *6*, 452-462.

Kies, U. (2001). Faltung oligomerer Proteine im Endoplasmatischen Retikulum und *in vitro*. PhD thesis, Technische Universität München.

Kim, P.S., and Baldwin, R.L. (1982). Specific intermediates in the folding reactions of small proteins and the mechanism of protein folding. Annu Rev Biochem *51*, 459-489.

Kimata, Y., Ishiwata-Kimata, Y., Ito, T., Hirata, A., Suzuki, T., Oikawa, D., Takeuchi, M., and Kohno, K. (2007). Two regulatory steps of ER-stress sensor Ire1 involving its cluster formation and interaction with unfolded proteins. J Cell Biol *179*, 75-86.

Kimata, Y., Oikawa, D., Shimizu, Y., Ishiwata-Kimata, Y., and Kohno, K. (2004). A role for BiP as an adjustor for the endoplasmic reticulum stress-sensing protein Ire1. J Cell Biol *167*, 445-456.

Kimura, T., Hosoda, Y., Sato, Y., Kitamura, Y., Ikeda, T., Horibe, T., and Kikuchi, M. (2005). Interactions among yeast protein-disulfide isomerase proteins and endoplasmic reticulum chaperone proteins influence their activities. J Biol Chem *280*, 31438-31441.

King, L.B., and Corley, R.B. (1989). Characterization of a presecretory phase in B-cell differentiation. Proc Natl Acad Sci U S A *86*, 2814-2818.

Knittler, M.R., and Haas, I.G. (1992). Interaction of BiP with newly synthesized immunoglobulin light chain molecules: cycles of sequential binding and release. EMBO J *11*, 1573-1581.

Kohler, G., and Milstein, C. (1975). Continuous cultures of fused cells secreting antibody of predefined specificity. Nature *256*, 495-497.

Kohno, K. (2010). Stress-sensing mechanisms in the unfolded protein response: similarities and differences between yeast and mammals. J Biochem *147*, 27-33.

Kulp, M.S., Frickel, E.M., Ellgaard, L., and Weissman, J.S. (2006). Domain architecture of protein-disulfide isomerase facilitates its dual role as an oxidase and an isomerase in Ero1p-mediated disulfide formation. J Biol Chem *281*, 876-884.

Lange, S., Schmitt, J., and Schmid, R.D. (2001). High-yield expression of the recombinant, atrazine-specific Fab fragment K411B by the methylotrophic yeast Pichia pastoris. J Immunol Methods *255*, 103-114.

Leitzgen, K., Knittler, M.R., and Haas, I.G. (1997). Assembly of immunoglobulin light chains as a prerequisite for secretion. A model for oligomerization-dependent subunit folding. J Biol Chem *272*, 3117-3123.

Levinthal, C. (1968). Are There Pathways For Protein Folding. J Chim Phys *85*, 44-45.

Levinthal, C. (1969). How to fold graciously. Mossbauer spectroscopy in biological systems. Proc Univ Illinois Bull *67*, 22-24.

Li, H., Sethuraman, N., Stadheim, T.A., Zha, D., Prinz, B., Ballew, N., Bobrowicz, P., Choi, B.K., Cook, W.J., Cukan, M., *et al.* (2006). Optimization of humanized IgGs in glycoengineered Pichia pastoris. Nat Biotechnol *24*, 210-215.

Lievremont, J.P., Rizzuto, R., Hendershot, L., and Meldolesi, J. (1997). BiP, a major chaperone protein of the endoplasmic reticulum lumen, plays a direct and important role in the storage of the rapidly exchanging pool of Ca2+. J Biol Chem *272*, 30873-30879.

Lilie, H., Rudolph, R., and Buchner, J. (1995). Association of antibody chains at different stages of folding: prolyl isomerization occurs after formation of quaternary structure. J Mol Biol *248*, 190-201.

Lin, H.Y., Masso-Welch, P., Di, Y.P., Cai, J.W., Shen, J.W., and Subjeck, J.R. (1993). The 170-kDa glucose-regulated stress protein is an endoplasmic reticulum protein that binds immunoglobulin. Mol Biol Cell *4*, 1109-1119.

Lu, T.T., and Cyster, J.G. (2002). Integrin-mediated long-term B cell retention in the splenic marginal zone. Science *297*, 409-412.

Luo, B.H., Carman, C.V., and Springer, T.A. (2007). Structural basis of integrin regulation and signaling. Annu Rev Immunol *25*, 619-647.

Mains, P.E., and Sibley, C.H. (1983). The requirement of light chain for the surface deposition of the heavy chain of immunoglobulin M. J Biol Chem *258*, 5027-5033.

Marcinowski, M., Holler, M., Feige, M.J., Baerend, D., Lamb, D.C., and Buchner, J. (2011). Substrate discrimination of the chaperone BiP by autonomous and cochaperone-regulated conformational transitions. Nat Struct Mol Biol *18*, 150-158.

Martoglio, B., and Dobberstein, B. (1998). Signal sequences: more than just greasy peptides. Trends Cell Biol *8*, 410-415.

Matlack, K.E., Misselwitz, B., Plath, K., and Rapoport, T.A. (1999). BiP acts as a molecular ratchet during posttranslational transport of prepro-alpha factor across the ER membrane. Cell *97*, 553-564.

Melnick, J., Dul, J.L., and Argon, Y. (1994). Sequential interaction of the chaperones BiP and GRP94 with immunoglobulin chains in the endoplasmic reticulum. Nature *370*, 373-375.

Misselwitz, B., Staeck, O., Matlack, K.E., and Rapoport, T.A. (1999). Interaction of BiP with the J-domain of the Sec63p component of the endoplasmic reticulum protein translocation complex. J Biol Chem *274*, 20110-20115.

Molinari, M., and Helenius, A. (1999). Glycoproteins form mixed disulphides with oxidoreductases during folding in living cells. Nature *402*, 90-93.

Nakatsukasa, K., Nishikawa, S., Hosokawa, N., Nagata, K., and Endo, T. (2001). Mnl1p, an alpha -mannosidase-like protein in yeast Saccharomyces cerevisiae, is required for endoplasmic reticulum-associated degradation of glycoproteins. J Biol Chem *276*, 8635-8638.

Nelson, A.L., and Reichert, J.M. (2009). Development trends for therapeutic antibody fragments. Nat Biotechnol *27*, 331-337.

Nguyen, T.H., Law, D.T., and Williams, D.B. (1991). Binding protein BiP is required for translocation of secretory proteins into the endoplasmic reticulum in Saccharomyces cerevisiae. Proc Natl Acad Sci U S A *88*, 1565-1569.

Ning, D., Junjian, X., Qing, Z., Sheng, X., Wenyin, C., Guirong, R., and Xunzhang, W. (2005). Production of recombinant humanized anti-HBsAg Fab fragment from Pichia pastoris by fermentation. J Biochem Mol Biol *38*, 294-299.

Nishikawa, S., Brodsky, J.L., and Nakatsukasa, K. (2005). Roles of molecular chaperones in endoplasmic reticulum (ER) quality control and ER-associated degradation (ERAD). J Biochem *137*, 551-555.

Nishikawa, S., and Endo, T. (1997). The yeast JEM1p is a DnaJ-like protein of the endoplasmic reticulum membrane required for nuclear fusion. J Biol Chem *272*, 12889-12892.

Nishikawa, S., Hirata, A., and Endo, T. (2008). Nuclear inner membrane fusion facilitated by yeast Jem1p is required for spindle pole body fusion but not for the first mitotic nuclear division during yeast mating. Genes Cells *13*, 1185-1195.

Nishikawa, S.I., Fewell, S.W., Kato, Y., Brodsky, J.L., and Endo, T. (2001). Molecular chaperones in the yeast endoplasmic reticulum maintain the solubility of proteins for retrotranslocation and degradation. J Cell Biol *153*, 1061-1070.

Norgaard, P., Westphal, V., Tachibana, C., Alsoe, L., Holst, B., and Winther, J.R. (2001). Functional differences in yeast protein disulfide isomerases. J Cell Biol *152*, 553-562.

Ogunjimi, A.A., Chandler, J.M., Gooding, C.M., Recinos, A., and Choudary, P.V. (1999). High-level secretory expression of immunologically active intact antibody from the yeast Pichia pastoris. Biotechnol Lett *21*, 561-567

Okamura, K., Kimata, Y., Higashio, H., Tsuru, A., and Kohno, K. (2000). Dissociation of Kar2p/BiP from an ER sensory molecule, Ire1p, triggers the unfolded protein response in yeast. Biochem Biophys Res Commun *279*, 445-450.

Oliver, J.D., van der Wal, F.J., Bulleid, N.J., and High, S. (1997). Interaction of the thiol-dependent reductase ERp57 with nascent glycoproteins. Science *275*, 86-88.

Onuchic, J.N., Wolynes, P.G., Luthey-Schulten, Z., and Socci, N.D. (1995). Toward an outline of the topography of a realistic protein-folding funnel. Proc Natl Acad Sci U S A *92*, 3626-3630.

Ou, W.J., Cameron, P.H., Thomas, D.Y., and Bergeron, J.J. (1993). Association of folding intermediates of glycoproteins with calnexin during protein maturation. Nature *364*, 771-776.

Parlati, F., Dominguez, M., Bergeron, J.J., and Thomas, D.Y. (1995). Saccharomyces cerevisiae CNE1 encodes an endoplasmic reticulum (ER) membrane protein with sequence similarity to calnexin and calreticulin and functions as a constituent of the ER quality control apparatus. J Biol Chem *270*, 244-253.

Pilon, M., Schekman, R., and Romisch, K. (1997). Sec61p mediates export of a misfolded secretory protein from the endoplasmic reticulum to the cytosol for degradation. EMBO J *16*, 4540-4548.

Potgieter, T.I., Cukan, M., Drummond, J.E., Houston-Cummings, N.R., Jiang, Y., Li, F., Lynaugh, H., Mallem, M., McKelvey, T.W., Mitchell, T., *et al.* (2009). Production of monoclonal antibodies by glycoengineered Pichia pastoris. J Biotechnol *139*, 318-325.

Promlek, T., Ishiwata-Kimata, Y., Shido, M., Sakuramoto, M., Kohno, K., and Kimata, Y. (2011). Membrane aberrancy and unfolded proteins activate the endoplasmic reticulum stress sensor Ire1 in different ways. Mol Biol Cell *22*, 3520-3532.

Ptitsyn, O.B. (1995). How the molten globule became. Trends Biochem Sci *20*, 376-379.

Rakestraw, J.A., Sazinsky, S.L., Piatesi, A., Antipov, E., and Wittrup, K.D. (2009). Directed evolution of a secretory leader for the improved expression of heterologous proteins and full-length antibodies in Saccharomyces cerevisiae. Biotechnol Bioeng *103*, 1192-1201.

Rapoport, T.A. (2007). Protein translocation across the eukaryotic endoplasmic reticulum and bacterial plasma membranes. Nature *450*, 663-669.

Richter, K., Haslbeck, M., and Buchner, J. (2010). The heat shock response: life on the verge of death. Mol Cell *40*, 253-266.

Rothlisberger, D., Honegger, A., and Pluckthun, A. (2005). Domain interactions in the Fab fragment: a comparative evaluation of the single-chain Fv and Fab format engineered with variable domains of different stability. J Mol Biol *347*, 773-789.

Russell, S.J., Ruddock, L.W., Salo, K.E., Oliver, J.D., Roebuck, Q.P., Llewellyn, D.H., Roderick, H.L., Koivunen, P., Myllyharju, J., and High, S. (2004). The primary substrate binding site in the b' domain of ERp57 is adapted for endoplasmic reticulum lectin association. J Biol Chem *279*, 18861-18869.

Sakoh-Nakatogawa, M., Nishikawa, S., and Endo, T. (2009). Roles of protein-disulfide isomerase-mediated disulfide bond formation of yeast Mnl1p in endoplasmic reticulum-associated degradation. J Biol Chem *284*, 11815-11825.

Saris, N., and Makarow, M. (1998). Transient ER retention as stress response: conformational repair of heat-damaged proteins to secretion-competent structures. J Cell Sci *111 (Pt 11)*, 1575-1582.

Schirrmann, T., Al-Halabi, L., Dubel, S., and Hust, M. (2008). Production systems for recombinant antibodies. Front Biosci *13*, 4576-4594.

Schlenstedt, G., Harris, S., Risse, B., Lill, R., and Silver, P.A. (1995). A yeast DnaJ homologue, Scj1p, can function in the endoplasmic reticulum with BiP/Kar2p via a conserved domain that specifies interactions with Hsp70s. J Cell Biol *129*, 979-988.

Shamu, C.E., and Walter, P. (1996). Oligomerization and phosphorylation of the Ire1p kinase during intracellular signaling from the endoplasmic reticulum to the nucleus. EMBO J *15*, 3028-3039.

Shaw, A.S., Rottier, P.J., and Rose, J.K. (1988). Evidence for the loop model of signal-sequence insertion into the endoplasmic reticulum. Proc Natl Acad Sci U S A *85*, 7592-7596.

Shen, Y., and Hendershot, L.M. (2005). ERdj3, a stress-inducible endoplasmic reticulum DnaJ homologue, serves as a cofactor for BiP's interactions with unfolded substrates. Mol Biol Cell *16*, 40-50.

Shimizu, Y., Meunier, L., and Hendershot, L.M. (2009). pERp1 is significantly up-regulated during plasma cell differentiation and contributes to the oxidative folding of immunoglobulin. Proc Natl Acad Sci U S A *106*, 17013-17018.

Shusta, E.V., Raines, R.T., Pluckthun, A., and Wittrup, K.D. (1998). Increasing the secretory capacity of Saccharomyces cerevisiae for production of single-chain antibody fragments. Nat Biotechnol *16*, 773-777.

Sidrauski, C., and Walter, P. (1997). The transmembrane kinase Ire1p is a site-specific endonuclease that initiates mRNA splicing in the unfolded protein response. Cell *90*, 1031-1039.

Silberstein, S., Schlenstedt, G., Silver, P.A., and Gilmore, R. (1998). A role for the DnaJ homologue Scj1p in protein folding in the yeast endoplasmic reticulum. J Cell Biol *143*, 921-933.

Simpson, E.R., Herold, E.M., and Buchner, J. (2009). The folding pathway of the antibody V(L) domain. J Mol Biol *392*, 1326-1338.

Spector, D.L., Goldman, R.D., and Leinwand, L.A.e. (1998). Cells, a laboratory manual. Volume 1: Culture and Biochemical Analysis of Cells. Cold Spring Harbour Laboratry Press.

Tian, G., Xiang, S., Noiva, R., Lennarz, W.J., and Schindelin, H. (2006). The crystal structure of yeast protein disulfide isomerase suggests cooperativity between its active sites. Cell *124*, 61-73.

Tyson, J.R., and Stirling, C.J. (2000). LHS1 and SIL1 provide a lumenal function that is essential for protein translocation into the endoplasmic reticulum. EMBO J *19*, 6440-6452.

Ushioda, R., Hoseki, J., Araki, K., Jansen, G., Thomas, D.Y., and Nagata, K. (2008). ERdj5 is required as a disulfide reductase for degradation of misfolded proteins in the ER. Science *321*, 569-572.

Valkonen, M., Penttila, M., and Saloheimo, M. (2003). Effects of inactivation and constitutive expression of the unfolded- protein response pathway on protein production in the yeast Saccharomyces cerevisiae. Appl Environ Microbiol *69*, 2065-2072.

van Anken, E., Pena, F., Hafkemeijer, N., Christis, C., Romijn, E.P., Grauschopf, U., Oorschot, V.M., Pertel, T., Engels, S., Ora, A., *et al.* (2009). Efficient IgM assembly and secretion require the plasma cell induced endoplasmic reticulum protein pERp1. Proc Natl Acad Sci U S A *106*, 17019-17024.

Vashist, S., and Ng, D.T. (2004). Misfolded proteins are sorted by a sequential checkpoint mechanism of ER quality control. J Cell Biol *165*, 41-52.

Vembar, S.S., Jonikas, M.C., Hendershot, L.M., Weissman, J.S., and Brodsky, J.L. (2010). J domain co-chaperone specificity defines the role of BiP during protein translocation. J Biol Chem *285*, 22484-22494.

Vinci, F., Catharino, S., Frey, S., Buchner, J., Marino, G., Pucci, P., and Ruoppolo, M. (2004). Hierarchical formation of disulfide bonds in the immunoglobulin Fc fragment is assisted by protein-disulfide isomerase. J Biol Chem *279*, 15059-15066.

Vitu, E., Kim, S., Sevier, C.S., Lutzky, O., Heldman, N., Bentzur, M., Unger, T., Yona, M., Kaiser, C.A., and Fass, D. (2010). Oxidative activity of yeast Ero1p on protein disulfide isomerase and related oxidoreductases of the endoplasmic reticulum. J Biol Chem *285*, 18155-18165.

Walter, P., and Johnson, A.E. (1994). Signal sequence recognition and protein targeting to the endoplasmic reticulum membrane. Annu Rev Cell Biol *10*, 87-119.

Wang, C.C., and Tsou, C.L. (1993). Protein disulfide isomerase is both an enzyme and a chaperone. FASEB J *7*, 1515-1517.

Wegele, H., Haslbeck, M., Reinstein, J., and Buchner, J. (2003). Sti1 is a novel activator of the Ssa proteins. J Biol Chem *278*, 25970-25976.

Wegrzyn, R.D., and Deuerling, E. (2005). Molecular guardians for newborn proteins: ribosome-associated chaperones and their role in protein folding. Cell Mol Life Sci *62*, 2727-2738.

Welihinda, A.A., and Kaufman, R.J. (1996). The unfolded protein response pathway in Saccharomyces cerevisiae. Oligomerization and trans-phosphorylation of Ire1p (Ern1p) are required for kinase activation. J Biol Chem *271*, 18181-18187.

Werner, E.D., Brodsky, J.L., and McCracken, A.A. (1996). Proteasome-dependent endoplasmic reticulum-associated protein degradation: an unconventional route to a familiar fate. Proc Natl Acad Sci U S A *93*, 13797-13801.

Wesolowski, J., Alzogaray, V., Reyelt, J., Unger, M., Juarez, K., Urrutia, M., Cauerhff, A., Danquah, W., Rissiek, B., Scheuplein, F., *et al.* (2009). Single domain antibodies: promising experimental and therapeutic tools in infection and immunity. Med Microbiol Immunol *198*, 157-174.

Wetlaufer, D.B. (1973). Nucleation, rapid folding, and globular intrachain regions in proteins. Proc Natl Acad Sci U S A *70*, 697-701.

Xu, X., Azakami, H., and Kato, A. (2004a). P-domain and lectin site are involved in the chaperone function of Saccharomyces cerevisiae calnexin homologue. FEBS Lett *570*, 155-160.

Xu, X., Kanbara, K., Azakami, H., and Kato, A. (2004b). Expression and characterization of Saccharomyces cerevisiae Cne1p, a calnexin homologue. J Biochem *135*, 615-618.

Yamada, T. (2011). Therapeutic monoclonal antibodies. Keio J Med *60*, 37-46.

Ye, Y., Meyer, H.H., and Rapoport, T.A. (2001). The AAA ATPase Cdc48/p97 and its partners transport proteins from the ER into the cytosol. Nature *414*, 652-656.

Zhang, Y., Nijbroek, G., Sullivan, M.L., McCracken, A.A., Watkins, S.C., Michaelis, S., and Brodsky, J.L. (2001). Hsp70 molecular chaperone facilitates endoplasmic reticulum-associated protein degradation of cystic fibrosis transmembrane conductance regulator in yeast. Mol Biol Cell *12*, 1303-1314.

6 *Abbreviations*

Ac	acetylglucosamine
aUC	analytical centrifugation
CD	circular dichroism
CSSR	core stress sensing region
Da	Dalton
ER	endoplasmic reticulum
ERAD	endoplasmic reticulum associated degradation pathway
g	gram
GdmHCl	guanidine hydrochloride
Glc	glucose
GRAS	generally regarded as safe
h	hour
HPLC	high pressure liquid chromatography
Ig	immunoglobulin
k	kilo
l	liter
M	mol liter^{-1}
Man	mannose
min	minute
MW	molecular weight
MWCO	molecular weight cut off
OD	optical density
oN	over night
PDI	protein disulfide isomerase
rpm	revolutions per minute
RT	room temperature
s	second
SEM	scanning electron microscopy
UPR	unfolded protein response
v/v	volume in volume
WT	wild type
w/v	weight in volume

Acknowledgements

Firstly, I would like to thank to my supervisor, Prof. Dr. Johannes Buchner, for giving me the opportunity to work in his group on an exciting and stimulating project within excellently equipped labs. I would like to thank him for all the advice he has given me during my PhD. project, for his patience, understanding and encouragement.

A special thanks goes to Dr. Martin Haslbeck for all the helpful discussions, for answering all my questions and for encouraging and supporting me all the time.

I would like to thank Emma Harding, PhD. for introducing me to many methods of protein science, for her friendship and encouragement.

Additionally, I would like to express my gratitude to Linda M**.** Hendershot, PhD. and Yuichiro Shimizu, PhD. for providing the glycerol stocks of pERp1 expressing *E. coli* cultures.

Many thanks to Dr. Klaus Richter for the aUC-analysis, Helmut Krause for doing the MS-measurements and Bettina Richter for taking the SEM-pictures.

Furthermore, I would like to thank Mrs. Susanne Hilber who has always been very helpful and understanding.

Thanks also to the technicians Bianca Ludwig and Anja Osterauer for their support throughout the lab's daily routine.

I thank also my lab and office mates as well as to all my colleagues for a pleasant working atmosphere. In particular, I would like to say thanks to B.Z., T.K., E.K., E.H. and A.R. for their friendship and help in many ways.

Finally, I would like to thank H.B., J.F. and S.B. for their constant support, their understanding and always having time for me. Last but not least, I would like to thank my husband Hans Georg for his love, encouragement and never-ending patience and for always being there.

Declaration

I, Eva Seedig, hereby declare that this thesis was prepared by me independently and using only the references and resources stated here. The work has not been submitted to any audit commission or published so far.

Hiermit erkläre ich, Eva Seedig, dass ich die vorliegende Arbeit selbständig verfasst und keine anderen als die angegebenen Quellen und Hilfsmittel verwendet habe. Die Arbeit wurde bisher keiner Prüfungskommission vorgelegt und auch nicht veröffentlicht.

_____

Eva Seedig

Garching, ……